

“PETROLOGY OF THE ANDESITIC VOLCANISM WITHIN THE BOYALI  
FLYSCH - NORTHERN TURKEY”

A THESIS SUBMITTED TO  
THE GRADUATE SCHOOL OF NATURAL AND APPLIED SCIENCES  
OF  
MIDDLE EAST TECHNICAL UNIVERSITY

BY

REMZİYE EZGİ ÇAKIROĞLU

IN PARTIAL FULFILLMENT OF THE REQUIREMENTS  
FOR  
THE DEGREE OF MASTER OF SCIENCE  
IN  
THE DEPARTMENT OF GEOLOGICAL ENGINEERING

SEPTEMBER 2017



Approval of the thesis:

**PETROLOGY OF THE ANDESITIC VOLCANISM WITHIN THE BOYALI  
FLYSCH -NORTHERN TURKEY**

submitted by **REMZİYE EZGİ ÇAKIROĞLU** in partial fulfillment of the  
requirements for the degree of **Master of Science in Geological Engineering**  
**Department, Middle East Technical University** by,

Prof. Dr. Gülbin Dural Ünver  
Dean, Graduate School of **Natural and Applied Sciences**

\_\_\_\_\_

Prof. Dr. Erdin Bozkurt  
Head of Department, **Geological Engineering**

\_\_\_\_\_

Prof. Dr. M. Cemal Göncüoğlu  
Supervisor, **Geological Engineering Dept., METU**

\_\_\_\_\_

**Examining Committee Members:**

Prof. Dr. Semih Gürsu  
Geological Engineering Dept., Muğla Sıtkı Koçman University

\_\_\_\_\_

Prof. Dr. M. Cemal Göncüoğlu  
Geological Engineering Dept., METU (retired)

\_\_\_\_\_

Doç. Dr. Kaan Sayıt, METU  
Geological Engineering Dept., METU

\_\_\_\_\_

Yrd.Doç.Dr. Fatma (Toksoy) Köksal  
Geological Engineering Dept., METU

\_\_\_\_\_

Yrd.Doç.Dr. Ali İmer  
Geological Engineering Dept., METU

\_\_\_\_\_

**Date:** \_\_\_\_\_

**I hereby declare that all information in this document has been obtained and presented in accordance with academic rules and ethical conduct. I also declare that, as required by these rules and conduct, I have fully cited and referenced all material and results that are not original to this work.**

Name, Last name: Remziye Ezgi akırođlu

Signature :

## **ABSTRACT**

### **PETROLOGY OF THE ANDESITIC VOLCANISM WITHIN THE BOYALI FLYSCH - NORTERN TURKEY**

Çakırođlu, Remziye Ezgi

MSc., Department of Geological Engineering

Supervisor : Prof. Dr. Mehmet Cemal G6ncüođlu

September 2017,98 pages

The Araç-Boyalı Flysch Basin, a foreland basin formed following the closure of the Intra-Pontide Ocean during the Late Cretaceous-Late Paleocene on the platform of the Sakarya Composite Terrane contains a large number of dykes and sills. Dykes that intrude the deformed flysch sediments and also the olistolits, are covered by the volcano-sedimentary rocks of Mid-Eocene age. Majority of the dykes contain chilled margins and flow structures characterized by large plagioclase phenocrystals and amigdules filled with calcite and zeolite. Among the flysch sediments, lava flows up to 50 m thickness include massive and pillow lavas, lava and pillow breccias. Pillow lavas within the olistostromes were formed by submarine volcanism and accumulated by gravitational sliding.

The lavas are dominantly plagioclase and pyroxene phyric and a few include biotite. Lavas as well as the dykes are variably altered, most of them showing chloritization, epidotization and carbonatization. Dykes are dominantly andesitic, and range from sub alkaline to alkaline basalts. Majority of lava and dyke samples are of calc alkaline character. Harker diagrams are in accordance with plagioclase, pyroxene and biotite

fractionation, as well as fractionation of Fe-Ti oxides. Tectono-magmatic discrimination diagrams of lavas as well as the dykes are indicative for destructive plate margin volcanism.

Regional geological constraints together with geochemical characteristics of the volcanic rocks are in favour of extension in continental back-arc setting within the Sakarya Composite Terrane above the N-ward subducting Izmir-Ankara oceanic lithosphere of Neotethys.

Keywords: Central Pontide, Late Cretaceous-Paleocene, Back-arc volcanism, Sakarya Continent, dykes

## ÖZ

### **BOYALI FİLİŞİNDEKİ ANDEZİTİK VOLKANİZMANIN PETROLOJİSİ, KUZEY- TÜRKİYE**

Çakıroğlu, Remziye Ezgi

Yüksek lisans., Jeoloji Mühendisliği

Tez Yöneticisi: Prof. Dr. Mehmet Cemal Göncüoğlu

Eylül 2017, 98 sayfa

Araç-Boyalı Fliş havzası Intra-Pontid Okyanusu'nun kapanışıyla oluşmuş bir önülke basenidir. Geç Kretase-Geç Paleosen döneminde Sakarya Kompozit Birliği platformunun üzerinde oluşmuştur. Çok miktarda dayk ve sil içermektedir. Deforme flişsedimanlarını ve olistolitleri kesen dayklar Orta-Eosen yaşlı volkano-sedimanter kayaçlarla örtülmüştür. Daykların çoğu iri plajioklasfenokristalleri , kalsit ve zeolit dolgulu amigdüller, “chilled magrin” ve akma yapıları içermektedir. Flişsedimanlarının arasında, 50 m'ye kadar lav akmaları masif ve yastık lavlar, lav breşleri ve yastık lav breşleri içermektedir. Olistostromların arasında yastık lavlar denizaltı volkanizması ile oluşmuş, yerçekimi kaymalarıyla toplanmıştır.

Lavlar ağırlıklı olarak plajioklas ve piroksen fenokristalleri içermektedir. Az sayıda örnekte biyotite de rastlanmıştır. Lavlar ve dayklar değişen düzeylerde alterasyona uğramış ve kloritleşme, epidotlaşma, karbonatlaşma sergilemektedir. Dayklar, ağırlıklı andezitik kompozisyondadır, subalkalen-alkalen bileşim göstermektedir. Lav ve dayk örnekleri kalk alkalen karakterdedir. Harker diyagramları plajioklas, piroksen ve biyotit fraksiyonlaşmasıyla, aynı zamanda Fe-Ti oksitlerin oluşumuyla uyumludur. Lavların ve daykların tektono-magmatik ayırım diyagramları yakınlaşan levha sınırı volkanizmasına işaret etmektedir.

Bölgesel jeolojik bulgular, jeokimyasal karakterlerle birlikte düşünöldüğünde incelenen volkanik kayalar Neotetis'in İzmir-Ankara kolunun Kuzeye Sakarya Kompozit Birliđi'nin altına dalması ile kıtasal kabuk üzerinde gerilme ile gelişen yay-ardı magmatizmasını göstermektedir.

Anahtar Kelimeler: Orta Pontid, Üst Kretase-?Paleosen, Yay-ardı volkanizması, Sakarya Kıtası, dayklar

**To my family**

## ACKNOWLEDGEMENTS

I would like to express my sincere gratitude to my supervisor Prof. Dr. M. Cemal Göncüoğlu for his patience, guidance, advice and criticism throughout my thesis, his understanding approach during the life challenges I have gone through during this period. I have learned a lot from his approaches to debatable issues; ethics of science/work discipline, as well as his way of explaining/ teaching a phenomenon. He is one of the best lecturers I've ever attended the classes of. I feel privileged to have had the chance to learn from his scientific knowledge and experience, which I (probably everyone) would call "legendary" and also his wisdom.

I'm deeply grateful to Prof. Dr. Asuman G. Türmenoğlu for her motivation, advice and everything she has taught me as an admirable lecturer/ a scientist, an idol as a successful woman and one of the loveliest persons I have ever known; as well as her comments about the clay minerals and alterations products in my samples and recommendations about further possible studies.

I would like to thank Dr. Kaan Sayıt and Dr. Giuseppe Ottria for their help about geochemistry and evaluating data about dykes; all the honorable members of the examining committee for their advice and support, and the geoscientists of the University of Pisa for their hospitality.

I would like to extend my thanks to all my friends in METU; in METU-GEO: D. P., G. G.; my friends from Izmir for their friendship and moral support; as for other friends; especially "D.", "M.K.", "A.I.", "as well as "N." deserves endless "thank you"s.

Finally I am indebted to my family and all of my honorable lecturers from Izmir, Dokuz Eylül University from whom I learned invaluable geological and non-geological values, knowledge and wisdom.

## TABLE OF CONTENTS

ABSTRACT.....	v
ÖZ .....	vii
DEDICATION.....	ix
ACKNOWLEDGMENTS .....	x
TABLE OF CONTENTS.....	xi
LIST OF FIGURES/ILLUSTRATIONS/SCHEMES .....	xiii
LIST OF TABLES.....	xviii
CHAPTERS	
1. INTRODUCTION .....	1
1.1. Purpose and Scope .....	1
1.2. Geographic Setting .....	2
1.3. Methods of Study.....	3
1.3.1.Field Work .....	4
1.3.2.Laboratory Work.....	4
1.4.Previous Work .....	4
1.4.1. General Geology .....	5
1.4.1.1. Istanbul Zonguldak Terrane.....	5
1.4.1.2.Intra-Pontide Suture.....	7
1.4.1.3. Sakarya Composite Terrane.....	8
1.4.1.4.Izmir-Ankara-Erzincan Suture.....	9
2. GEOLOGY OF THE STUDY AREA .....	13
2.1.Regional Geology .....	13
2.2.Local Geology.....	15
2.2.1.Taraklı Flysch .....	15
2.2.2.Boyalı Unit.....	23
2.2.2.1.Lavas .....	23

2.2.2.2.Dykes.....	29
2.2.2.2.1.Field Observations.....	29
2.2.2.2.2.Orientation of Dykes .....	34
3. PETROGRAPHY .....	37
3.1.Introduction .....	37
3.2.Petrography of Boyalı Volcanics .....	37
3.2.1..Basalts .....	38
3.2.2. Andesites .....	47
4. PETROLOGY GEOCHEMISTRY .....	57
4.1. Introduction .....	57
4.2. Method .....	57
4.3. Alteration.....	57
4.4. Major Element Chemistry .....	64
4.5.Trace and Rare Earth Element Chemistry .....	72
4.6. Classification.....	79
4.7.Tectonomagmatic Discrimination .....	79
4.8. Source.....	84
6. DISCUSSION AND CONCLUSIONS.....	87
REFERENCES.....	91

## LIST OF FIGURES

### FIGURES

- Figure 1** Location map of the study area shown on the simplified tectonic map of Anatolia and its surroundings showing the distribution of major plate boundaries, tectonic belts, Neotethyan ophiolites (Jurassic–Cretaceous), and Eocene volcanic units (Altunkaynak and Dilek, 2013).....3
- Figure 2** Terrane Map of Turkey (Göncüoğlu et al., 1997).....5
- Figure 3.** Generalized columnar section of the Sakarya Composite Terrane's cover in NW Anatolia (Saner, 1980; Altıner et al, 1991; Göncüoğlu, 1997)..... 15
- Figure 4.** Geological map of the study area (Catanzariti et al., 2013) 1) Alluvial deposits; 2) Pliocene deposits; 3) Middle Eocene deposits; 4) Lower Eocene deposits; 5) Low-Grade Metamorphic Unit; 6) Arkotdag Mélange; 7) Basalts; 8) Taraklı Flysch, slide-block in shaly-matrix; 9) Taraklı Flysch, orthoconglomerates; 10) Taraklı Flysch, thin-bedded turbidites; 11) Jurassic-Cretaceous limestones; 12) Granites; 13) Cataclastic zones; 14) Main strike-slip faults; 15) Main faults; 16) Thrust faults; 17) Stratigraphic boundaries; 18) Bedding; 19) Vertical bedding; 20) S1 foliation; 21) Vertical S1; 22) S2 foliation, 23) A1 fold axes; 24) A2 fold axes with vergence; 25) Horizontal A2 fold axes; 26) High-angle strike-slip faults; 27) Low-angle thrust faults; 28) Approximate locations of the dyke and lava samples 29) Trace of the geological cross-section. B) Geological cross-section.....18
- Figure 5.** Thin-bedded turbidites of the Taraklı Flysch observed along the Boyalı Creek.....19
- Figure 6** Conglomerates of the Taraklı Flysch in the southeast of Boyalı.....20
- Figure 7** Slide-block of a recrystallized limestone in a fine-grained matrix in the south of Boyalı.....21
- Figure 8** Slide-block of Triassic red quartz-arenites next to Devonian-Carboniferous limestones in the southeast of Boyalı.....21
- Figure 9** Massive lavas, distributed among the flysch sediments.....24
- Figure 10** A dyke having a thickness of about 80 cm is intruding the lavas (Coordinates: N 41.01063- E033.31744) and a thinner dyke of about 30 cm is observed

in lavas at another outcrop nearby (Coordinates: N 41.01334- E033.31488).....	24
<b>Figure 11</b> Contact of massive lavas with deformed sediments of the flysch (Coordinates: N 41.01334- E033.31488).....	25
<b>Figure 12</b> Ellipsoidal pillow lavas of about 10-20 cm in diameter (Coordinates: N41.01063-E033.31744).....	26
<b>Figure 13</b> Carbonate minerals have formed in cracks together with clay minerals and veins in pillow lavas (Coordinates: N41.01063-E033.31744).....	27
<b>Figure 14</b> Amigdules and vesicles are abundantly observed on pillow lavas (Coordinates: N 41.01063-E033.31744).....	27
<b>Figure 15</b> General view of the pillow lavas and pillow-breccias exposed in an area of about 2 meters on the side of the road by the Boyalı Creek where the ellipsoidal structure is best seen (Coordinates: N 41.01063° E033.31744°).....	28
<b>Figure 16</b> Breccias with pillow fragments that partially retains their ellipsoidal shape.....	29
<b>Figure 17</b> General view of a dyke intruding the flysch sediments.....	30
<b>Figure 18</b> A nearly horizontal dyke overlain by blocky debris-flows (Coordinates: N 41.01401-E033.31441).....	30
<b>Figure 19</b> Several dykes are intruding flysh sediments at different dip angles.....	31
<b>Figure 20</b> Two dykes of approximately 55-60 cm are intruding the flysch at different dip angles; the thicker dyke is a horizontal dyke (Coordinates: N 41.01401- E033.31441).....	32
<b>Figure 21</b> The contact of a dyke with deformed flysch sediments and chilled margin (Coordinates: N41.02446-E033.30330).....	33
<b>Figure 22</b> Vesicles on the surface of a dyke (Coordinates: N41.02446-E033.30330)...	33
<b>Figure 23</b> Flow structure on dykes (Coordinates: N 41.01334- E033.31488).....	34
<b>Figure 24</b> Strike and dip values of dykes plotted on the rose diagram.....	35
<b>Figure 25</b> Stereographic projections of dykes with respective paleostress fields.....	36
<b>Figure 26</b> Plagioclase and clinopyroxene minerals are observed as microphenocryst phases in a groundmass composed mainly of plagioclase microlites and Fe-oxides. (XPL; Plg: plagioclase; cpx; clinopyroxene).....	39
<b>Figure 27</b> Alteration to clay minerals is clearly observed on a plagioclase phenocrystal. Amygdules are filled by prehnite and pumpellyite minerals in this sample which displays both amygdaloidal and intersertal texture with the presence of glass in the	

groundmass (XPL; Plg: plagioclase).....	41
<b>Figure 28</b> Highly altered plagioclase phenocrystals in clusters (XPL; Plag: Plagioclase).....	41
<b>Figure 29</b> A subhedral augite phenocryst exhibiting second order birefringence colors and traces of 90 degrees of cleavage.....	41
<b>Figure 30</b> Orthopyroxene phenocrystal distinguished by typical cleavage and first order birefringence colors. Alteration to clay products on cleavage traces is evident (XPL)..	42
<b>Figure 31</b> Plagioclase exhibiting sieve texture and poikilitic texture with clinopyroxene and Fe-oxide inclusions (XPL; Plag: Plagioclase; Cpx: Clinopyroxene).....	42
<b>Figure 32</b> Subhedral augite phenocrystal in a highly altered matrix of plagioclase laths and smaller augite crystals (XPL; Plag: Plagioclase).....	43
<b>Figure 33</b> Sector zoning and oscillatory zoning observed in an augite phenocrystals (XPL).....	43
<b>Figure 34</b> Twinning and zoning is commonly observed in clinopyroxenes as well as orthopyroxenes. Also, Fe inclusions are common in pyroxene phenocrystals differing in sizes (XPL).....	45
<b>Figure 35</b> Simple twinning observed in clinopyroxene phenocrystals (XPL).....	45
<b>Figure 36</b> Anheadral clinopyroxene which is zoned and altered in a matrix of plagioclase microlites and plagioclase microphenocrystals (XPL).....	45
<b>Figure 37</b> A volcanic rock fragment composed of plagioclase, orthopyroxene and clinopyroxene minerals; as well as Fe-oxide inclusions (XPL).....	46
<b>Figure 38</b> Volcanic rock fragment composed of plagioclase minerals of various sizes and Fe-oxides exhibiting high levels of alteration (XPL).....	46
<b>Figure 39</b> Volcanic rock fragment containing lesser amounts plagioclase minerals as phenocrystals and microphenocrystals and Fe-oxides (XPL).....	47
<b>Figure 40</b> Plagioclase microphenocrystals in a matrix of plagioclase microlites, Fe- oxides, glass and alteration minerals (XPL; Plag: Plagioclase).....	48
<b>Figure 41</b> Zoned plagioclase crystal which includes Fe-oxide inclusions has altered to clay minerals. Alteration, which is also evident in the oscillatory layers, is especially concentrated in the innermost zones of the crystals (XPL).....	49
<b>Figure 42</b> Subheadral plagioclase phenocrystals in a cluster which exhibits sieve texture and glomeroporphyritic texture (XPL).....	50
<b>Figure 43</b> Quenching seen on a plagioclase phenocrystal which partly preserves its	

crystal boundaries and form.....	50
<b>Figure 44</b> Clusters of highly altered plagioclase phenocrystals with oxidized zones in the center (XPL).....	51
<b>Figure 45</b> Microlites are oriented according to the flow direction. Amygdules filled by prehnite and pumpellyite minerals exhibit a similar kind of orientation as well (XPL).....	52
<b>Figure 46</b> Plagioclase microlites are randomly oriented in some of the andesite samples. The matrix is composed of plagioclase microlites, clinopyroxenes, Fe-oxides and silica (XPL).....	52
<b>Figure 47</b> Subhedral to anhedral hornblendes are seen as phenocrystals and microphenocrystals; as well as inclusions in plagioclase minerals. They have been oxidized especially on the boundaries and often include Fe-oxide minerals.....	53
<b>Figure 48</b> Biotite phenocrystals and microphenocrystals altered to Fe-Ti minerals (XPL).....	54
<b>Figure 49</b> Biotite phenocrystal containing plagioclase mineral and opaque inclusions (XPL).....	54
<b>Figure 50</b> Chalcedony has been formed in cracks in a sample which includes plenty of hornblende crystals of various sizes altered to varying degrees of Fe-Ti minerals (XPL).....	55
<b>Figure 51</b> Amygdules, elongated according to the flow direction are filled with carbonate minerals and pumpellyite (XPL).....	55
<b>Figure 52</b> Major and trace elements plotted against Zr.....	59
<b>Figure 53</b> MgO% vs SiO <sub>2</sub> % Harker diagram.....	67
<b>Figure 54</b> CaO% vs SiO <sub>2</sub> % variation diagram.....	67
<b>Figure 55</b> Fe <sub>2</sub> O <sub>3</sub> % vs SiO <sub>2</sub> % variation diagram.....	68
<b>Figure 56</b> Al <sub>2</sub> O <sub>3</sub> % vs SiO <sub>2</sub> % variation diagram.....	68
<b>Figure 57</b> K <sub>2</sub> O% vs SiO <sub>2</sub> % variation diagram.....	69
<b>Figure 58</b> MnO% vs SiO <sub>2</sub> % variation diagram.....	69
<b>Figure 59</b> Na <sub>2</sub> O% vs SiO <sub>2</sub> % variation diagram.....	70
<b>Figure 60</b> P <sub>2</sub> O <sub>5</sub> % vs. SiO <sub>2</sub> % variation diagram.....	70
<b>Figure 61</b> TiO <sub>2</sub> % vs. SiO <sub>2</sub> % variation diagram.....	71
<b>Figure 62</b> Cr <sub>2</sub> O <sub>3</sub> % vs. SiO <sub>2</sub> % variation diagram.....	71
<b>Figure 63</b> Primitive mantle-normalized trace element patterns of a) dyke samples b)	

lava samples (Normalized values are from Sun and McDonough, 1989).....	76
<b>Figure 64</b> Chondrite normalized REE patterns a) for dyke samples b) for lava samples (Normalized values are from Sun and McDonough, 1989).....	77
<b>Figure 65</b> Chemical Classification of the dykes and lavas of the Boyalı Volcanics on the basis of immobile elements (Winchester and Floyd, 1977).....	79
<b>Figure 66</b> Zr vs Ti diagram of the Boyalı dykes (blue) and lavas (red) after Pearce (1982).....	80
<b>Figure 67</b> Zr-Ti/100-Y*3 diagram (Pearce and Cann, 1973) of the Boyalı dykes (blue) and lavas (red).....	81
<b>Figure 68</b> Zr/Y-Ti/Y diagram of the Boyalı dykes and lavas after Pearce and Gale, 1977).....	81
<b>Figure 69</b> Ti/1000 vs. V diagram Shervais (1982).....	82
<b>Figure 70</b> Zr-Ti/100-Y*3 diagram of the Boyalı dykes(blue) in lavas(red) after Pearce and Cann (1973).....	83
<b>Figure 71</b> Evolution lines of the studied volcanic rocks in Th-Yb vs. Ta-Yb diagram.	84
<b>Figure 72</b> Chondrite-normalized REE patterns a) for dyke samples b) for lava samples (normalizing values are from Sun and McDonough (1989).....	85

## LIST OF TABLES

<b>Table 1</b> Major element analysis of the studied samples.....	65
<b>Table 2</b> Trace and rare earth element analysis of the studied samples.....	72

## CHAPTER 1

### INTRODUCTION

#### 1.1. Purpose and Scope

Rocks of Turkey bear evidence of several oceans which have opened and closed in geologic history; during Palaeozoic to Cenozoic. Repeated geological processes and rearrangement of micro-continents lead to a now very complicated structure; due to several geological entities having been brought next to each other by convergence and then pulled away again by opening of a new ocean. These oceans are collectively called “Tethys” and as stated by many authors (i.e. Şengör and Yılmaz, 1980) Tethyan evolution; can be studied in two main phases; Palaeo-Tethyan and Neo-Tethyan. So far, the evolution of these oceans have been studied by many authors; Şengör and Yılmaz, 1981; Yılmaz et al., 1995; 1997; Göncüoğlu et al., 1997; Okay and Tüysüz, 1999; Stampfli, 2000; Robertson and Ustaömer, 2004.

The Intra-Pontide Suture and the Izmir-Ankara-Erzincan Suture represent branches of Northern Neotethys; which is a Mesozoic ocean that has been subject to many studies by various authors (i.e. Şengör and Yılmaz, 1981; Göncüoğlu and Türel, 1993; Okay and Tüysüz, 1999; Elmas and Yiğitbaş, 2001) The Izmir-Ankara-Erzincan suture, located between the Sakarya Continent in the north and the Anatolide-Tauride platform in the south, opening and closure ages of which is determined as mid Triassic and Late Cretaceous, represents northern Neotethys (e.g. Göncüoğlu et al., 1997) .

Many contrasting ideas about the Northern branches of Neotethys exist, which indicate that there is still work to be done to clearly enlighten the discussed points about the Intra-Pontide Suture and the Izmir-Ankara-Erzincan Suture. Although the region is affected by the North Anatolian Fault which results in difficulties obtaining

original features (Göncüoğlu et al., 1997), more detailed studies can uncover the unknown or false-known.

Late Cretaceous-Paleocene volcanism has been a subject of debate regarding to the geology of Turkey. According to some authors active subduction of an oceanic lithosphere produced these volcanics (as well as associated plutonics) and they represent arc magmatism. Whereas, a post-collisional origin is proposed by many other authors (e.g. Harris et al, 1994; Kadioğlu and Dilek 2010; Altunkaynak and Dilek, 2013). In addition to previous studies in western and eastern Pontides (e.g. Temizel et al., 2007; Altunkaynak and Dilek, 2013) it is important to contribute to studies from a region where only limited research is present (e.g. Peccerillo and Taylor, 1976) with volcanics of Boyalı area, in Central Pontides region.

Araç-Boyalı flysch basin is located in Araç and Boyalı districts of Kastamonu, north-central Turkey. It is classified as a foreland basin formed following the closure of the Intra-Pontide Ocean during the Late Cretaceous-Middle Paleocene on the platform of the Sakarya Composite Terrane. This study aims to examine the volcanism in the Boyalı region which is exposed both as lavas and several dykes. The petrographic and geochemical characteristics of the samples taken from lavas and dykes in the region are aimed to be investigated in order to aid in interpretation of the magmatism in the region; its source and tectonomagmatic position; to approach the paleogeographic setting with new geologic findings. The orientation of dykes are aimed to be evaluated in order to make an approach to which tectonic events these volcanics are related to within the perspective of geologic evolution. The tectonic events in the region between Late Cretaceous-Middle Eocene are taken into consideration to find the relation between the dyke formation and Late-Cretaceous-Paleocene volcanism.

## **1.2. Geographic Setting**

Study place is located in Boyalı, a town in the Kastamonu city of Turkey, situated in the geographical coordinates 41°41'0"N and 34°14'0"E and is in the southwest of Kastamonu and in the northwest of Çankırı.

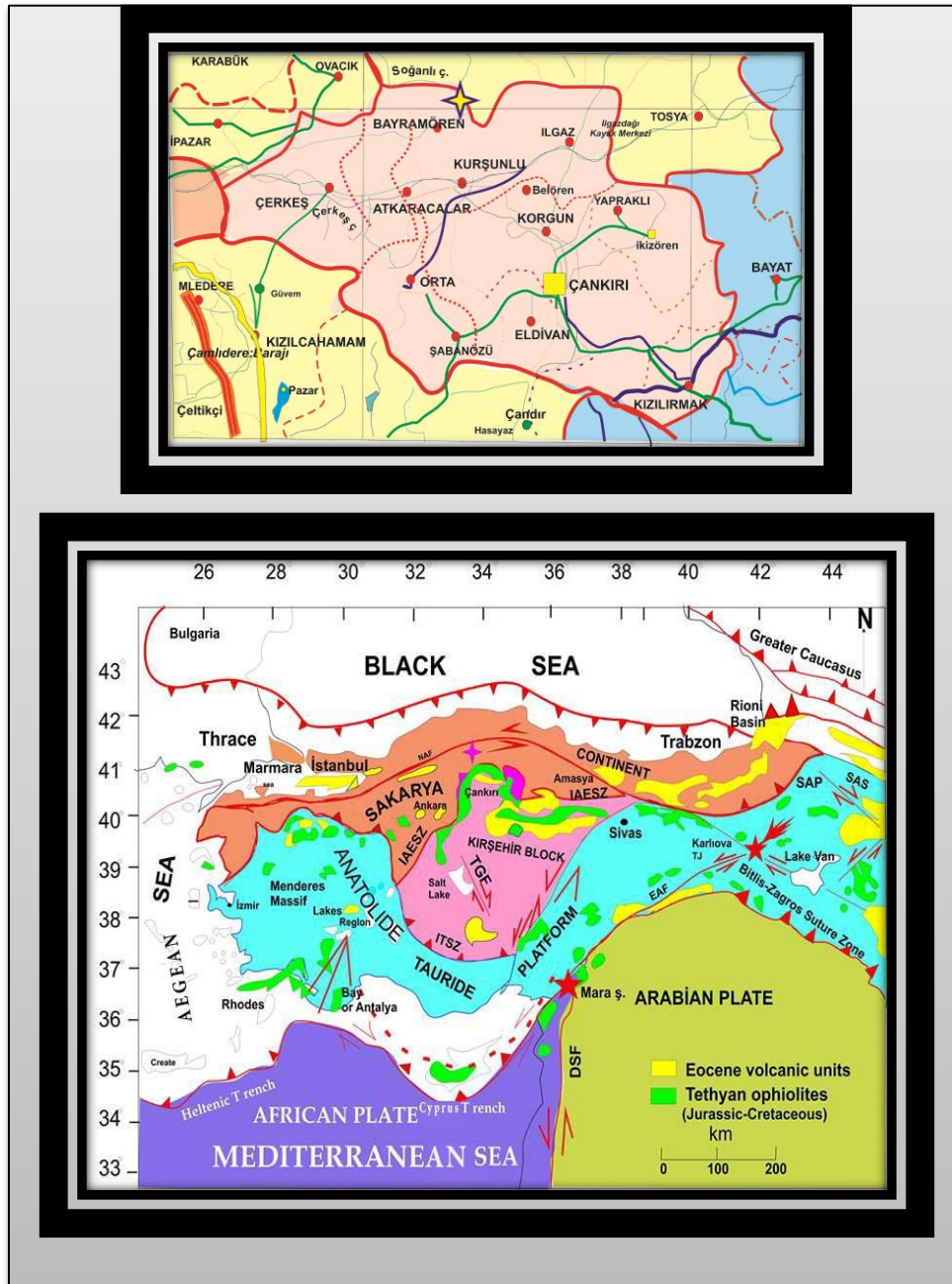


Figure 1. Location map of the study area shown on the simplified tectonic map of Anatolia and its surroundings showing the distribution of major plate boundaries, tectonic belts, Neotethyan ophiolites (Jurassic–Cretaceous), and Eocene volcanic units (Altunkaynak and Dilek, 2013).

### 1.3. Methods of Study

The methods used in this study are presented as follows:

### **1.3.1. Field Work**

During the summer of 2011, the field relations of dykes and lavas have been studied and approximately 30 samples have been collected. Samples were picked to make thin sections to examine under polarized microscope for petrographic determinations and to send appropriate ones to geochemical analysis. In autumn of 2012, in another field study strike and dip measurements were taken from the dykes in the basin.

### **1.3.2. Laboratory Work**

Several thin sections were prepared from the andesitic and basaltic lava and dyke samples collected in the field. Under the polarizing microscope these thin sections were studied to reveal their petrographic properties; identifying the mineral assemblages and textures, the relationships between them, as well as alteration products and comparing these properties observed in one sample, to the other; especially in efforts to find out if there is a relation between the lava samples and dyke samples; to aid in geochemical studies that will contribute to previous scientific discussions on the mechanisms that produced these volcanics.

10 selected samples from andesites and basalts were then sent to ACME Analytical Laboratories, Canada for geochemical analysis.

### **1.4. Previous Work**

A review of the previous studies regarding the Istanbul-Zonguldak terrane, Intra-Pontide suture, Sakarya Composite Terrane and Izmir-Ankara Erzincan suture (Figure 2) is given below, in terms of general characteristics of related units, together with controversial parts.

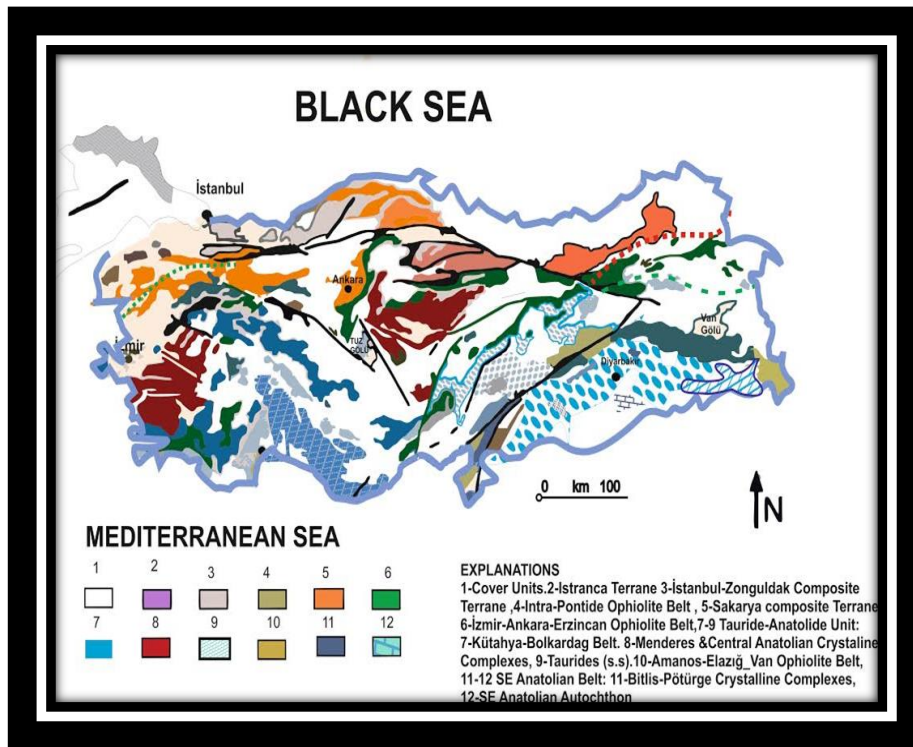


Figure 2. Terrane Map of Turkey (Göncüoğlu et al., 1997)

### 1.4.1. General Geology

#### 1.4.1.1. Istanbul-Zonguldak Terrane

Şengör et al (1981) first distinguished the “Istanbul Nappe”, the main bulk of which is made up of a fairly complete Palaeozoic succession known as the 'Palaeozoic of Istanbul', Cropping out in different localities beneath Mesozoic to Tertiary cover units, it forms a thin belt of 30 km wide and 200 km long. It is separated from the Sakarya Microcontinent to the south by the Intra-Pontide Suture Zone (Şengör and Yılmaz, 1981). The term “Istanbul Zone” was first used by Okay (1989) and “Istanbul Fragment” by Ustömer and Robertson (1993). The terrane was later termed “Istanbul-Zonguldak Unit” by Yiğitbaş and Elmas (1997).

Okay et al. (1994) explained how this terrane took its present-day position; as a result of investigation of the kinematic history of the opening of the Black Sea; revealing that one of two oceanic basins that constituted the Black Sea opened as a back-arc rift in the Cretaceous separating the Istanbul zone from the prent-day Odessa shelf; owing to the dextral Black Sea and the sinistral west Crimean transform faults; Istanbul

zone moved to the south of the Odessa shelf during the Late Cretaceous-Paleocene to finally collide in the early Eocene with a Cimmeride zone, to take its present-day position.

Istanbul Terrane was defined as a Peri-Gondwanan microplate that accreted to the Variscan Belt by the closure of the Rheic Ocean (Göncüoğlu et al., 1997; Yanev et al.2006).

Ustaömer and Robertson (1999) reported that the main exposures of the Palaeozoic of Istanbul are located in the Istanbul–Hereke, Çamdag, Bolu and Kastamonu areas and made up of ortho- and paragneisses, meta-gabbros, orthoamphibolites and amphibole-gneisses and oceanic basic igneous rocks intruded by arc-type granitoids. On top of this Cadomian-consolidated basement, a continued sequence of Early Ordovician-Late Carboniferous age is deposited.

Yanev et al (2006) pointed out that the overlying Paleozoic succession, represents a passive continental margin deposition from Early Ordovician to Early Devonian and is conformably overlain by Middle Devonian to lowermost Carboniferous slope-type sediments and flysch-type sediments of Viséan age. Continental clastics of Early Triassic age and an Alpine-type sequence of Triassic age unconformably overly this succession that is affected by Variscan deformation (Göncüoğlu et al., 1997).

As indicated by Göncüoğlu et. al (1997) and Yiğitbaş et al. (2004), slivers of an intra-oceanic island-arc, oceanic and continental crust were recognized in the unit, Cadomian- related accretion time of which is stated as the Late Neoproterozoic.

On the other hand, Zonguldak terrane has a common basement with the Istanbul Terrane with Pre-Cambrian granitoids (Chen et al, 2002). Late Silurian and the Early Devonian succession are separated by a distinct unconformity, which is interpreted as a Caledonian event by Göncüoğlu and Kozur (1998). Shelf-type carbonates and non-marine coal bearing units of Carboniferous age comprise the Middle Devonian and Early Carboniferous succession. Termed as a Permo-Triassic molasse-type deposition; continental clastics of middle Permian to Scythian age have unconformably deposited over the Paleozoic sequence (Yılmaz and Boztuğ, 1986; Göncüoğlu et al., 1997).

Alpine cover sequences overly a fault-controlled basement where basins of Mid Jurassic to Early Cretaceous age have formed (Göncüoğlu et al., 1997).

#### **1.4.1.2. Intra-Pontide Suture**

Being one of the two main Tethyan sutures of Turkey; Intra-Pontide suture remarks the subduction of one of the northern branch of Tethyan oceanic lithosphere, followed by continental collisions. Controversial ideas about the paleogeographic setting, opening and closure ages and evolution of this ocean together with its subduction polarity have been discussed by several authors. Furthermore, its presence has been questioned by some. (e.g., Kaya and Kozur, 1987; Elmas and Yigitbas, 2001; Robertson et al., 2004).

Şengör and Yılmaz (1981) denoted the stratigraphic, metamorphic and magmatic break in the boundary between Istanbul and Sakarya terranes as the Intra-Pontide suture.

Şengör et al. (1984) suggested that the northern branch of Neotethys constituted two oceans; Intra-Pontide Ocean between the Rhodope-Pontide and the Sakarya terranes and Izmir-Ankara-Erzincan Ocean between Sakarya and Tauride-Anatolide terranes.

Different scenarios about this controversial ocean that still keeps some of its mysteries can be summarized as below:

Some authors (Robertson and Dixon, 1984; Dercourt et al., 1986; Ustaömer and Robertson, 1997, 1999; Stampfli, 2000) interpreted the geologic data indicating remains of an ocean in the region as a Palaeotethyan ocean of Late Palaeozoic–Early Mesozoic age was subducted northwards beneath Eurasia during Early Mesozoic time.

According to some other authors (Şengör and Yılmaz 1981), within the Western Pontides and adjacent area along the southern margin of Eurasia, the ocean in question could not be called Palaeotethys and it is a different oceanic basin called the Intra-Pontide ocean, which had a life-span of Early Jurassic to Late Cretaceous–Early Tertiary. Its palaeo-tectonic setting together with the timing of events have been a

subject of discussion in many studies by different authors. (Yılmaz, 1990; Yılmaz et al., 1997; Göncüoğlu et al., 1987, 1992).

Elmas and Yiğitbaş (2001) proposed that only a single Northerly Neotethys was present and interpreted the presence of any late Mesozoic ophiolites in the Western Pontides as having been introduced by left-lateral strike-slip during Late Cretaceous time.

On the other hand, another contradictory approach was suggested by some authors (e.g. Kaya and Kozur, 1987) which suggests that a Neotethyan oceanic basin has never existed in the region.

#### **1.4.1.3. Sakarya Composite Terrane**

It is a 100-200km wide east-west trending belt covering almost the entire northern Anatolia. As explained in Altıner et al. (1991) it extends from the Biga Peninsula in the west to the Eastern Pontides in the east. The sedimentary sequence starts with Lower Jurassic sandstones, which rest on a complex basement; Göncüoğlu et al. (1997) defined this basement as containing pre-Alpine terranes and considered this terrane as a composite terrane due to its several different tectonic assemblage content; such as Variscan and Cimmerian continental and oceanic assemblages. Variscan massifs and the Cimmerian Karakaya Complex with Küre-Yusufeli ophiolites comprise the pre-Jurassic basement of the Sakarya Composite Terrane. The lower part of the overstep sequence was determined as Early Jurassic in age, followed by Jurassic-Cretaceous platform sediments. These are followed by slope-type sediments beginning from Late Cretaceous, and covered by flysch-type deposits with ophiolitic blocks pertaining to Intra-Pontide Ocean.

The crystalline basement of the Sakarya Composite Terrane, which can be divided in 3 parts, has been explained by various authors:

According to studies of various authors (Topuz et al., 2004; Okay et al., 2006; Nzegge and Satır, 2007) a high-grade Variscan metamorphic sequence of gneiss, amphibolites, marble and scarce metaperidotite, is dated to the Carboniferous by zircon and monazite ages from Pular, Kazdağ, Devrekani and Gümüşhane massifs (Okay et al.

2008). Ketin (1951) revealed that in the Pulur region, easternmost part of the Sakarya Zone, a unit of Upper Carboniferous molasse overlies the Variscan basement.

Small outcrops of Palaeozoic granitoids (Delaloye and Bingöl, 2000; Okay et al. 2002, 2006) are scattered throughout the Sakarya terrane and are unconformably overlain by Jurassic and younger sediments (Okay et al., 2008).

A Permo-Triassic subduction-accretion complex with Late Triassic blueschists and eclogites (Okay and Monié, 1997; Okay and et al., 2002) accreted to the margin of Laurussia during the Late Permian to Triassic; which is a low-grade metamorphic complex, called the lower Karakaya Complex (Okay et al., 2008).

Concerning the boundary between the Istanbul and Sakarya terranes, the area between the northern and southern branch of the North Anatolian Fault, is a tectonic zone called the Armutlu Ovacık Zone, which has been discussed by many authors (Yılmaz et al., 1995; Yiğitbaş et al., 1999; Elmas and Yiğitbaş, 2001; Robertson and Ustaömer, 2004). As stated by Akartuna (1968) and Göncüoğlu and Erendil (1990) this zone is made up of different types of metamorphic rocks and mélanges overlain unconformably by Eocene volcanic and sedimentary rocks.

#### **1.4.1.4. Izmir-Ankara-Erzincan Suture**

Izmir-Ankara-Erzincan suture, located between the Sakarya Continent in the north and the Anatolide-Tauride platform in the south, is one of the two major E-W trending ophiolite belts together with southern Neotethys (Southeast Anatolian Suture). Having once separated Laurussia and Gondwana, it represents northern Neotethys and holds information related to the elimination of this ocean (Okay and Tüysüz 1999; Bozkurt et al., 2000).

Assemblages of the Izmir-Ankara-Ocean were emplaced southward onto the Tauride-Anatolide Platform during Late Cretaceous. The North Anatolian Ophiolite Belt (NAOB) represents these assemblages. In Northwest, Anatolia units of Sakarya Composite Terrane tectonically overlie the ophiolites, whereas the ophiolites are thrust onto Tertiary basins in Central and East Anatolia. Huge bodies of almost complete supra-subduction zone-type ophiolitic sequences and tectonic mélanges of

the accretionary complex comprise NAOB (Göncüoğlu and Türeli, 1993; Göncüoğlu et al, 1997).

Eastwards continuation of Izmir-Ankara-Erzincan suture, which is segmenting having several loops, is extending further from the border with Georgia to the Lesser Caucasus, whereas in the west, across the Aegean Sea to the Vardar suture (Okay and Tüysüz, 1999).

Opening of this ocean is determined as mid Triassic, obtained from pelagic limestones and radiolarites associated with pillow-lavas in the mélangé (Göncüoğlu et al., 2001).

Closure of the Izmir-Ankara-Erzincan Ocean occurred with a subduction beneath the Sakarya continent in the north at the end of Cretaceous, which resulted in a marginal arc (Late Mesozoic-Tertiary Pontide Magmatic Arc) (Bektaş, 1987; Göncüoğlu et al. 1997).

Liassic epoch was considered to be one of the tectonically very active geologic periods of time according to Şengör and Yılmaz (1981); in Liassic, Cimmer continent experienced continuous destruction, Paleotethys continued closing; whereas on the south of this ocean; another ocean began to open as a peripheral basin and this is how Anatolide –Tauride Platform was shaped.

Görür et al (1983) made a study to provide sedimentological evidence for the opening of the northern branch of Neotethys in the Pontides. According to this study; the age of rifting and associated block faulting began along the southern border of the Pontides which lead to the opening of the northern branch of Neo - Tethys was suggested as the beginning or just before the Sinemurian.

Okay (1989) states that Izmir-Ankara-Erzincan suture refers to a Northern Neotethys ocean which existed between Sakarya terrane and Anatolide-Tauride platform. Most of the ophiolites found in the Anatolide-Tauride platform were attributed to the Izmir-Ankara-Erzincan suture.

Arguments about the age of opening suggested by Görür et al (1983), stating that Izmir-Ankara-Erzincan suture abruptly truncates the metamorphic Karakaya Complex along the whole length of the suture and no Karakaya Complex equivalents are known south of the suture. The absence of these units, could only be explained with immense

lateral movement across the suture in order to fit a Liassic opening scenario and the Triassic pelagic sediment and basic volcanic content of upper level nappes in the Taurides is indicative of presence of a continental margin during the Triassic to the north of Anatolide-Tauride platform.

The age of closure of the Izmir-Ankara-Erzincan Ocean has also been debated. According to Şengör and Yılmaz (1981) Anatolide Tauride Platform and the Pontides collided in Late Paleocene-Early Eocene. On the otherside Okay (1989) proposed a Late Cretaceous age for this collision based on investigation of blueschists in northwest Turkey. Another view is that, the collision might have been diachronous; therefore giving different ages for northwest Turkey where it started and for eastern Sakarya Zone as it was progressing; supported by island arc volcanism evidences that was found to have continued until Eocene, as stated by Okay (1989). However, later, by several authors (Göncüoğlu and Türelî 1993; Yalınız et al. 1996; Floyd et al. 1998) it was revealed that Izmir-Ankara segment of the northern Neo-tethyan Ocean closed during early Late Cretaceous time, along a north dipping intra-oceanic subduction zone.



## CHAPTER 2

### GEOLOGY OF THE STUDY AREA

#### 2.1. Regional Geology

Sakarya Composite Terrane, comprises a complex basement with units of continental and oceanic assemblages resulting from Variscan and Cimmerian orogeny; pre-Jurassic metamorphic and granites and the Karakaya tectonostratigraphic unit of Triassic age onto which an overstep sequence starting from Early Jurassic in age has deposited (e.g. Altner et al., 1991; Göncüoğlu et al., 1997). These are continental to shallow marine clastic rocks, overlying the tectonic structures (Yiğitbaş et al, 1999) which formed as a result of collision of Laurasia and Gondwana at that time, closing the Paleotethys ocean subduction accretion units of which are represented by the Karakaya Complex (Şengör et al., 1984; Göncüoğlu et al., 2000; Sayit et al., 2011). A detailed stratigraphic study of Rosso Ammonitico bearing Jurassic-Lower Cretaceous successions of the southern part of the North Western Anatolia, found as scattered outcrops in Edremit-Balya, Bursa, Bilecik, Mudurnu-Nallıhan-Beyazır, Aktaş-Çerkeş regions by Altner et al. (1991) reveals a continuous succession of the Upper-Triassic to Lower Cretaceous sedimentary rocks, overlying the remaining of the Karakaya orogeny, starting from clastics (e.g. Hettangian conglomerates and coarse sandstones) and followed upwards, unconformably giving way to carbonate deposition, is accompanied by tuffaceous volcanism. Carbonate deposition also continues in Lower Cretaceous, whereas in Upper Cretaceous clastics and volcanic levels take over. This succession displays local changes due to subsidence and uplift of different areas of North Western Anatolia at different times. In the Upper Cretaceous, as Saner (1980) stated; sandstone-shale alternation that includes lava

lenses at some localities in the region, and absence of volcanic activity, lenses of limestone at others. An overall deepening of the sea resulted in subsidence of the area as a whole, giving way to flysch deposition in Mid Upper Cretaceous, which continued to be laid down as long as the deepening of the basin continued. At the end of Upper Cretaceous, tectonic control over deposition, regression of the sea from south to north is evident, resulting in pelagic and shaley deposition in the north; as well as local sliding of limestones towards north as olistoliths and turbidite formation, as the sea bottom was elevated. On top of the slope-type sediments from Upper Cretaceous and onward, an unconformable unit; Albian-Cenomanian pelagic limestones showing a transition to turbidite deposits is observed. These turbidite deposits, ranging in age from Late Cretaceous to Paleocene, are reported as Taraklı Flysch, they represent the top of the Sakarya Terrane (Catanzariti et al., 2013). These flysch-type deposits include ophiolitic blocks, derived from the northerly Intra-Pontide Ocean (Göncüoğlu et al, 1997). Onto this unit, tectonic units of Istanbul-Zonguldak Terrane and the Intra-Pontide suture zone are thrust over (Catanzariti et al., 2013).

In the Paleocene sea, clastics were deposited at delta environments, and in other parts that were not affected by deltas, limestone deposition is observed. Eocene marks a time of new transgression, which gave way to molasse type deposits. A generalized columnar section (Figure 3) based on the study of Altner et al. (1991) and Saner (1980) was presented by Göncüoğlu et al (1997).

Along the geotraverse Kursunlu-Araç, the ophiolite units, the Arkotdag Melange, the High-Grade Metamorphic Unit and the Low-Grade Metamorphic unit were observed as an imbricate stack, which was thought to have occurred as a result of multiple thrustings that brought oceanic and continental units together. These units tectonically overly Sakarya Terrane and are overlain by the Istanbul-Zonguldak Terrane. On top of the rock units of the Intra-Pontide Suture zone area, sedimentary deposits of Early Eocene were deposited. North-Anatolian Fault Zone, has affected this area with strike-slip tectonics and caused modification of the original relationships of the rock units of the Intra-Pontide zone.

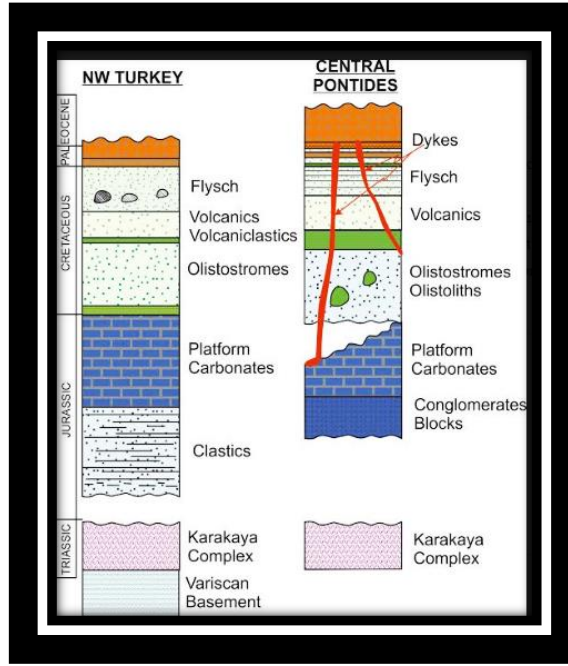


Figure 3. Generalized columnar section of the Sakarya Composite Terrane's cover in NW Anatolia (Saner, 1980; Altiner et al., 1991; Göncüoğlu et al., 1997).

## 2.2. Local Geology

### 2.2.1. Taraklı Flysch

Boyalı area is a locality where it is possible to observe the deposits at the top of the Sakarya Terrane; relations of Istanbul-Zonguldak and Sakarya terranes, and the Intra-Pontide suture that formed due to the convergence between them during Late Cretaceous to Early Tertiary; therefore it is important in terms of holding information useful for a paleogeographic reconstruction (Catanzariti et al., 2013). The succession at the top, that represents the sedimentary cover of the Sakarya Terrane are termed the Taraklı Flysch, onto which tectonic units of Istanbul-Zonguldak Terrane and the Intra-Pontide suture zone are thrust over (Saner 1977; Catanzariti et al., 2013). In the area, Taraklı Flysch is observed as an east-west-trending strip to the north of Kurşunlu and Ilgaz and along the Akçay and Boyalıçay valleys between the Aylı mountain in the north and Gürgenli and Köklüce Mountains in the south. Stratigraphic,

paleontological and structural study of these units is of great importance as a guide to more precise reconstruction of the Intra-Pontide suture (Catanzariti et al., 2013).

At the base of Sakarya continent, as summarized in Elmas and Yiğitbaş. (2001), different metamorphic units with tectonic contacts are found (Yılmaz 1981; Yılmaz et al., 1995). On top of this, Liassic deposits, composed dominantly of clastics, which shows lateral facies changes including Ammonitico-rosso facies rocks and is transitional to shallow sea clastics, have deposited as a result of transgression, in a horst-graben system controlled by active tectonics (Görür et al.,1983). This unit is overlain by a sequence of oolitic and clastic limestones at the base, pink-white micritic limestone of Jurassic age at upper levels, called as the Bilecik formation (e.g. Saner, 1977; Yılmaz, 1981; 1990; Yılmaz et al., 1990; 1995; Altiner et al., 1991). Jurassic neritic limestones laterally and vertically are transitional to white, thin bedded, cherty limestones named as Soğukçam formation (which crops out in the Bayramören region, south of Boyalı; Fig. 7). Soğukçam limestone is observed as a highly deformed unit, folded in many localities in the region and is characterized by medium-bedded bioclastic levels containing microfossils. Several planctonic and bentic microfossils were determined by Altiner et al. (1991); and it is accepted as Callovian-Aptian of age. It also includes radiolarian chert blocks. Unit was deposited in slope/basin environment. On top of these, pelagic limestones, radiolarite and mudstones, Cenomanian-Turonian of age called as Vezirhan formation were deposited. The Taraklı Flysch is an Upper Cretaceous-Lower Tertiary succession unconformably overlying a complex of metamorphic rocks and granitoids, Permian limestones, Karakaya-type sedimentary and volcano-sedimentary successions and their Liassic cover as indicated by Saner (1977) for Gölpazarı Group that has fast facies changes, in Geyve region, NW Anatolia.

As defined by Saner (1980) (under the name of Yenipazar formation) the depositional sequence in flysch facies is a sandstone-shale alternation containing volcanics. An extended definition of Yenipazar formation was used by Sevin and Aksay (2002). According to this definition, the unit composed of grayish green colored, fine to medium bedded sandstone-shale alternation and green and brown colored volcanics, green colored marl and white, beige, red and pink colored thin bedded micritic (pelagic –semi pelagic) limestone and minor amounts of conglomerate, showing

gradual transition to Soğukçam formation that it overlies, whereas having also local tectonic contacts. This represents Vezirhan formation and Gölpazarı group of Saner (1980), upper half of Hamamboğazı formation and Yenipazar formation of Göncüoğlu et al. (2001), Vezirhan and Yenipazar formations of Altıner et al.(1991). Yenipazar formation is accepted as Albian-Paleocene, because it was cut by Meyildere volcanics of Upper Paleocene-Lower Eocene of age. Unit was deposited in slope/basin environment and ended deposition in shelf environment (Sevin and Aksay, 2002).

Thickening and coarsening feature demonstrated by a transition from thin bedded turbidites to medium grained arenites and calcareous coarse-grained turbidite lithofacies ending with a level of slide-block in shaly matrix lithofacies is interpreted as a fast catastrophic event predating the closure and deformation of the basin, which is considered typical of syntectonic sedimentation in a foredeep environment (Catanzariti et al., 2013)

Within the clastic rocks, arenites that range from quartz-poor mixed type to calcilithites contain rock fragments that are determined to be granitoids, in rare amounts metamorphic rocks such as gneisses, metaquartzites, fine-grained schists and mica-schists, and widespread intra- and extra-basinal carbonate rocks. Intrabasinal carbonate fragments in the calcareous coarse grained turbidites indicate that a carbonate platform of the same age supplied material to the arenites, whereas carbonate platform derived rocks of Jurassic-Early Cretaceous age are the source of carbonate extrabasinal fragments. On the other hand, arenites do not have any rock fragments derived from ophiolites. Considering the lithic fragments in the arenites debris that are indicative of a continental margin and the composition of the main slide-blocks in the uppermost part of the succession, Istanbul-Zonguldak Terrane was thought to be the most probable source area of the Taraklı Flysch. Calcareous nanofossils revealed an Early Maastrichtian age for the lowermost level of the flysch in the area; whereas for the uppermost part was formed in Middle Paleocene age (Catanzariti et al., 2013). A geological map of the study area is presented below (Figure 4):

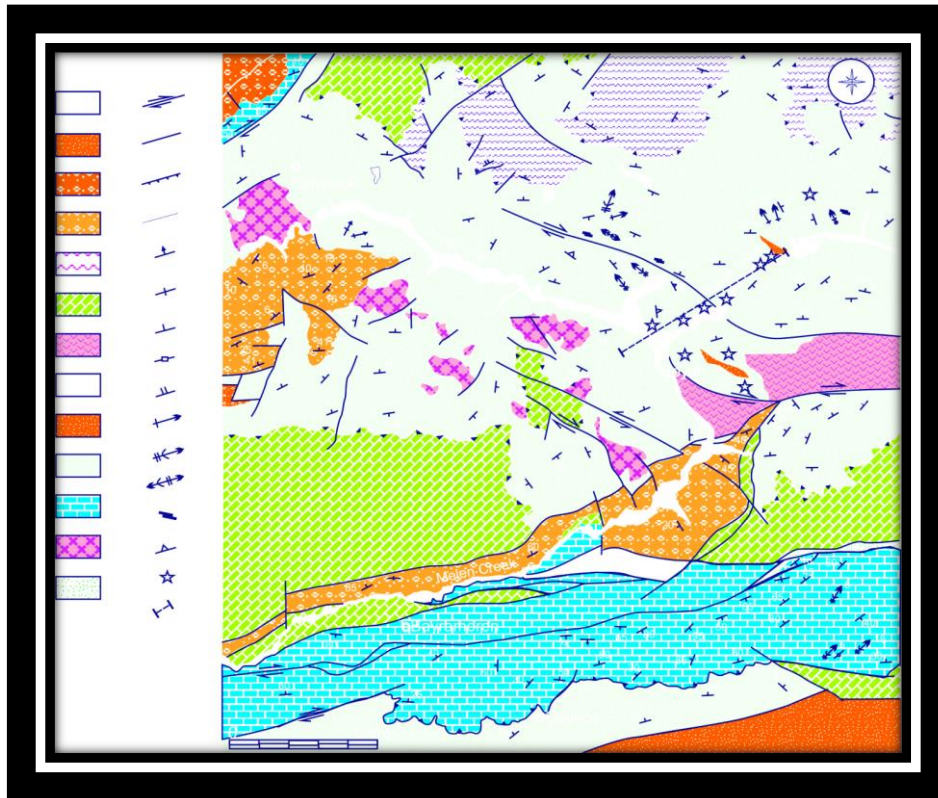


Figure 4. Geological map of the study area (Catanzariti et al., 2013) 1) Alluvial deposits; 2) Pliocene deposits; 3) Middle Eocene deposits; 4) Lower Eocene deposits; 5) Low-Grade Metamorphic Unit; 6) Arkotdag Mèlange; 7) Basalts; 8) Taraklı Flysch, slide-block in shaly-matrix; 9) Taraklı Flysch, orthoconglomerates; 10) Taraklı Flysch, thin-bedded turbidites; 11) Jurassic-Cretaceous limestones; 12) Granites; 13) Cataclastic zones; 14) Main strike-slip faults; 15) Main faults; 16) Thrust faults; 17) Stratigraphic boundaries; 18) Bedding; 19) Vertical bedding; 20) S1 foliation; 21) Vertical S1; 22) S2 foliation, 23) A1 fold axes; 24) A2 fold axes with vergence; 25) Horizontal A2 fold axes; 26) High-angle strike-slip faults; 27) Low-angle thrust faults; 28) Approximate locations of the dyke and lava samples 29) Trace of the geological cross-section. B) Geological cross-section..

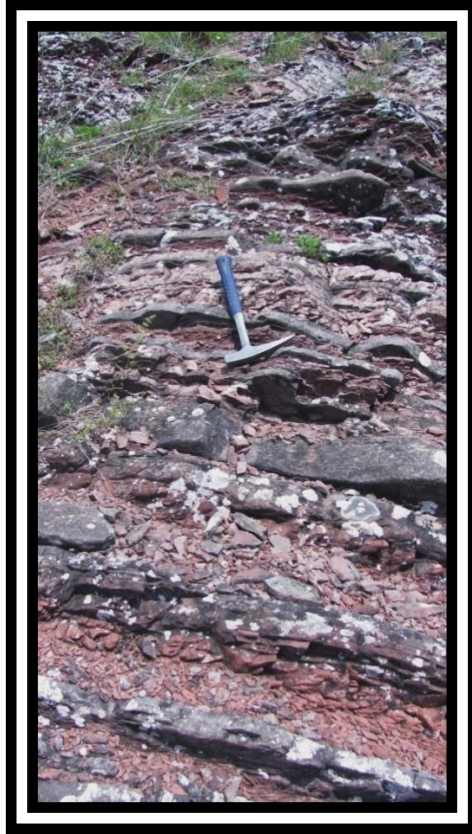


Figure 5. Thin-bedded turbidites of the Taraklı Flysch observed along the Boyalı Creek.

Medium part of the Taraklı Flysch contains dam-thick level of well-rounded clast- to matrix-supported conglomerates (Figure 6). The pebbles were found to be granite-dominated of composition, and they were thought to have derived from high density erosive flows connected to a coarse-grained river delta system (Catanzariti et al., 2013).

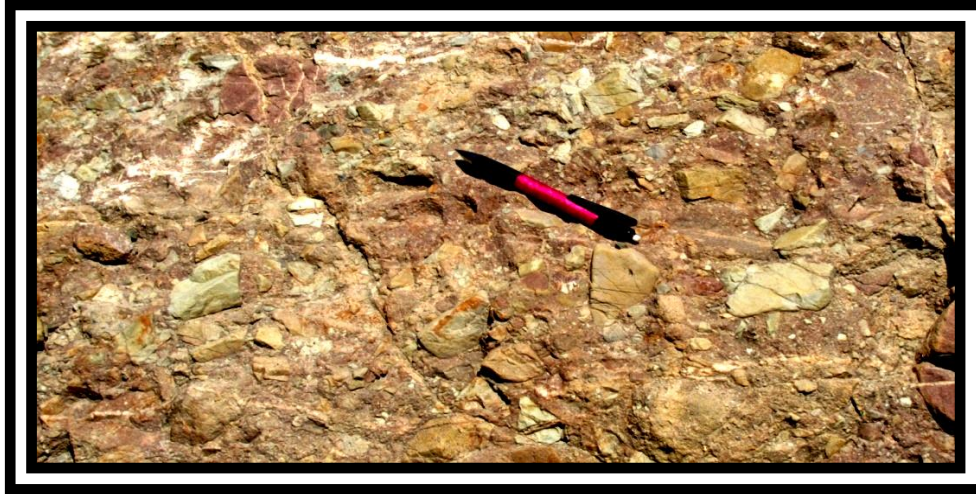


Figure 6. Conglomerates of the Taraklı Flysch in the southeast of Boyalı.

Clast-supported orthoconglomerates to coarse arenites compose the calcareous coarse-grained turbidites lithofacies, which were mainly derived from debris flows and high density turbidity currents. The debris is characterized by a quasi-monomict composition, indicating extra-basinal carbonatic clasts (Catanzariti et al., 2013).

Several slide blocks (Figure 10) have been observed in the upper part of the succession, surrounded by a fine grained matrix. Catanzariti et al. (2013) indicates that these slide blocks are mainly granitoids, orthogneisses, metagabbros/amphibolites, Jurassic carbonatic turbidites next to Ordovician quartz arenites, black shales, crinoidal and brachiopod-bearing Devonian-Carboniferous limestones and probably Triassic red quartz arenites (Figure 7 and 8); and they typically represent Istanbul-Zonguldak Terrane; are therefore important for the reconstruction of the region.



Figure 7. Slide-block of a recrystallized limestone in a fine-grained matrix in the south of Boyalı.



Figure 8. Slide-block of Triassic red quartz-arenites next to Devonian-Carboniferous limestones in the southeast of Boyalı.

Detailed study of the succession revealed important implications for the paleotectonic setting. Clear thickening and coarsening feature (thin bedded turbidites to medium grained arenites and calcareous coarse-grained turbidite lithofacies ending with a level

of slide-block in shaly-matrix lithofacies) was considered as the fast catastrophic event that predates the closure of the basin and its deformation by Catanzariti et al. (2013). This evolution is typical of syn-tectonic sedimentation in a foredeep environment.

Petrographically, arenites range from quartz-poor mixed arenites up to calcilithites. Mono- and polycrystalline quartz and feldspar make up the extra-basinal siliciclastic framework. Rock fragments are determined to be commonly granitoids, whereas metamorphic rock fragments such as gneisses, metaquartzites, fine-grained schists and mica-schists are found too, in rare amounts. The intra- and extra-basinal carbonate fragments are present in all samples. Carbonate platform derived rocks of Jurassic-Early Cretaceous age are the source of carbonate extra-basinal fragments. Intra-basinal carbonate fragments in the calcareous coarse grained turbidites indicate that a carbonate platform of the same age supplied material to the arenites. On the other hand, arenites do not have any rock fragments derived from ophiolites. As a result, a continental basement is proposed for the source area of these sediments, which include granitoids, metamorphic rocks, felsic volcanic rocks and the relative sedimentary covers, represented by extra-basinal non coeval carbonate rock successions. All together, these are indicative of a continental margin. Consequently, considering the lithic fragments in the arenites debris and the composition of the main slide-blocks in the uppermost part of the succession, Istanbul-Zonguldak Terrane was thought to be the most probable source area of the Taraklı Flysch.

To identify the age of the Taraklı flysch, calcareous nannofossils were used, which revealed an Early Maastrichtian age for the lowermost level of the studied succession; whereas for its top, a Middle Paleocene age was proposed (Catanzariti et al., 2013).

As a result of a detailed study of the deformation pattern, Catanzariti et al. (2013) mentioned that two main deformation phases were identified, one of the which was found to have occurred due to emplacement of the Istanbul-Zonguldak Terrane with the ophiolites of the Intra-Pontide Suture and *mélange* at its base over the Taraklı Flysch. Based on the youngest deposits involved in the deformation, the age of this phase was estimated between Middle Paleocene and Early Eocene.

Structures of the second phase can be regarded as related to the flower structures developed due to North Anatolian Fault Zone tectonics. Miocene age was estimated for this phase, based on studies of the inception of the North Anatolian Fault Zone (e.g. Bozkurt, 2001).

### **2.2.2. Boyalı Unit**

The Late Cretaceous-Early Tertiary volcanic activity that forms a parallel belt to the Eocene volcanics in the Pontic chain, consisting of andesitic lavas, tufts and agglomerates interbedded with neritic calcareous sediments and marly and arenaceous flysch; and occurs as a volcano-sedimentary complex, as mentioned by Peccerillo and Taylor (1976) who did a study on outcrops lying E-W between Kastamonu and Araç. According to their study, the relationship between volcanics and Eocene flysch is clear and that in the area andesitic lavas, tufts, agglomerates and breccias occur.

Boyalı, a district of Kastamonu, located on the south of Araç is a critical locality where Late Cretaceous-Early Tertiary volcanism is observed in Kastamonu area. In the basin, large number of andesitic dykes are found as intruding the deformed flysch sediments and olistolites; whereas the volcanism is also expressed as massive and pillow lavas as well which can easily be noticed among the basin sediments, together with pillow breccias. Field observations on the volcanic rocks in Boyalı area are given as follows:

#### **2.2.2.1. Lavas**

In Boyalı, lava flows can be observed in different forms; pillow lavas, massive lavas that reach 50 m in thickness and pillow breccias (Figure 9), which are intruded by several dykes (Figure 9, 10 and 11). They are distributed among the flysch sediments approximately 5 km to the north following the Boyalı Creek line and more or less the same distance to the south of the Boyalı Village. The road to the village offers a great sight to lava occurrences to be easily detected.

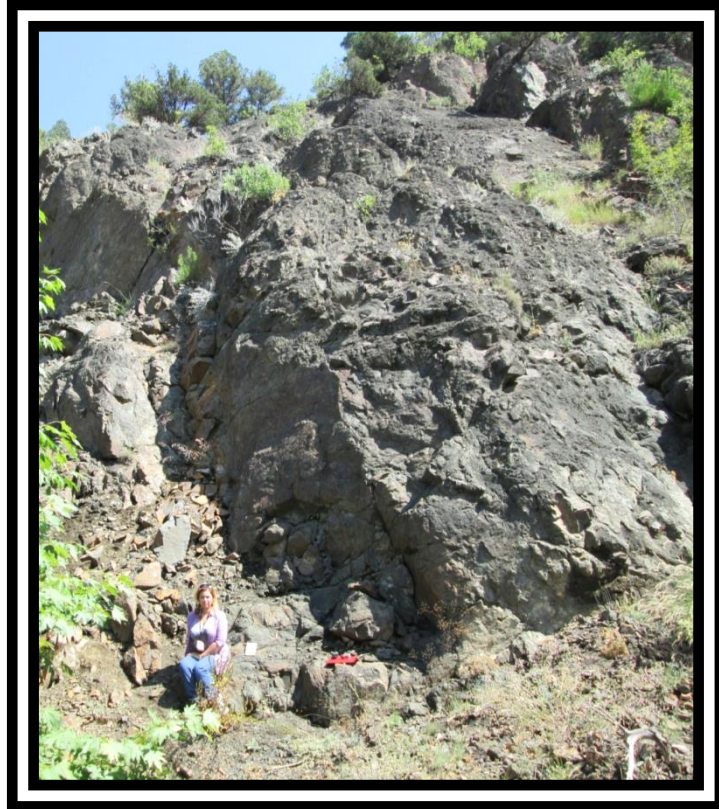


Figure 9. Massive lavas, distributed among the flysch sediments.



Figure 10. A dyke having a thickness of about 80 cm is intruding the lavas (Coordinates: N 41.01063- E033.31744) and a thinner dyke of about 30 cm is observed in lavas at another outcrop nearby (Coordinates: N 41.01334- E033.31488).

Lavas in the basin are observed as interbedded with the marly, arenaceous flysch (Figure 5).



Figure 11. Contact of massive lavas with deformed sediments of the flysch  
(Coordinates: N 41.01334- E033.31488).

Pillow lavas are easily detectable by their ellipsoidal structures (Figure 12). They offer a dark grey, altered surface they are around 30 cm in diameter, whereas some are elongated and usually as long as 50 cm (Figure 7). Alteration products such as carbonates and palagonite can be seen in figures 13 and 14 and 15. Vesicles and amigdules filled with carbonates are widespread among them (Figure 13).



Figure 12. Ellipsoidal pillow lavas of about 10-20 cm in diameter (Coordinates: N41.01063-E033.31744).



Figure 13. Carbonate minerals have formed in cracks together with clay minerals and veins in pillow lavas (Coordinates: N41.01063-E033.31744).



Figure 14. Amygdules and vesicles are abundantly observed on pillow lavas (Coordinates: N 41.01063-E033.31744).

Pillow lavas formed as a result of submarine volcanism, in contact with water and they accumulated just like the olistostromes observed in the region, by submarine gravity sliding.



Figure 15. General view of the pillow lavas and pillow-breccias exposed in an area of about 2 meters on the side of the road by the Boyalı Creek where the ellipsoidal structure is best seen (Coordinates: N 41.01063° E033.31744°).

Lava breccias are identified by fragmented appearance; the angular volcanic fragments they contain, that range between 2-10 cm in size and formed by transportation of loose volcanic material by gravity.



Figure 16 . Breccias with pillow fragments that partially retains their ellipsoidal shape.

#### **2.2.2.2. Dykes**

##### **2.2.2.2.1. Field Observations**

Several dykes are observed approximately 5 km to the north following the Boyalı Creek line and more or less the same distance to the south of the Boyalı Village. They have a large range in thickness; while some of them are really thin; about 30 cm, there are some that reach 260 cm in thickness. Their inclination also varies; they are observed as intruding the flysch sediments, as well as the olistoliths in different angles (Figure 17, 18, 19 and 20). Some of them being nearly horizontal (Figure 17), while dip angle of others differ in a great range (Figure 18). They are covered by volcano-sedimentary rocks of Mid-Eocene age.



Figure 17. General view of a dike intruding the flysch sediments.



Figure 18. A nearly horizontal dyke overlain by blocky debris-flows (Coordinates: N 41.01401-E033.31441).



Figure 19. Several dykes are intruding flysch sediments at different dip angles.



Figure 20. Two dykes of approximately 55-60 cm are intruding the flysch at different dip angles; the thicker dyke is a horizontal dyke (Coordinates: N 41.01401-E033.31441).

A distinctive feature observed on most of the dikes; especially the wider ones, is a fine grained texture at the contact zones with Taraklı flysch; in other words chilled margins where the melt crystallized rapidly (Figure 21).

Another characteristic common in Boyalı dikes is vesicular structure. On the altered outcrops of the dykes, abundant vesicles are observed (Figure 22).

Flow structures, giving the rock a porphyritic character as well, is another commonly observed structure that strike to the eye by subparallel arrangements of lath-shaped plagioclase phenocrystals (Figure 23).



Figure 21. The contact of a dyke with deformed flysch sediments and chilled margin  
(Coordinates: N41.02446-E033.30330).



Figure 22. Vesicles on the surface of a dyke (Coordinates: N41.02446-E033.30330).



Figure 23. Flow structure on dikes (Coordinates: N 41.01334- E033.31488).

#### **2.2.2.2.2. Orientation of Dykes**

Because of pressure increase in a magma chamber, dikes grow upward and place in the crust in a subparallel or subvertical way, as it is also observed in the Boyalı region. As stated by Nakamura (1976) tectonic stress orientation can be determined by using volcanic rocks as a tool, using the relation between volcanic processes and extensive fracturing which is dependent on non-magmatic stress acting on the region, affecting also the orientation of dikes. The relation between the orientation of dikes and the regional stress field can occur in three possible ways; dike trends could coincide with the maximum compressional or the intermediate stress axis, or could concentrate in a direction normal to the minimum compressional axis. If these trends of dikes are linear within each volcanic area and in adjacent areas, or change gradually among them, it could be possible to say that the regional stress is at the same time a tectonic one, affecting the volcanic structures in the region in a relating way (Nakamura, 1976). The relation between the palaeostress distribution and orientation of dikes was based on several studies pointing to the control of orientation of a dike by the prevailing stress axis in the crust, as shown by e.g. Anderson (1972), as the crust is cracked perpendicular to the  $\sigma_3$ , making way for a dike to follow and enlarge, during the

injection of the dike, the dike strike is parallel to the  $\sigma_1$ - $\sigma_2$  plane and the normal to the dike is formed in accordance to the least prevailing stress  $\sigma_3$ .

Aiming to estimate the palaeostress distribution in the Boyalı region during the volcanic activity, the orientations of several dikes were measured. strike and dip values of these dikes were then evaluated using the WinTensor program to obtain palaeostress tensors from the data.

The obtained paleostress tensor indicates that these dykes formed in an extensional strike-slip tectonic regime with horizontal maximum and minimum stress axes oriented NE-SW and NW-SE, respectively (Figure 24).

In Figure 25, strike values are plotted on a rose diagram, which indicates NE-SW directions, at about N20E and N70E minimum and maximum values.

While a wide scatter is observed in the measured strikes of the dikes, the most prominent direction shown by the strikes of the dikes is NE-SW. This strike value is concordant with the expected rifting direction in the basin.

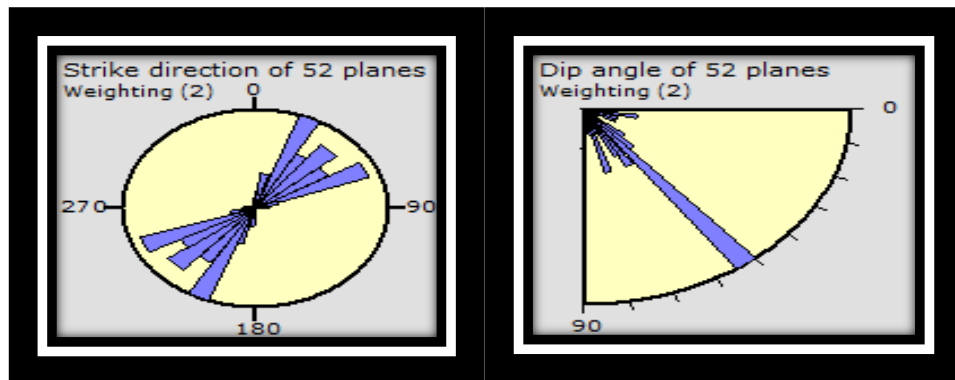


Figure 24. Strike and dip values of dykes plotted on the rose diagram.

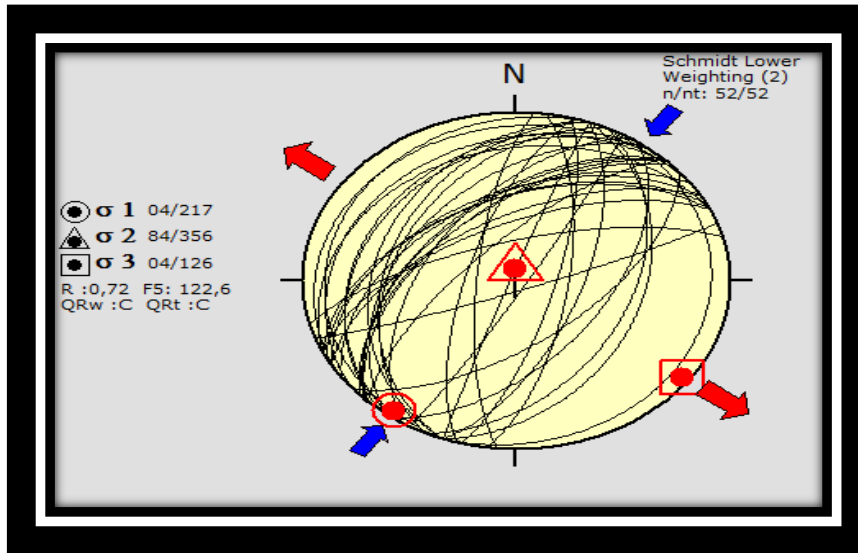


Figure 25. Stereographic projections of dykes with respective paleostress fields.

## **CHAPTER 3**

### **PETROGRAPHY**

#### **3.1. Introduction**

In order to gain insights regarding to the petrographic properties, several rock samples have been collected from the Boyalı area. These rock samples, which have been grouped as lavas and dykes according to their mode of occurrence in the field, have been identified as basaltic and andesitic rocks and turned into thin sections to be examined under the polarized microscope to obtain more detailed information. Despite the effects of post magmatic alteration, which is also evident from macroscopic studies, varying from sample to sample, samples which are as free from alteration as possible, have been chosen.

#### **3.2. Petrography of Boyalı Volcanics**

Boyalı volcanics forms of which differ from lava flows to pillow lavas, lava breccias to dykes, texturally and mineralogically, were determined as basalts and andesites; which were observed as greyish-black fine grained rocks, with orange-brown altered parts and occasional plagioclase phenocrysts. Aphanitic, porphyritic and vesicular textures were also commonly observed in the field.

Results obtained from the microscopic studies and geochemical analyses are in accordance with the field observations. In addition, the mineral content of volcanic rocks exhibit similarities and a distinct dissimilarity of neither petrographic nor textural properties is nonexistent.

Phenocryst phases and abundances differ from sample to sample, detailed explanation of which is provided below:

### 3.2.1. Basalts

Basalts of Boyalı area are grayish-black in color in hand specimen and display aphanitic and vesicular texture. They have orange-brown oxidized parts. In general, basalt samples contain several cracks and joints which resulted in the formation of alteration products; such as carbonate filled veins and cracks which are apparent in hand specimen.

Mineralogical composition of basalts can be listed as: Plagioclase, clinopyroxene, orthopyroxene and Fe-Ti oxides, titanite and apatite and accessory phases. Groundmass is holocrystalline in most samples; yet hypocrySTALLINE samples are present as well, so volcanic glass can also be mentioned among the constituents of the basalts. Hydrous phases such as biotite or hornblende haven't been detected neither in macroscopic nor microscopic examinations.

Microphenocrysts are composed of plagioclase and clinopyroxene minerals; orthopyroxene is not present in the microphenocryst phases whereas plagioclase microlites are abundant in the groundmass. In some samples they are observed together with anhedral or subhedral clinopyroxenes. Fe-Ti oxides are observed frequently in most of the samples, like in andesitic ones; disseminated in the groundmass as small round crystals. They are often aligned according to the flow direction. Volcanic glass is also present in some of the basaltic rocks giving them the hypocrySTALLINE texture (Figure 26).

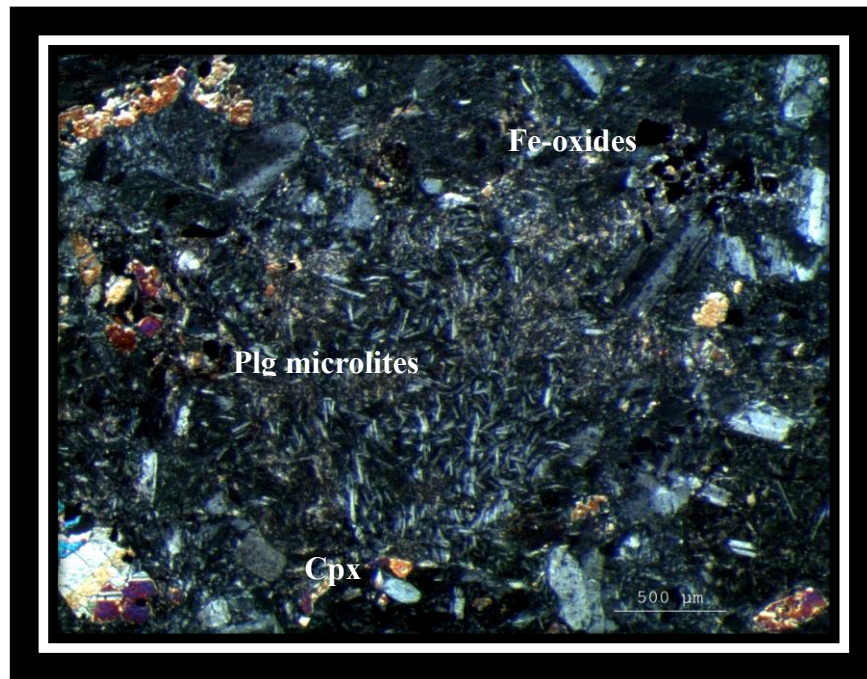


Figure 26. Plagioclase and clinopyroxene minerals are observed as microphenocryst phases in a groundmass composed mainly of plagioclase microlites and Fe-oxides.

(XPL; Plg: plagioclase; cpx; clinopyroxene)

Porphyritic texture is dominantly present in the basaltic rocks, whereas clusters of plagioclase and pyroxene phenocrysts are observed in gathered forms displaying glomeroporphyritic texture in some samples.

Vesicular and amygdaloidal textures are also commonly observed; where carbonates, prehnite and pumpellyite minerals and chalcedony or other forms of silica fill in most of the vesicles. Prehnite minerals, one of the vesicle-filler type of minerals can be classified as secondary mineral assemblage along with pumpellyite minerals and are indicative of hydrothermal alteration. They are detectable by their yellowish-green colors, radial or nodular forms, low relief and absence of any pleochroism. Pumpellyite minerals display acicular to fibrous, generally radiating and greenish colours. Both have anomalous interference colours. Intersertal texture is present in hypocrySTALLINE samples. Similar to andesitic ones, alteration to clay minerals is also common in basaltic samples; most explicitly observed on plagioclase minerals. In addition carbonate minerals are also observed as replacing primary phases (Figure 27).

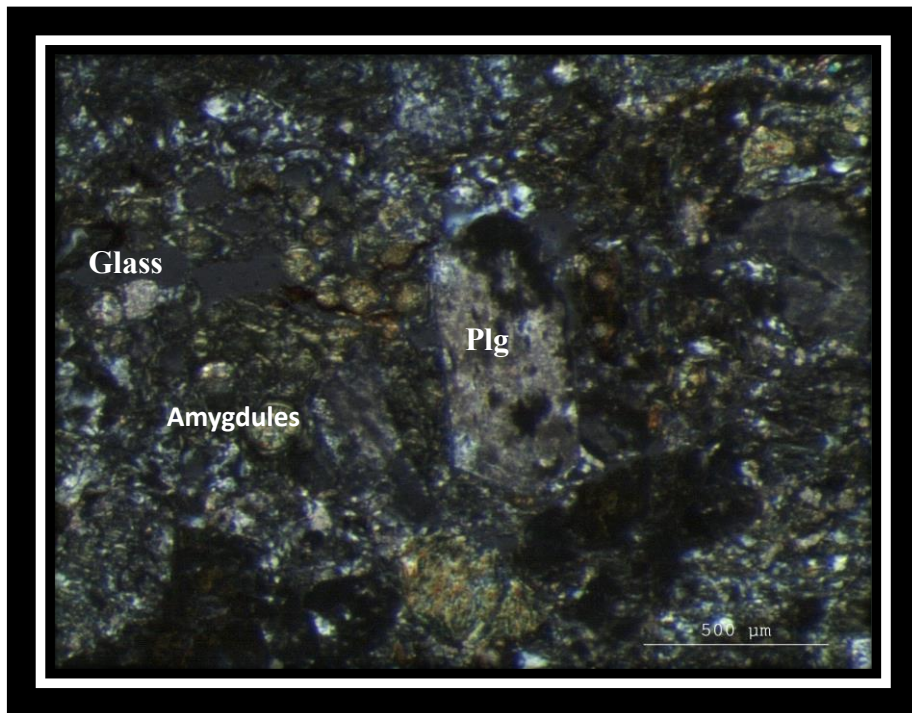


Figure 27. Alteration to clay minerals is clearly observed on a plagioclase phenocrystal. Amygdules are filled by prehnite and pumpellyite minerals in this sample which displays both amygdaloidal and intersertal texture with the presence of glass in the groundmass (XPL; Plg: plagioclase).

The most abundant phenocryst phase is plagioclase. It can be observed in various sizes, occurring both as phenocrysts and microphenocrysts in addition to microlites. Sieve texture is commonly observed in plagioclase minerals, whereas clear plagioclases also occur. Zoned plagioclases can also abundantly be observed. Carbonatization and alteration to clay is intense in some samples; whereas alteration of plagioclases occur in varying degrees in others (Figure 28).

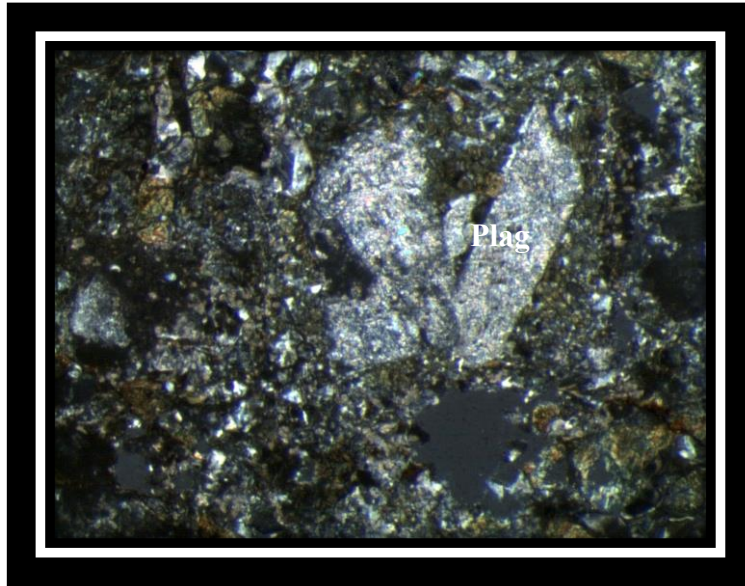


Figure 28. Highly altered plagioclase phenocrysts in clusters (XPL; Plag: Plagioclase).

The second most abundant phase, pyroxene minerals, occur both as clinopyroxenes and orthopyroxenes (Figure 29 and 30). While the abundance of clinopyroxenes is much higher than that of orthopyroxenes, both occur as phenocrysts. Clinopyroxenes occur as microphenocrysts as well. Pyroxenes show partly preserved crystal outlines in general; therefore they are mostly observed as subhedral crystals. Augites are distinguished easily by their birefringence colors and cleavage planes (Figure 29).



Figure 29. A subhedral augite phenocryst exhibiting second order birefringence colors and traces of 90 degrees of cleavage.

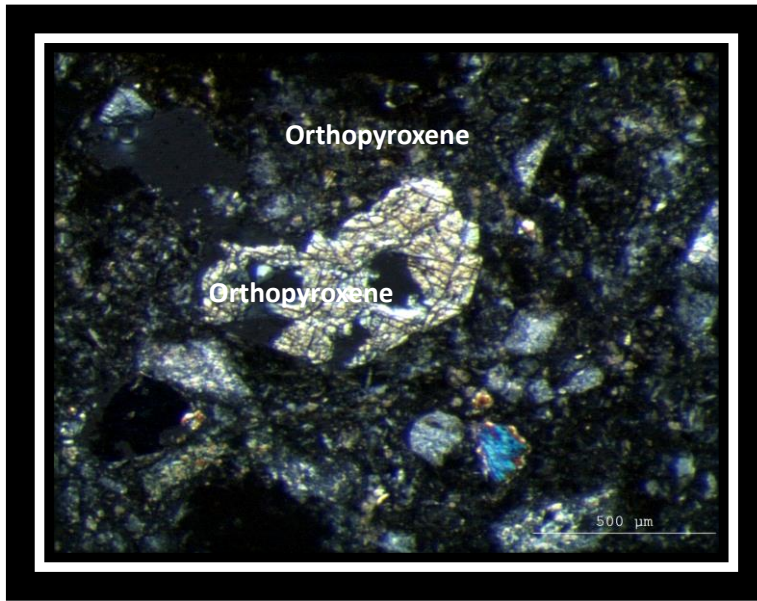


Figure 30. Orthopyroxene phenocrystal distinguished by typical cleavage and first order birefringence colors. Alteration to clay products on cleavage traces is evident (XPL).

Alteration along cleavage planes is observed commonly on pyroxenes. Some clinopyroxenes are found as inclusions in plagioclase minerals; displaying a poikilitic texture (Figure 31).

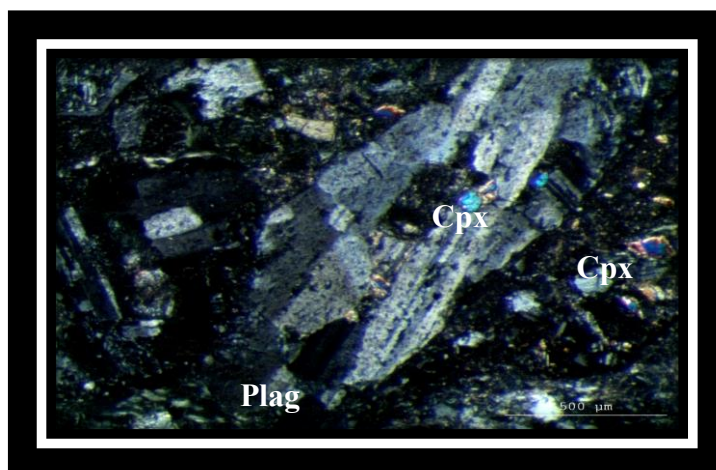


Figure 31. Plagioclase exhibiting sieve texture and poikilitic texture with clinopyroxene and Fe-oxide inclusions (XPL; Plag: Plagioclase; Cpx: Clinopyroxene).

Twinning is commonly observed in clinopyroxenes, whereas rarely orthopyroxenes exhibit simple twinning as well. Some of the clinopyroxene crystals exhibit sector zoning; some of them are characterized by oscillatory zoning features. Inclusions are common amongst them and in some samples it is possible to observed different types of zoning; in addition to inclusions in a single crystal (Figure 32, 33, 34, 35 and 36).

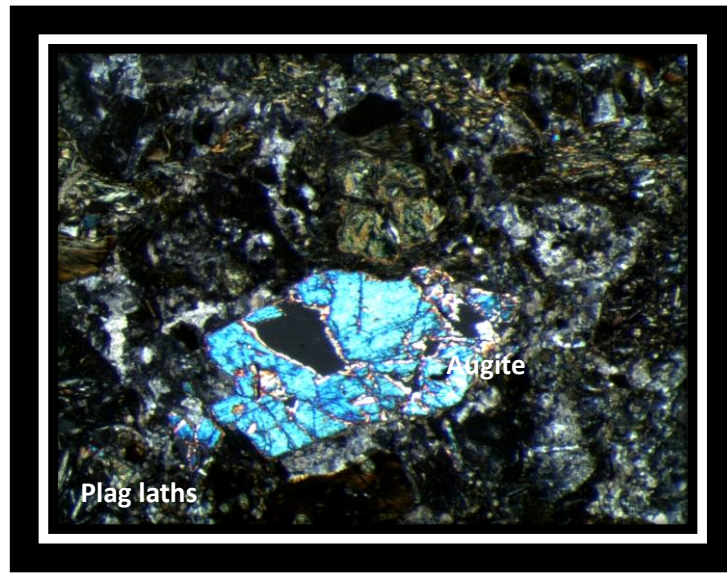


Figure 32. Subhedral augite phenocrystal in a highly altered matrix of plagioclase laths and smaller augite crystals (XPL; Plag: Plagioclase).

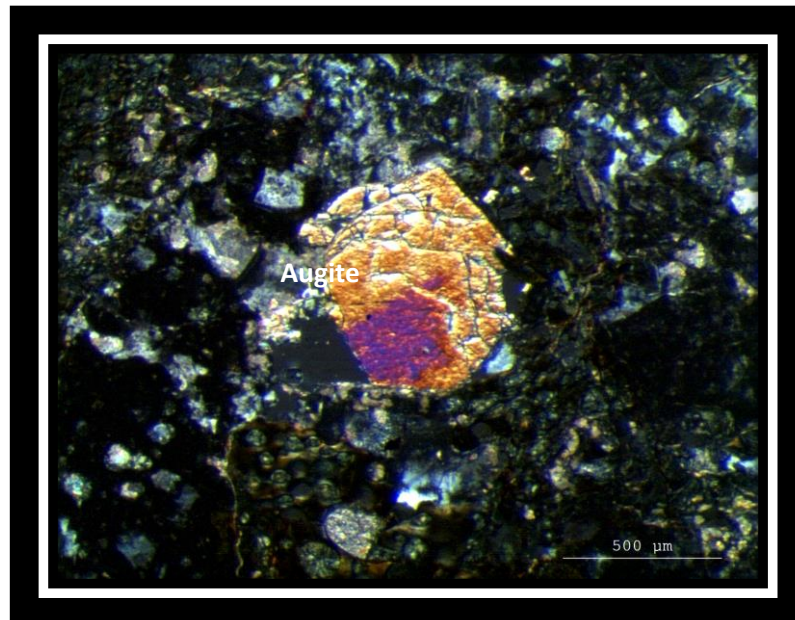


Figure 33. Sector zoning and oscillatory zoning observed in an augite phenocrystals (XPL).



Figure 34. Twinning and zoning is commonly observed in clinopyroxenes as well as orthopyroxenes. Also, Fe inclusions are common in pyroxene phenocrysts differing in sizes (XPL).

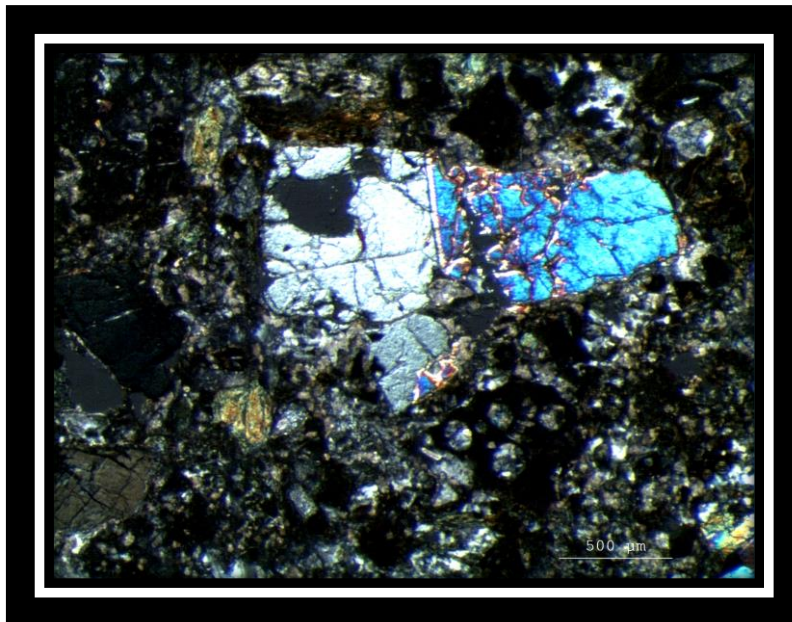


Figure 35. Simple twinning observed in clinopyroxene phenocrysts (XPL).

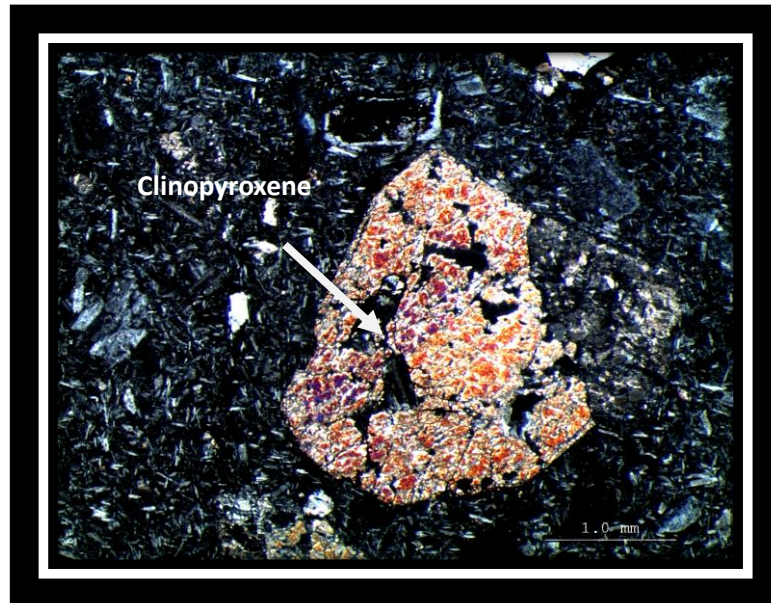


Figure 36. Anheadral clinopyroxene which is zoned and altered in a matrix of plagioclase microlites and plagioclase microphenocrystals (XPL).

As accessory phase, Fe-Ti oxides occur abundantly in basaltic samples. Their abundance differ from sample to sample, yet they are observed as disseminated in the groundmass as small rounded crystals. They occur in mafic phases as well. Titanite and apatite are observed as less common accessory phases. Whereas there has been no titanite inclusions in any mafic phases; apatite is seen in some of them; leading to conclusion that titanite crystallized as a later phase.

In some of the samples, volcanic rock fragments are easily noticed by fine grained matrix features exhibiting a darker color then that of the groundmass of the main thin section and different sizes of wholly crystallized essential minerals (Figure 37, 38 and 39).



Figure 37. A volcanic rock fragment composed of plagioclase, orthopyroxene and clinopyroxene minerals; as well as Fe-oxide inclusions (XPL).

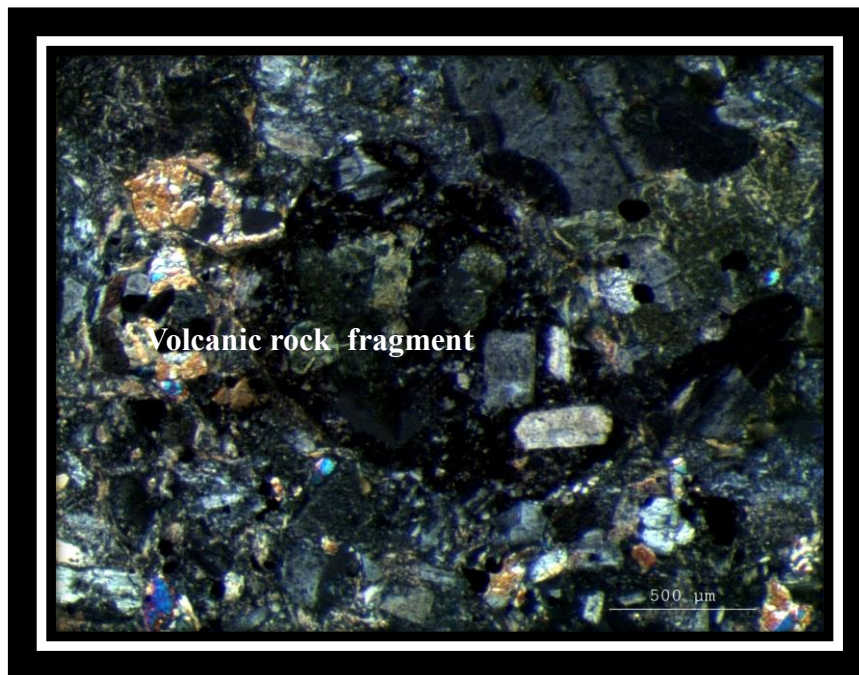


Figure 38. Volcanic rock fragment composed of plagioclase minerals of various sizes and Fe-oxides exhibiting high levels of alteration (XPL).



Figure 39. Volcanic rock fragment containing lesser amounts plagioclase minerals as phenocrysts and microphenocrysts and Fe-oxides (XPL).

### 3.2.2. Andesites

Andesite hand specimens have a grayish-pinkish color. In some samples porphyritic texture is observed where plagioclase phenocrysts are aligned as laths, according to flow direction. In addition to plagioclase, clinopyroxene, orthopyroxene, biotite and hornblende are also observed as phenocryst phases.

Similar to basaltic rocks, the most abundant phenocryst is plagioclase observed in andesitic thin section samples as well. The size of plagioclase minerals vary from sample to sample and also within a sample. In some of the andesite thin sections plagioclase is observed almost only as microlites, with one or two phenocrysts having formed; exhibiting a bimodal distribution of grain size. On the other hand, other andesite thin sections include abundant phenocrysts of variable sizes; including microphenocrysts in addition to microlites (Figure 40).

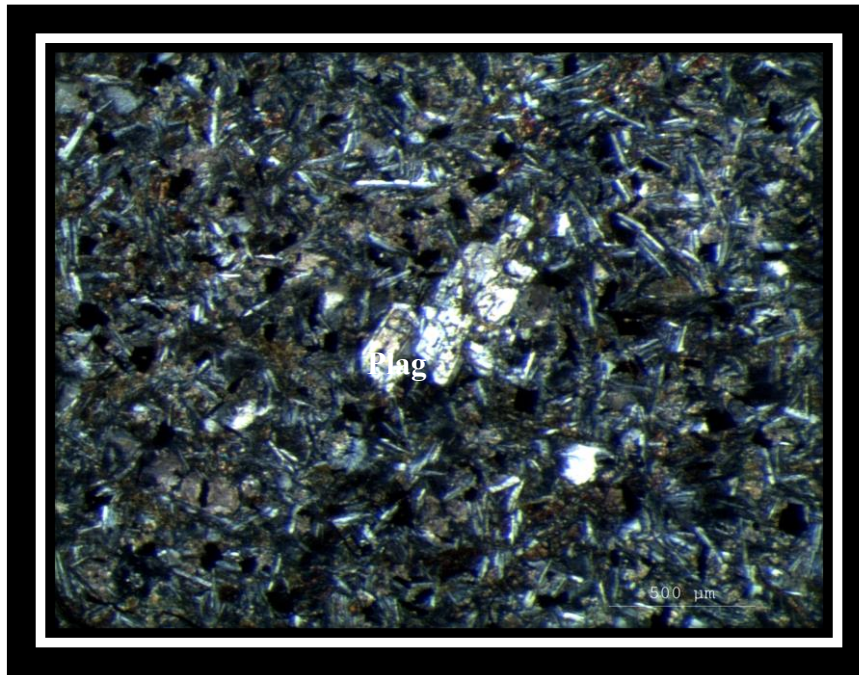


Figure 40. Plagioclase microphenocrystals in a matrix of plagioclase microlites, Fe-oxides, glass and alteration minerals (XPL; Plag: Plagioclase)

Some of plagioclase phenocrysts show intense alteration to carbonates and clay minerals. Especially the alteration to clay minerals seem to mask the mineral's textural features such as compositional or oscillatory zoning. However despite masked by alteration, zoned crystals are abundant in andesitic rocks; especially oscillatory zoning is one of the most common feature of plagioclases (Figure 41).

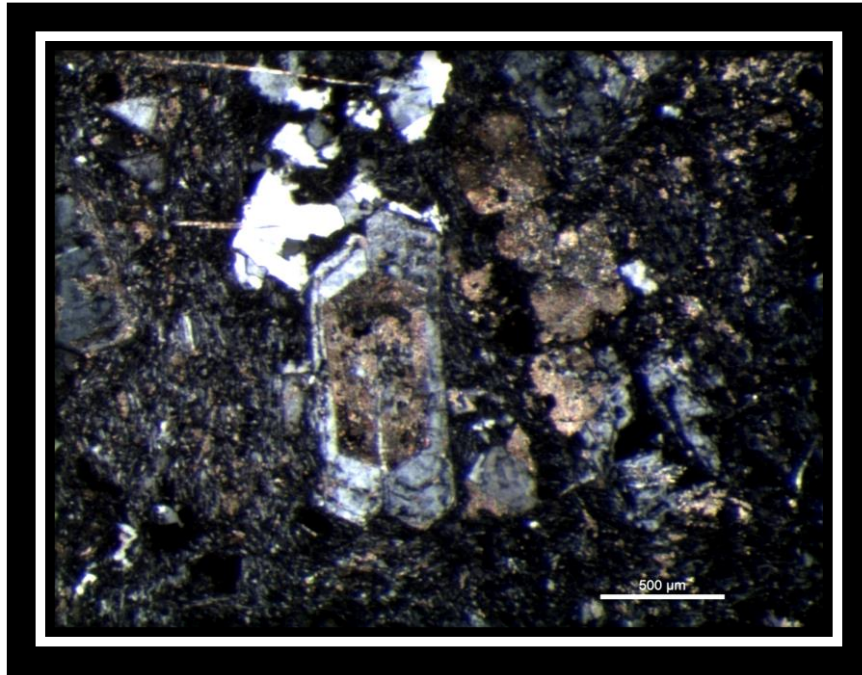


Figure 41. Zoned plagioclase crystal which includes Fe-oxide inclusions has altered to clay minerals. Alteration, which is also evident in the oscillatory layers, is especially concentrated in the innermost zones of the crystals (XPL).

Sieve texture is another feature commonly observed in plagioclase phenocrysts. However an important observation that needs to be noted is that in a single sample some plagioclases exhibit sieve texture; whereas others seem to have remained unaffected by the magma conditions that permit this texture to form. This characteristic of andesitic rocks points to magma mixing. Some of the altered plagioclase phenocrystals also show quenching (Figure 42 and 43).

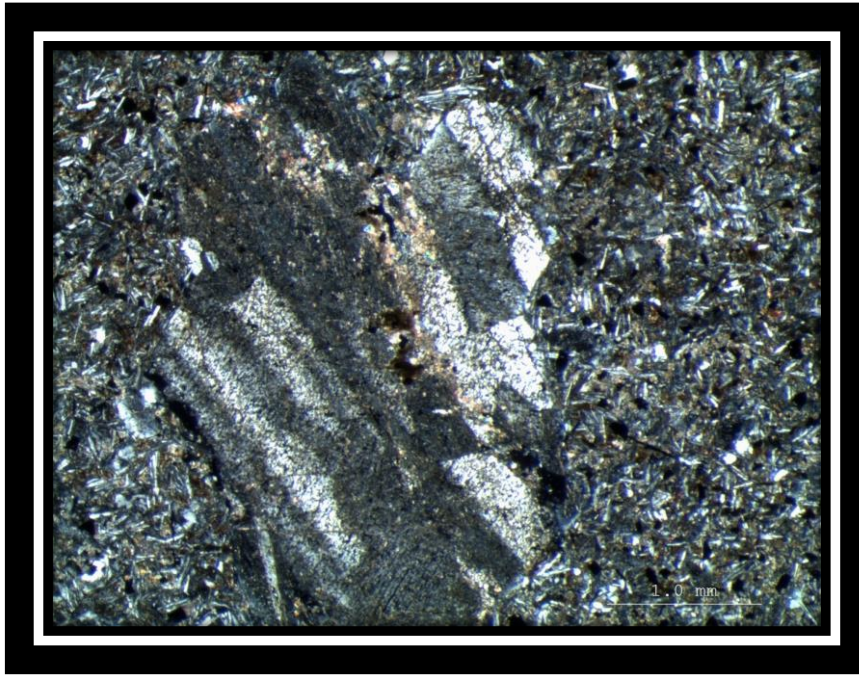


Figure 42. Subhedral plagioclase phenocrysts in a cluster which exhibits sieve texture and glomeroporphyritic texture (XPL).



Figure 43. Quenching seen on a plagioclase phenocrystal which partly preserves its crystal boundaries and form.

Polysynthetic twinning is common in either of them which makes plagioclase phenocrysts easily recognizable with this characteristic feature; although partly masked by alteration to carbonate and clay minerals.

Glomeroporphyritic texture, another commonly observed feature of andesitic rocks; is observed mainly where plagioclase minerals occur in clusters with biotite minerals; as well as in separate clusters (Figure 44).

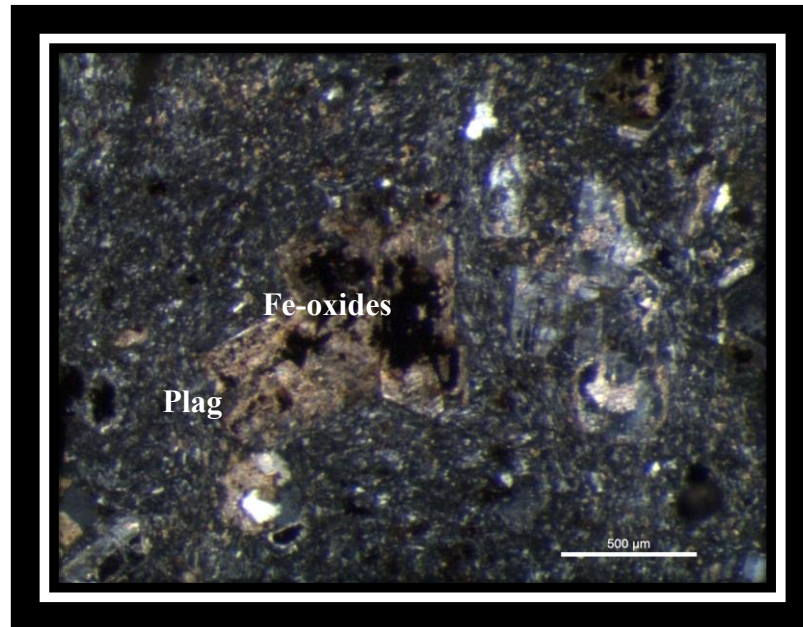


Figure 44. Clusters of highly altered plagioclase phenocrysts with oxidized zones in the center (XLP).

Some of the plagioclase phenocrysts include pyroxene inclusions. This indicates that pyroxene had already formed while plagioclase was newly forming; so it is an indicative of crystallization sequence.

Orientation of microlites is another characteristic of andesitic rocks, which demonstrate a flow texture in most of the samples. Parallel to the flow direction of the lava, gas bubbles seem to have elongated as well (Figure 45 and 46).

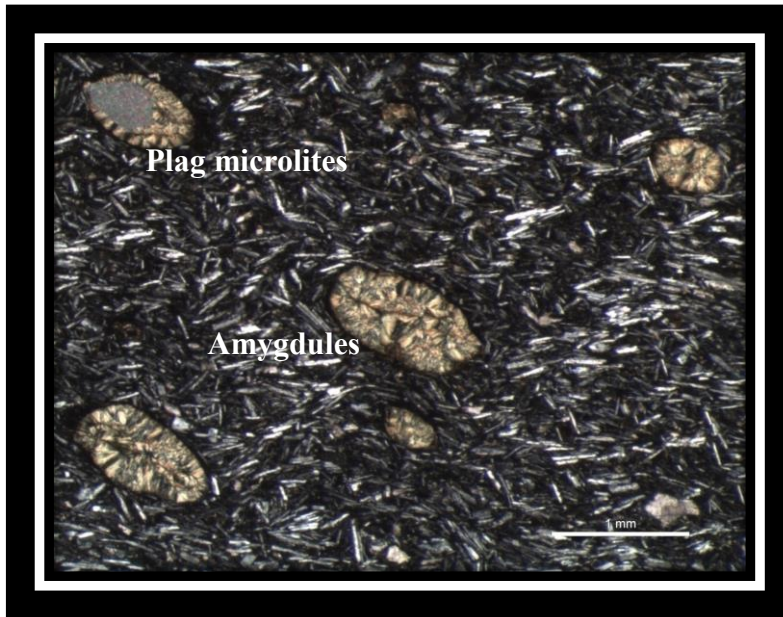


Figure 45. Microlites are oriented according to the flow direction. Amygdules filled by prehnite and pumpellyite minerals exhibit a similar kind of orientation as well (XPL).

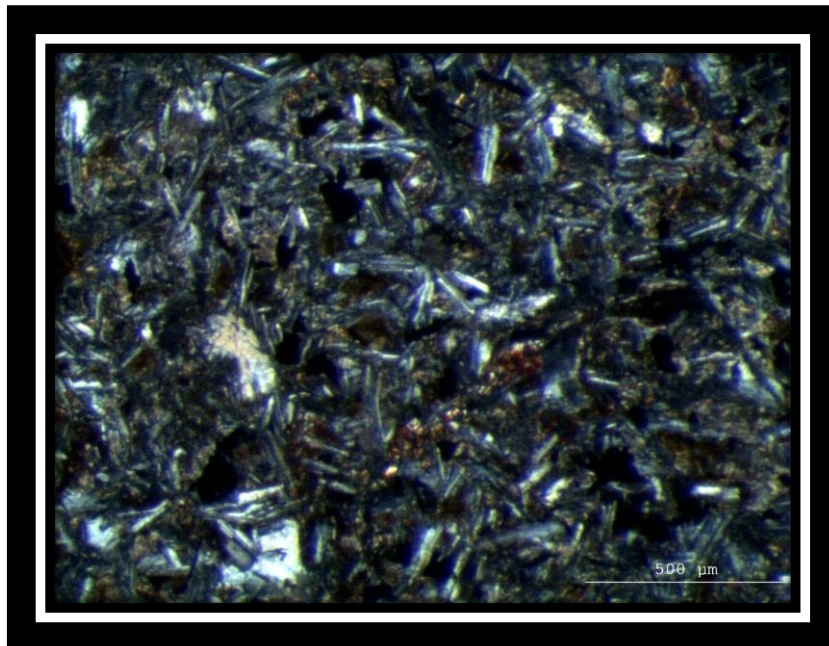


Figure 46. Plagioclase microlites are randomly oriented in some of the andesite samples. The matrix is composed of plagioclase microlites, clinopyroxenes, Fe-oxides and silica (XPL).

Pyroxenes are also seen abundantly in andesitic rocks as phenocryst phases. Their composition has been identified to range from augite (clinopyroxenes) to enstatite (orthopyroxenes) by petrographic methods. Orthopyroxenes are rare compared to augites and they are observed in phenocryst phases in clusters with augites or as separate crystals; whereas augites are seen in various sizes, including microphenocrysts and groundmass size as well.

Some of the augites are zoned; exhibiting ‘sector-zoning’ which indicates different regions of the crystal with different composition; pointing at rapid growth of the mineral. Twinning is another common feature of augites as several crystals exhibit simple twinning. Opaque inclusions are observed in some augite crystals.

Hornblende, although rare in abundance, is another phenocryst phase seen in andesitic rocks.. It is observed as green, subhedral crystals, crystal boundaries of which are thick and dark in color; indicating reaction rims that formed around them due to disequilibrium conditions in the magma, whereas hornblende crystallization is considered as mineralogical evidence for water content in the magma (Figure 47).

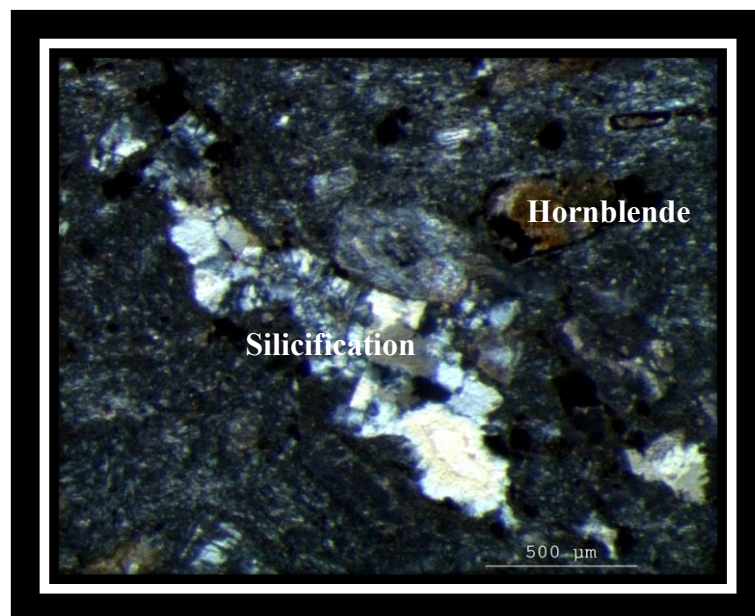


Figure 47. Subhedral to anhedral hornblendes are seen as phenocrystals and microphenocrystals; as well as inclusions in plagioclase minerals. They have been oxidized especially on the boundaries and often include Fe-oxide minerals.

Biotite has been observed as phenocrysts and microphenocrysts, distinguished by their characteristic one-dimensional cleavage. Due to alteration to Fe-Ti minerals, some of the crystals appear opaque. This alteration is most prominent at the crystal boundaries, forming dark rims in some of the biotite phenocrysts (Figure 48). In addition to opaque inclusions, some of the biotite phenocrysts contain plagioclase minerals (Figure 48 and 49).

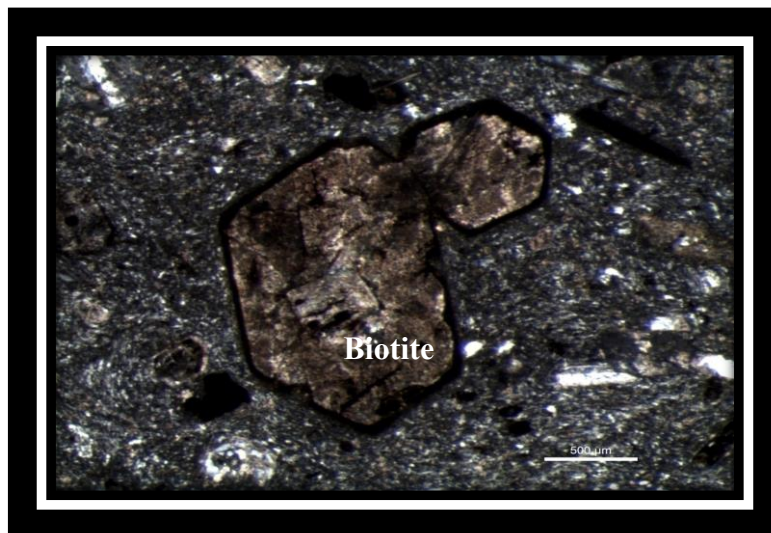


Figure 48. Biotite phenocrysts and microphenocrysts altered to Fe-Ti minerals (XPL).



Figure 49. Biotite phenocrystal containing plagioclase mineral and opaque inclusions (XPL).

The crystallization sequence can be given as Fe-Ti oxides, followed by proxene, then plagioclase and afterwards hornblende according to the textural relationships.

Amydules are filled with prehnite and pumpellyite minerals in some of the andesitic samples; which occur together with carbonate minerals, whereas others lack this feature. In addition, silicification (chalcedony) has also been detected (Figure 50 and 51).

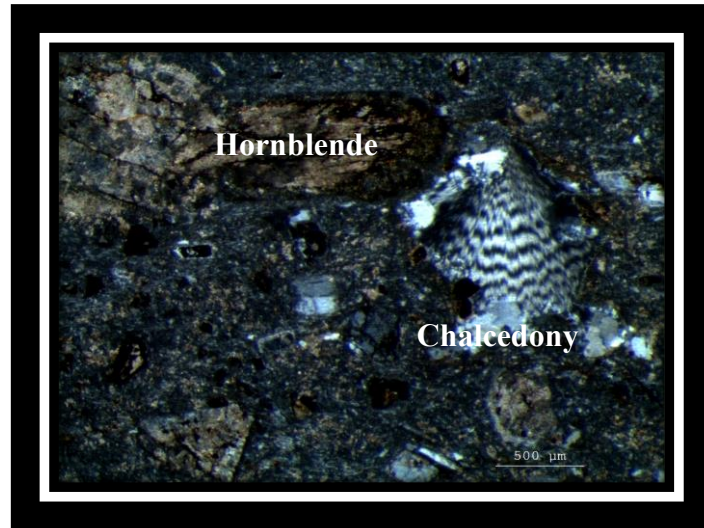


Figure 50. Chalcedony has been formed in cracks in a sample which includes plenty of hornblende crystals of various sizes altered to varying degrees of Fe-Ti minerals (XPL).

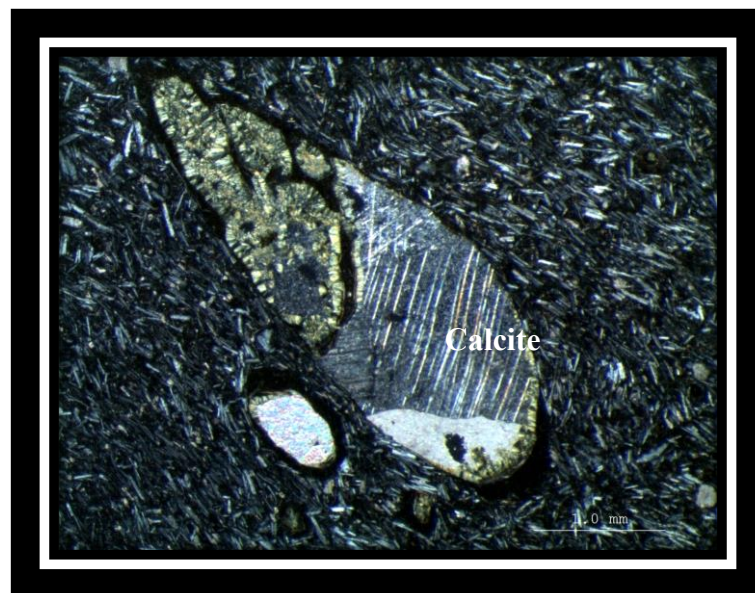


Figure 51. Amygdules, elongated according to the flow direction are filled with carbonate minerals and pumpellyite (XPL).

Some of the andesitic samples contain volcanic rock fragments, distinguished by a dark groundmass mostly composed of opaque minerals and plagioclase microlites

## **CHAPTER 4**

### **PETROLOGY –GEOCHEMISTRY**

#### **4.1. Introduction**

In this chapter, geochemical characteristics of andesitic and basaltic lava and dyke samples are presented. Major element variations together with trace and rare earth element chemistry is evaluated, in addition to tectonomagmatic discrimination, origin and petrogenesis of the Boyalı volcanic are discussed. Samples were first examined under the petrographic microscope in order to choose most representative ones; to eliminate possible affects of alteration on geochemical properties as much as possible, relatively less altered samples were determined as representative ones and were sent to geochemical analysis in ACME laboratories, Canada.

#### **4.2. Method**

14 samples; 10 of them belonging to dikes 4 to lavas were collected from study areas and chosen under the microscope. In order to obtain the most accurate results possible, the most fresh samples were picked due to the fact that alkali elements are mobile during weathering and metamorphism and altered samples may be misleading by falling onto wrong areas in classification. Chosen samples were analyzed by Inductively Coupled Plasma-Atomic Emission Spectrometry ICP-AES for major elements and Inductively Coupled Plasma-Mass Spectrometry (ICP-MS) for trace and rare earth (REE) elements, using powdered samples of 200 mesh-size for whole rock geochemical analyses in ACME Analytical Laboratories (Canada).

#### **4.3. Alteration**

Secondary products such as clay minerals, carbonates and zeolites observed clearly in petrographic examination on thin sections are indicative of an evident alteration

process which has affected a great amount of essential minerals. The affect of alteration is also supported by geochemical analysis that reveals variable yet high LOI (minimum 3.0; up to 7.8) values.

The average value of LOI values is 4.55 for dykes and and it is 4 for lava samples. These are moderate values, however the LOI measurements show that some samples are relatively more altered than the others.

The precaution of careful sampling is not an adequate method to omit alteration affects wholly; as any means of macroscopic examination is not sufficient to eliminate highly altered parts of a sample in order to obtain accurate geochemical results. Therefore in order to handle any possible remaining alteration with caution it is useful to test element mobility. Otherwise the results might lead to mistaken results in petrological investigations. For this reason, Zr element, which is one of the HFS (High field strength elements) is used as fractionation index, based on its incompatible and immobile character which indicates that the mineral is resistant to being carried away by fluids causing alteration and changes in the chemistry of the rock.

When the trends of the major and trace element content of the examined samples evaluated by comparison to increasing Zr content are taken into consideration, it is possible to say that overall a coherent linear trend is observable; with a few exceptions caused by a few samples. These are the samples displaying relatively higher LOI values than the average. As the elements plotted against Zr are also characterized by immobile affinities in general, an influence of post-magmatic processes forming secondary minerals, such as weathering by hydrothermal alteration, changing the overall content and combination of elements to make up a new mineral, is not in question.

Mobility and immobility of the elements are tested according to their relation with respect to Zr concentrations (Figure 52); elements that demonstrate a consistent trend can be regarded as immobile, whereas others, which lack an evident correlation and are scattered can be regarded as immobile and those are the ones to be more careful about while interpreting petrological diagrams because they are effected by low grade alteration and do not reflect original abundances.

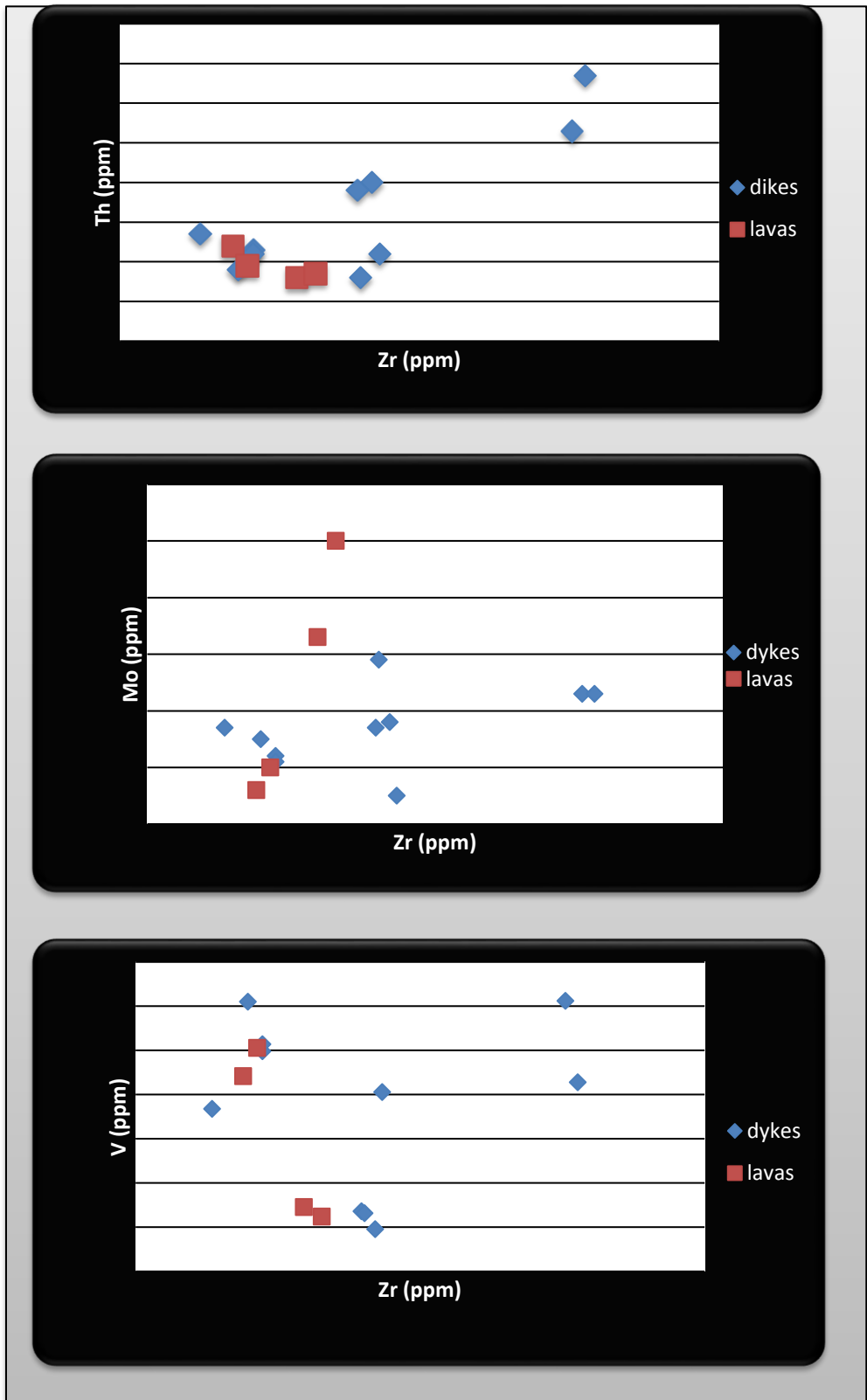


Figure 52. Major and trace elements plotted against Zr.

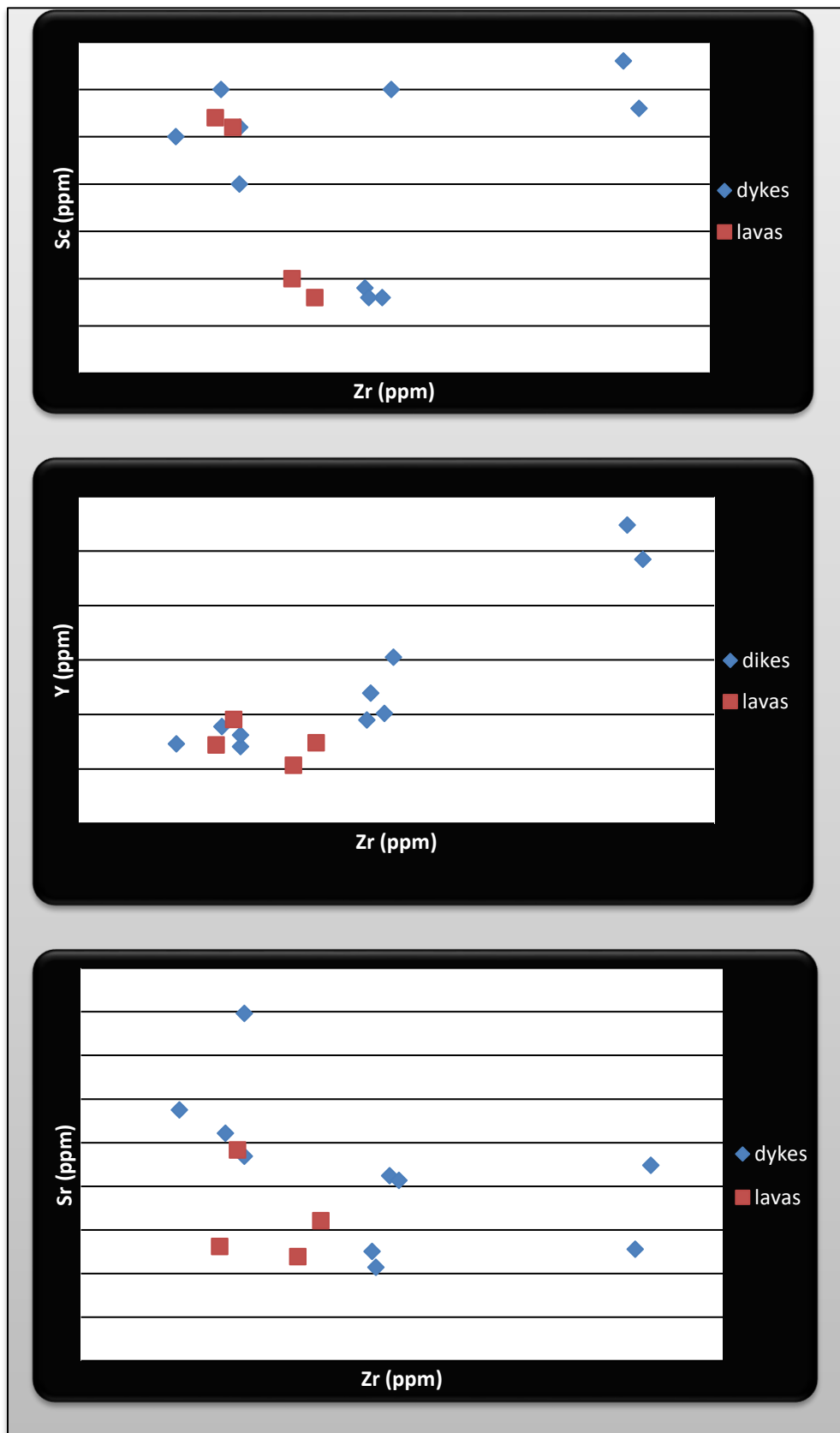


Figure 52. Continued.

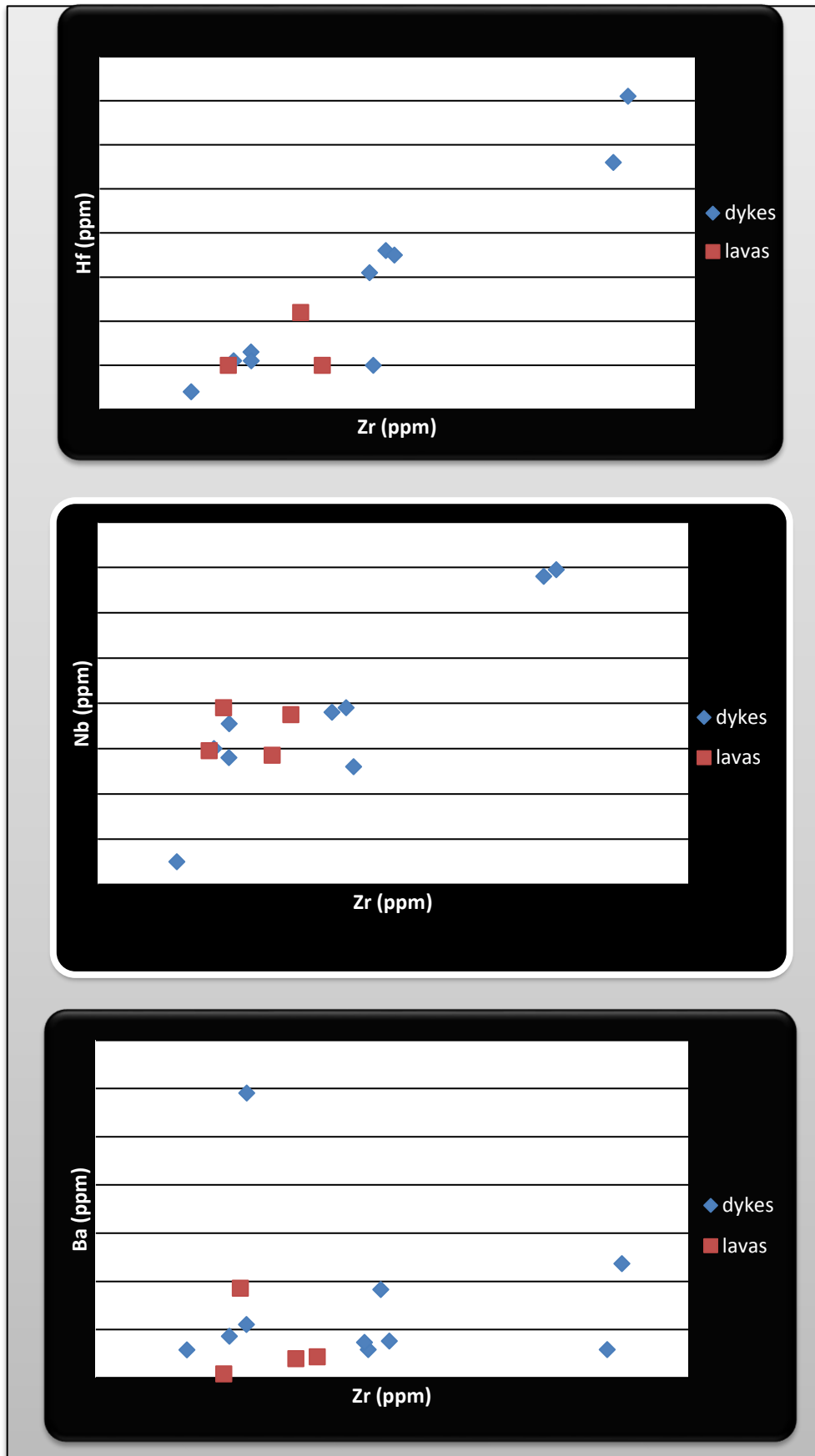


Figure 52. continued.

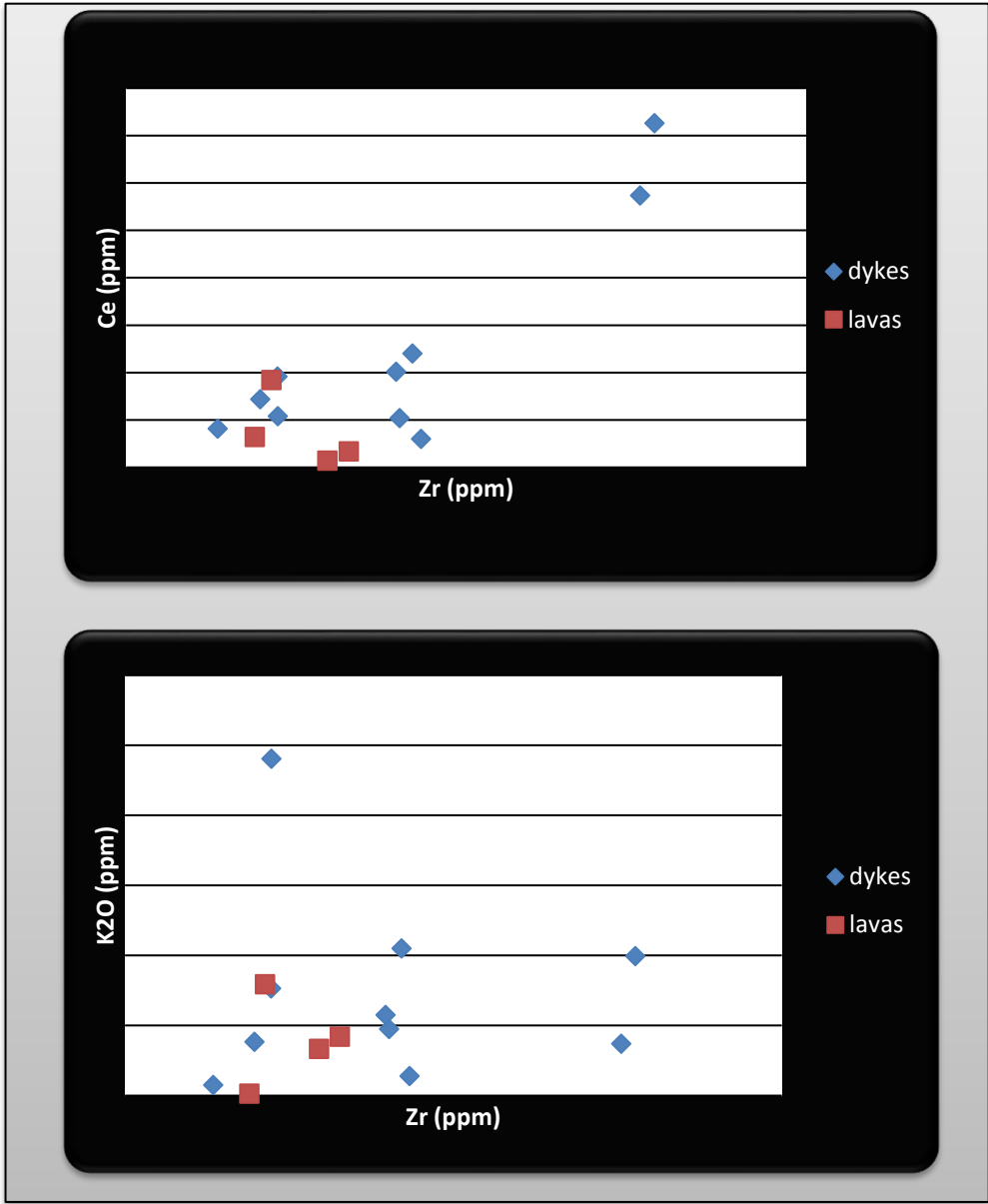


Figure 52. continued.



Within this perspective, CaO, K<sub>2</sub>O, Ba, Sr, Sc, V and Mo show clear mobility. Therefore attention should be paid on these oxides and elements when interpreting geochemical trends.

#### 4.4. Major Element Chemistry

Basalts, basaltic andesites and andesites are both characterized by a wide range of major element composition (Table 1). When dykes and lavas are evaluated together, there is a large variation in silica contents (46.79 to 62.88 wt.%). Lava samples are represented by SiO<sub>2</sub> (wt.%) contents 51.25, 52.00, 62.88 and 62.87, whereas dykes have SiO<sub>2</sub> contents in a greater range, varying from 46.79 to 60.61. One of the dyke samples and 2 of the lava samples have the highest silica values which are over 60 %. However, when the samples with highest SiO<sub>2</sub> contents are checked, petrographic examinations reveal that they display considerable amounts of silicification that happened as a post-magmatic process in the cracks, therefore this can be considered as a result of alteration. Overall, when silica contents are evaluated, majority of the samples are low silica (wt.%SiO<sub>2</sub><58) samples. “Loss on ignition” (LOI) values that indicate how fresh the investigated rocks are, vary between 3.0 to 7.8 (wt.%); average of LOI values being 4.55 for dykes and 4 for lava samples. As much as the attention put on selecting the least altered samples; still the examined ones display silicification, carbonatization, zeolitization and clay replacement, as clearly observed under the polarized microscope. The high LOI measurements highlights an important point to consider; it is possible that especially in samples with higher LOI values, some of the elements; alkalis, alkaline earths and large ion lithophile elements have been mobile due to post eruption processes, which means some of the results including these elements may differ from the original composition.

A wide range is also observed in alkali contents 2.49 to 7.69 wt.% in Na<sub>2</sub>O contents of dikes; whereas lavas as characterized by a narrower range, displaying the values 5.80, 5.40, 3.79 wt.% and 3.30 wt.%. K<sub>2</sub>O contents range between 0.15 to 4.81 for dikes and for lavas values are between 0.03 and 1.59 wt.%.

Half of the lava samples display high FeO contents (7.45 and 8.04wt.%) whereas the other half displays lower amounts (2.56 and 5.13 wt.%). Dike samples are characterized by generally high FeO contents ranging between 5.84 to 9.51 wt.%, with

one exception. One of the dike samples display a much lower FeO content; 3.07 wt.%.

MgO contents of half of the lavas are high (4.88 and 6.09 wt.%) and the other half have low values (0.77 and 1.71). For dikes, these values are between 0.89 to 6.59 wt.%, displaying a wide range. MgO values for lavas are much less than average values of dykes, therefore lava samples can said to be more evolved. The lowest value belongs to the same sample which displays lower FeO content than the rest. To provide a better aspect on the evolution degrees of the samples, when the Mg numbers are evaluated; for dikes the number is between 22 and 44 for lavas 23 and 43.

Table 1. Major element analysis of the studied samples.

	SiO <sub>2</sub>	Al <sub>2</sub> O <sub>3</sub>	Fe <sub>2</sub> O <sub>3</sub>	MgO	CaO	Na <sub>2</sub> O	K <sub>2</sub> O	TiO <sub>2</sub>	P <sub>2</sub> O <sub>5</sub>	MnO	Cr <sub>2</sub> O <sub>3</sub>	LOI	TOTAL	Mg #
	(wt %)	(wt %)	(wt %)	(wt %)	(wt %)	(wt %)	(wt %)	(wt %)	(wt %)	(wt %)	(wt %)	%		
Sample														
IPS-01 (dike)	50.04	17.16	9.15	6.59	5.77	4.91	0.77	0.97	0.25	0.14	0.015	3.9	95.765	0.4445743
IPS-02 (dike)	52.38	17.45	10.26	5.06	3.55	5.92	1.53	0.89	0.29	0.10	0.007	3.77	97.437	0.3885365
IPS-03 (dike)	53.29	14.60	11.37	4.82	4.82	2.49	4.81	0.72	0.21	0.11	0.023	6.36	97.263	0.4289945
IPS-04 (dike)	53.21	18.27	12.48	3.00	3.49	7.69	0.15	0.57	0.24	0.14	0.012	3.8	99.252	0.2662132
IPS-05 (dike)	54.09	15.85	13.60	2.99	3.76	5.51	1.99	1.86	0.47	0.17	0.008	3.0	100.298	0.2490422
IPS-06 (dike)	56.71	17.75	14.71	1.93	3.11	7.43	1.15	0.77	0.26	0.12	0.009	4.2	103.949	0.2478268
IPS-07 (dike)	57.75	18.41	15.82	1.83	4.11	4.79	2.10	0.73	0.26	0.11	0.012	3.3	105.922	0.23860
REC-14 (dike)	46.79	18.30	16.93	4.83	4.21	5.68	0.28	1.52	0.25	0.16	0.007	7.8	98.957	0.3513489
REC-15 (dike)	49.91	16.47	18.04	4.22	8.37	2.80	0.74	1.97	0.41	0.16	0.009	4.1	103.099	0.3073363
REC-16 (lava)	52.00	15.88	19.15	4.88	4.74	5.80	1.59	1.02	0.34	0.19	0.026	5.0	105.616	0.3957716
REC-17 (lava)	51.26	16.13	20.26	6.09	7.24	5.40	0.03	0.74	0.23	0.12	0.016	3.6	107.516	0.4311439
REC-18 (dike)	60.61	17.49	21.37	0.89	6.12	4.19	0.95	0.72	0.23	0.16	0.020	5.1	112.750	0.224843
REC-19 (lava)	62.88	17.27	22.49	0.77	7.06	3.79	0.84	0.60	0.20	0.08	0.036	3.6	116.016	0.230924
REC-20 (lava)	62.87	15.96	23.60	1.71	5.09	3.30	0.67	0.61	0.11	0.06	0.024	3.8	114.004	0.2500417

TiO<sub>2</sub> content of lavas are between 0.60 and 1.02 wt.%, dikes display values 0.72-1.97 wt.%. Most of the lava and dike samples display a restricted range; which implies derivation from a single source. However, Some of the dyke samples have relatively higher contents TiO<sub>2</sub> above 1 wt.%; which could have resulted from fractionation of iron-titanium oxide minerals.

When TiO<sub>2</sub>, MgO, CaO and Na<sub>2</sub>O concentrations are evaluated, overall, lavas are more homogenous in terms of these elements, displaying similar values. P<sub>2</sub>O<sub>5</sub> values are generally higher in dykes ranging between 0.23 and 0.47%.

In Harker diagrams (Figures 53-62) it is difficult to decide exactly whether the lava samples exhibit parallel trends with dike samples or not, due to scarcity of the samples and some scattered trends. However, they seem to be in correlation with the overall trends of dyke samples.

SiO<sub>2</sub> vs Al<sub>2</sub>O<sub>3</sub> trend is quite scattered. From MgO vs SiO<sub>2</sub> and FeO vs SiO<sub>2</sub> diagrams, a negative correlation is observed in oxides with increasing silica. MnO is a little bit difficult to interpret but, a decrease can be inferred with increasing silica. Alkali contents are variable due to alteration. Although a little bit scattered K<sub>2</sub>O increases with increasing silica, and a decrease is observed in Na<sub>2</sub>O. CaO is a little bit difficult to interpret, if a scatter of a few samples is omitted, it is possible to say that a negative trend can be observed with increasing silica, however lava samples cannot be interpreted. The scatter can be caused of secondary calcitization reflected in the analysis, as petrographic studies revealed these samples include calcitization as a secondary mineral phase. P<sub>2</sub>O<sub>5</sub> trend also can be interpreted as decreasing with increasing silica, although it is again a little scattered which gets in the way of obtaining more accurate data. This might indicate fractionation of apatite. The evident gradual decrease in MgO with increasing silica is indicative of ferro-magnesian mineral fractionation. This is also supported by a similar trend in FeO vs SiO<sub>2</sub> and Cr<sub>2</sub>O<sub>3</sub>.

Although the trend is difficult to interpret for Al<sub>2</sub>O<sub>3</sub>; decrease in Fe<sub>2</sub>O<sub>3</sub>, MgO, CaO and P<sub>2</sub>O<sub>5</sub> and TiO<sub>2</sub> with increasing SiO<sub>2</sub> is in correlation with what is expected of calc-alkaline rocks.

Some of the scatter in the diagrams might be due to secondary alteration processes, as also revealed by petrographic studies, however, as disequilibrium textures determined under the microscope indicate, magma mixing might also be reflected in the variation diagrams and cause scatter in the trends. When the scatter trends are evaluated; a comparison with previously conducted Harker diagrams of oxides and trace elements versus Zr to check alteration affect reveals the oxides that show scatter here are the ones that showed inconsistent trends with Zr and therefore a magma mixing effect is less possible.

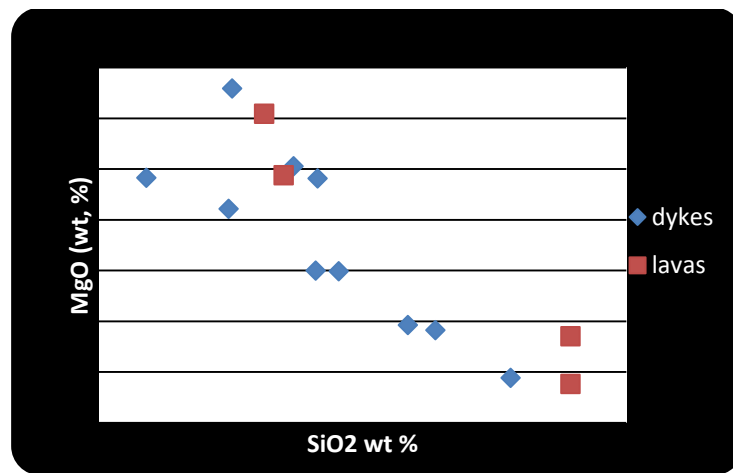


Figure 53. MgO% vs SiO<sub>2</sub> % Harker diagram.

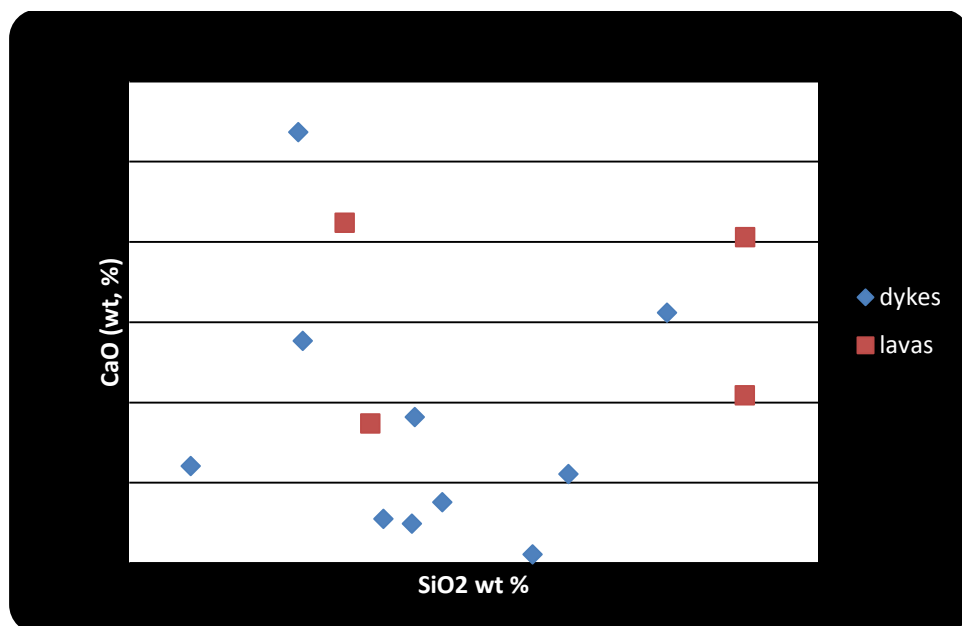


Figure 54. CaO% vs SiO<sub>2</sub> % variation diagram.

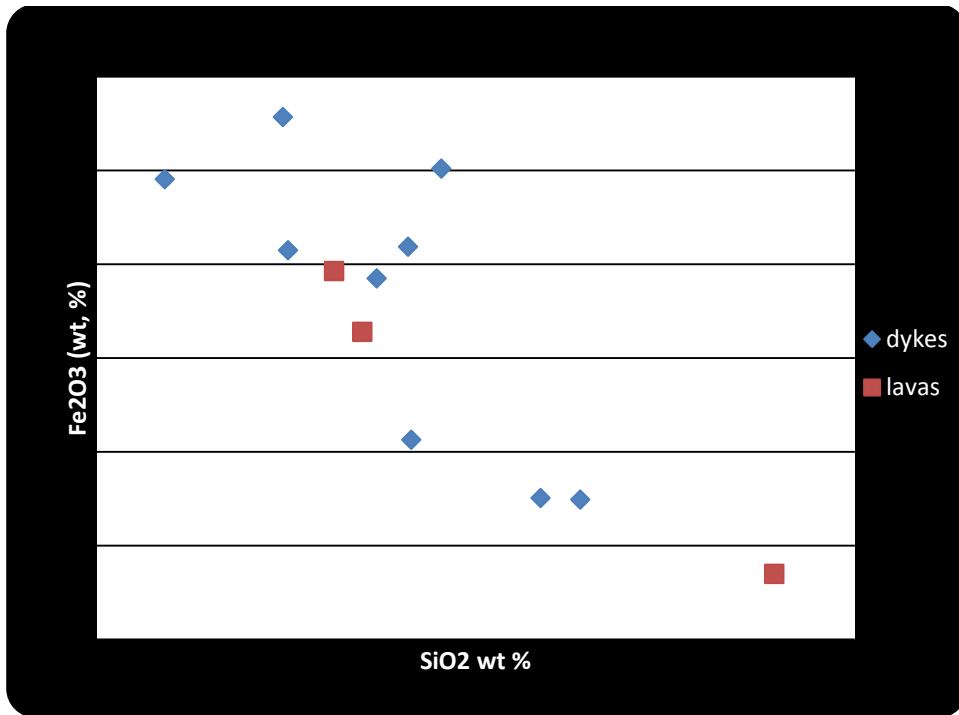


Figure 55. Fe<sub>2</sub>O<sub>3</sub>% vs SiO<sub>2</sub> % variation diagram.

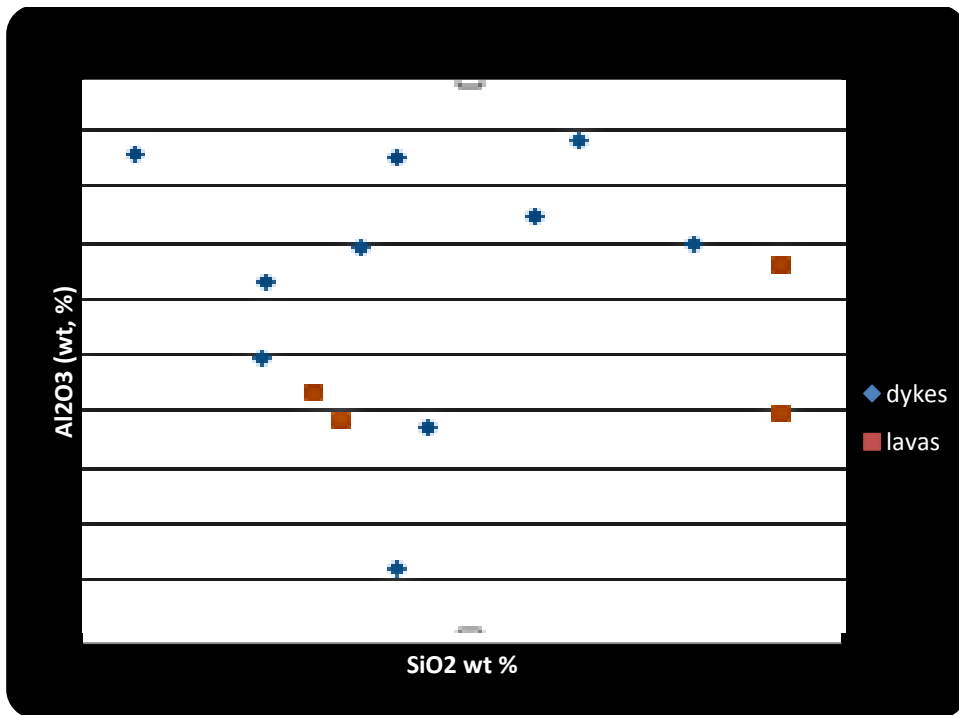


Figure 56. Al<sub>2</sub>O<sub>3</sub>% vs SiO<sub>2</sub> % variation diagram.

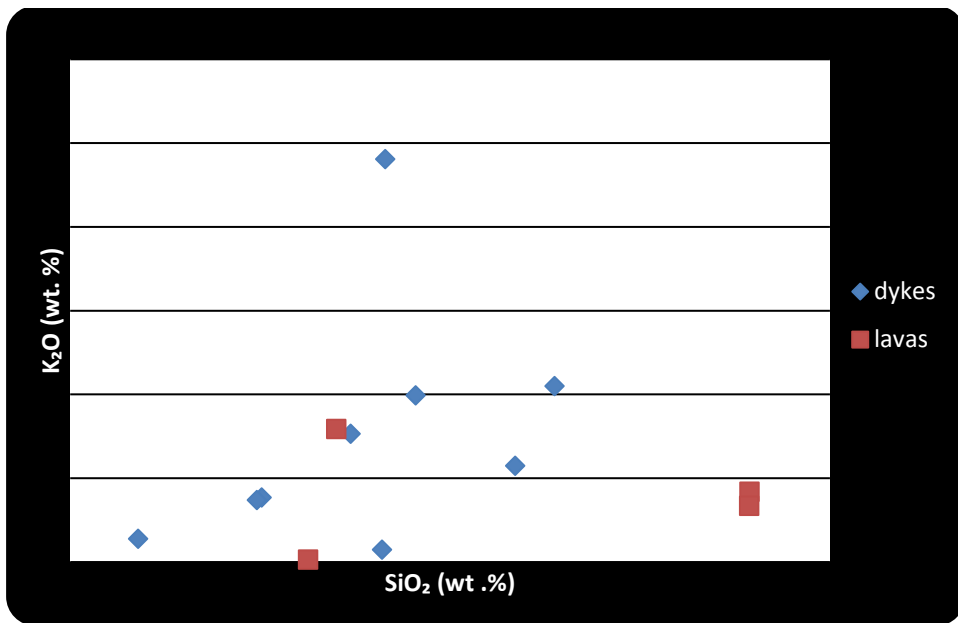


Figure 57. K<sub>2</sub>O% vs SiO<sub>2</sub> % variation diagram.

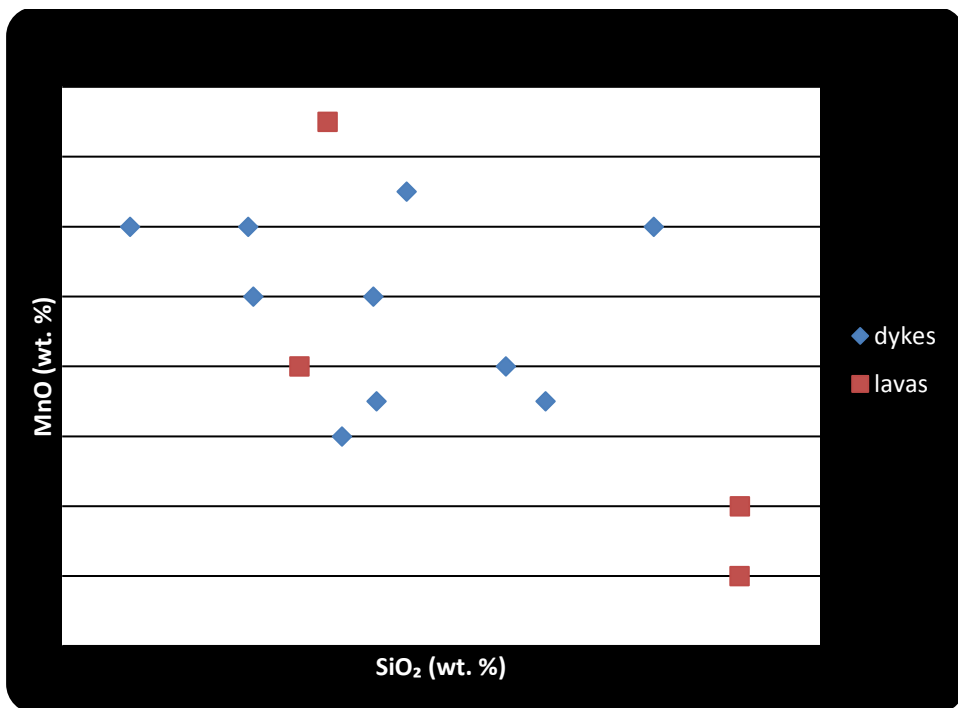


Figure 58. MnO% vs SiO<sub>2</sub> % variation diagram.

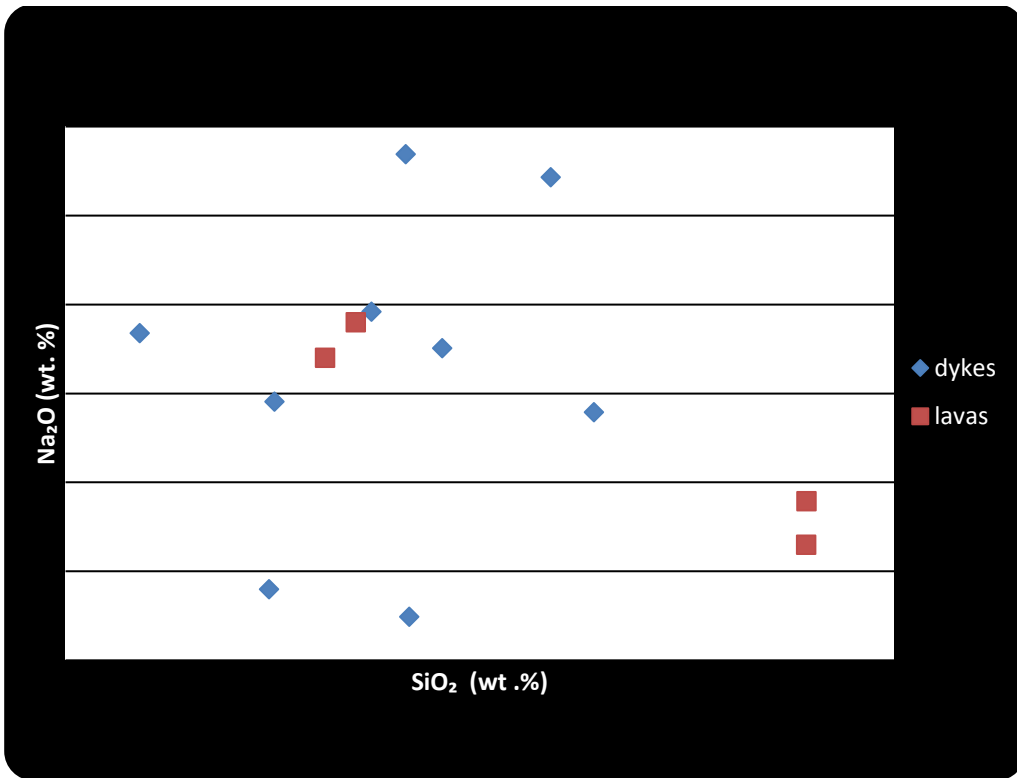


Figure 59. Na<sub>2</sub>O% vs SiO<sub>2</sub> % variation diagram.

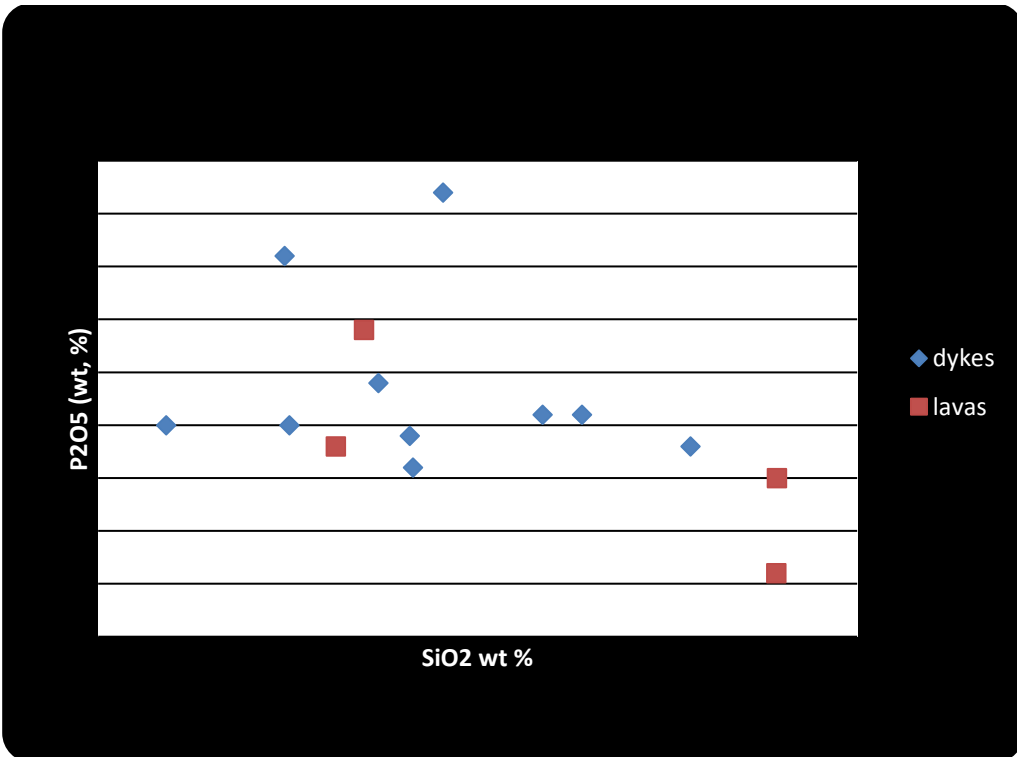


Figure 60. P<sub>2</sub>O<sub>5</sub> % vs. SiO<sub>2</sub> % variation diagram.

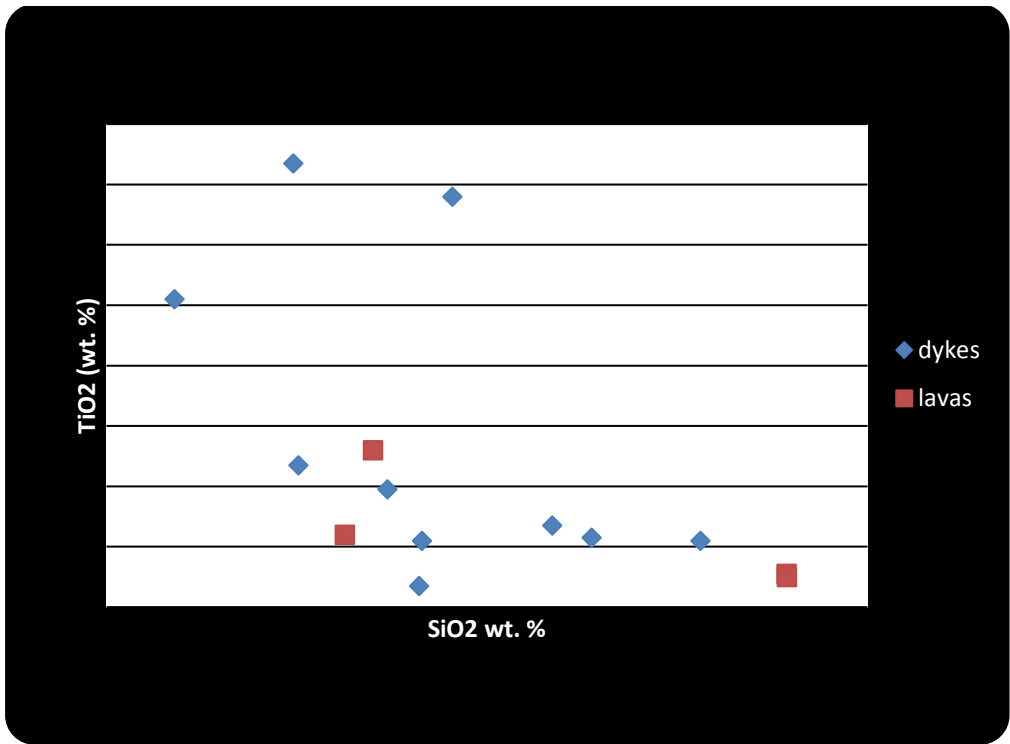


Figure 61. TiO<sub>2</sub> % vs. SiO<sub>2</sub> % variation diagram.

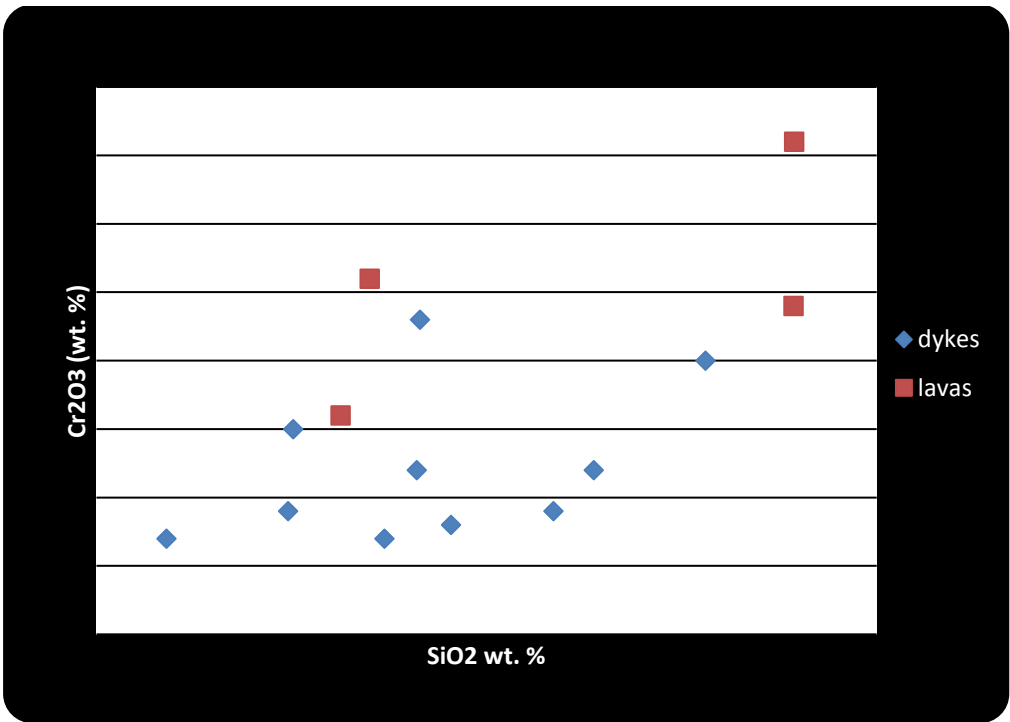


Figure 62. Cr<sub>2</sub>O<sub>3</sub> % vs. SiO<sub>2</sub> % variation diagram

#### 4.5. Trace and Rare Earth Element Chemistry

Trace elements, that are present in much lower concentrations in rocks than major elements also differ from them in another property; they are incorporated into the crystal structure of fewer minerals. This is an important point as it aids in many petrological interpretations; e.g. making approaches to magmatic differentiation or magma source. Trace element analysis of the samples is given in Table 2.

Table 2. Trace and rare earth element analysis of the studied samples.

	Ba	Be	Co	Cs	Ga	Hf	Nb	Rb	Sn	Sr
	PPM	PPM	PPM	PPM	PPM	PPM	PPM	PPM	PPM	PPM
<b>Sample</b>										
IPS-01 (dyke)	172	1	30.1	1.4	16.4	2.1	8.0	19.3	1	521.7
IPS-02 (dyke)	221	<1	24.8	0.1	15.8	2.3	7.6	29.0	1	796.4
IPS-03 (dyke)	1182	<1	23.3	0.6	13.1	2.1	9.1	86.5	1	468.7
IPS-04 (dyke)	116	<1	25.3	<0.1	13.7	1.4	3.0	3.2	1	575.0
IPS-05 (dyke)	474	<1	18.7	0.2	16.7	8.1	15.9	43.6	3	448.5
IPS-06 (dyke)	147	<1	11.6	0.2	16.4	4.1	9.6	19.5	1	250.6
IPS-07 (dyke)	366	<1	10.8	0.8	17.5	4.6	9.8	43.9	1	424.6
REC-14 (dyke)	153	8	21.0	0.6	19.6	4.5	7.2	11.8	<1	413.8
REC-15 (dyke)	117	<1	28.6	0.5	18.1	6.6	15.6	18.7	1	255.7
REC-16 (lava)	372	<1	33.0	0.2	15.8	2.0	9.8	19.1	<1	483.5
REC-17 (lava)	16	<1	27.3	<0.1	17.5	2.0	7.9	0.5	<1	262.0
REC-18 (dyke)	117	7	9.1	0.5	17.2	4.2	7.2	14.1	<1	214.6
REC-19 (lava)	87	<1	5.5	0.4	15.1	3.2	9.5	11.7	<1	321.0
REC-20 (lava)	79	15	13.6	0.7	14.4	2.4	7.7	10.6	<1	239.0

Table 2. continued

	Nd	Sm	Eu	Gd	Tb	Dy	Ho	Er	Tm	Yb	Lu
	PPM	PPM	PPM	PPM	PPM	PPM	PPM	PPM	PPM	PPM	PPM
<b>Sample</b>											
IPS-01 (dyke)	14.4	3.29	1.09	3.48	0.56	3.15	0.65	1.91	0.28	1.64	0.26
IPS-02 (dyke)	16.7	3.33	0.94	3.35	0.54	3.10	0.60	1.70	0.25	1.66	0.25
IPS-03 (dyke)	12.1	2.60	0.84	2.63	0.45	2.52	0.52	1.42	0.21	1.45	0.22
IPS-04 (dyke)	11.6	2.74	0.84	2.66	0.44	2.58	0.55	1.55	0.24	1.50	0.24
IPS-05 (dyke)	29.8	7.51	1.85	8.62	1.52	8.61	1.88	5.55	0.84	5.43	0.82
IPS-06 (dyke)	14.3	3.15	1.02	3.44	0.61	3.42	0.74	2.13	0.33	2.31	0.36
IPS-07 (dyke)	16.7	3.38	1.02	3.52	0.60	3.49	0.74	2.39	0.35	2.46	0.39
REC-14 (dyke)	13.7	4.39	1.29	5.06	0.90	5.34	1.13	3.63	0.52	3.52	0.47
REC-15 (dyke)	30.5	7.45	1.70	8.82	1.56	8.60	2.00	5.85	0.87	5.22	0.79
REC-16 (lava)	18.4	3.56	1.15	3.74	0.57	3.55	0.65	1.89	0.28	1.66	0.24
REC-17 (lava)	12.4	2.59	0.75	2.90	0.43	2.53	0.52	1.53	0.22	1.52	0.22
REC-18 (dyke)	14.0	3.19	1.10	3.46	0.65	3.93	0.83	2.30	0.37	2.08	0.41
REC-19 (lava)	12.0	2.29	0.87	2.69	0.42	2.30	0.44	1.57	0.20	1.29	0.23
REC-20 (lava)	11.8	2.03	0.69	1.82	0.33	1.78	0.36	1.10	0.14	0.98	0.18

Table 2. continued

	Ta	Th	U	V	W	Zr	Y	La	Ce	Pr
	PPM	PPM	PPM	PPM	PPM	PPM	PPM	PPM	PPM	PPM
<b>Sample</b>										
IPS-01 (dyke)	0.4	1.8	0.5	305	<0.5	78.8	17.8	11.1	27.2	3.47
IPS-02 (dyke)	0.4	2.2	0.7	249	2.9	89.0	16.2	12.7	29.6	3.60
IPS-03 (dyke)	0.4	2.3	0.6	257	3.2	89.1	14.1	12.7	25.4	2.95
IPS-04 (dyke)	0.1	2.7	0.7	184	4.0	53.7	14.6	11.5	24.1	3.02
IPS-05 (dyke)	1.1	6.7	1.8	214	4.9	310.7	48.5	22.8	56.3	6.86
IPS-06 (dyke)	0.8	3.8	1.0	68	5.4	158.7	19.0	13.5	30.1	3.39
IPS-07 (dyke)	0.7	4.0	1.1	48	4.0	168.3	20.2	14.2	32.0	3.65
REC-14 (dyke)	0.4	2.2	0.7	203	<0.5	173.3	30.5	9.0	23.0	3.22
REC-15 (dyke)	1.0	5.3	1.6	306	0.7	302.1	54.8	21.4	48.7	6.49
REC-16 (lava)	0.5	1.9	0.7	253	<0.5	85.3	19.1	14.2	29.2	3.58
REC-17 (lava)	0.4	2.4	0.7	221	<0.5	75.6	14.4	12.4	23.2	2.67
REC-18 (dyke)	0.4	1.6	0.6	66	0.9	160.8	23.9	13.2	25.2	3.26
REC-19 (lava)	0.6	1.7	0.5	62	<0.5	130.8	14.8	11.8	21.7	2.70
REC-20 (lava)	0.7	1.6	0.4	73	<0.5	118.2	10.7	12.4	20.7	2.55

Table 2. continued

	Mo	Cu	Pb	Zn	Ni	As	Cd	Sb	Bi	Ag	Au	Hg	Tl	Se
	PPM	PPM	PPM	PPM	PPM	PPM	PPM	PPM	PPM	PPM	PPB	PPM	PPM	PPM
<b>Sample</b>														
IPS-01 (dyke)	1.5	162.2	2.2	59	17.4	1.1	<0.1	<0.1	<0.1	<0.1	1.7	<0.01	<0.1	<0.5
IPS-02 (dyke)	1.1	32.5	2.6	70	12.5	1.9	<0.1	<0.1	<0.1	<0.1	1.3	<0.01	<0.1	<0.5
IPS-03 (dyke)	1.2	56.4	2.1	52	30.1	1.7	<0.1	<0.1	<0.1	<0.1	1.3	<0.01	<0.1	<0.5
IPS-04 (dyke)	1.7	168.5	3.2	81	8.6	0.9	<0.1	<0.1	<0.1	<0.1	2.2	<0.01	<0.1	<0.5
IPS-05 (dyke)	2.3	104.6	8.9	98	6.3	0.6	0.1	<0.1	<0.1	<0.1		<0.01	<0.1	<0.5
IPS-06 (dyke)	1.7	29.4	4.8	66	4.0	1.0	<0.1	<0.1	<0.1	<0.1	<0.5	0.01	<0.1	<0.5
IPS-07 (dyke)	1.8	26.4	6.0	68	5.1	1.2	0.2	<0.1	<0.1	<0.1	<0.5	0.04	<0.1	<0.5
REC-14 (dyke)	0.5	71.3	3.7	93	9.3	1.2	<0.1	<0.1	0.2	<0.1	<0.5	0.13	<0.1	<0.5
REC-15 (dyke)	2.3	111.8	5.3	74	12.7	<0.5	<0.1	<0.1	<0.1	<0.1	1.0	0.01	<0.1	<0.5
REC-16 (lava)	1.0	643.4	3.1	73	45.6	18.5	0.1	<0.1	<0.1	<0.1	1.9	<0.01	<0.1	<0.5
REC-17 (lava)	0.6	100.0	3.9	62	27.9	0.8	0.1	<0.1	<0.1	<0.1	9.8	<0.01	<0.1	<0.5
REC-18 (dyke)	2.9	20.5	4.3	20	11.4	1.0	<0.1	<0.1	<0.1	<0.1	<0.5	0.02	<0.1	<0.5
REC-19 (lava)	5.0	21.8	0.8	13	17.1	<0.5	<0.1	<0.1	<0.1	<0.1	<0.5	<0.01	<0.1	<0.5
REC-20 (lava)	3.3	24.1	1.1	26	13.8	0.6	<0.1	<0.1	<0.1	<0.1	<0.5	<0.01	<0.1	<0.5

REE, with atomic numbers between 57 (La) and 72 (Lu), characterized by relatively large ionic radii, HFSE (Ti, Zr, Y, Nb, Hf, P, Th,..) and transition metals (Sc, V, Cr) have been proven to be relatively immobile during low temperature alteration processes in basic rocks. Therefore, these are the elements that can be utilized as petrogenetic indicators, and are used to make related interpretations (Pandit et al., 2011 and references therein; Pearce et al. 1984; Winchester and Floyd, 1976, 1977).

Large ion lithophile elements (LILE), characterized by large ionic radii, and low charges are largely incompatible with respect to mantle phases; therefore they tend to concentrate in the liquid unless a particular mineral with large sites accommodates them in the crystal structure.

Both groups of dyke and lava samples show enrichment in LILE and LREE however some samples exhibit higher enrichment levels. There are some differences in shape and pattern of a few samples, which is important to investigate as it might be related to distinct source characteristics. However, difference in patterns are created by a few elements and in general do not stray apart from the rest of the patterns.

A marked peak is observed in K and Th (and Sr) for most of the lava and dike samples.

All of the dike samples show a peak at Ba whereas most of the lava samples show a trough at Ba (Figure 63). Peaks at Ba and K can be considered as a result of mobilization. Peaks at Ta and Th elements are noteworthy. Dyke and lava samples display a great amount compositional variation in Ba and Sr elements; this can be interpreted as a result of mobilization. When preferential partitioning of these components into feldspars is considered, this could reflect variations in fractionation amounts of plagioclase; however secondary processes have a non-negligible effect on Boyalı volcanics. In addition, for samples with strikingly different amounts; magma represented by these samples is likely to have experienced differing amounts of feldspar, as well as biotite fractionation. This is also reflected in the petrographical examinations; given that the presence and abundance of these minerals vary in thin sections.

Most of the samples exhibit enrichment in Rb. This is also due to feldspar fractionation has removed, as it removes Sr and K from the liquid, remaining melt is progressively enriched in Rb.

Most of the samples exhibit LILE (Sr, K, Rb, Cs, Ba) enrichment. This was probably an effect of fluids expelled from the subducting slab that influx into the mantle wedge to initiate melting of the lithospheric mantle and cause LILE enriched melts to be generated. So enrichment of LILE, together with depletion of HFSE (Ti, Nb, Ta, Hf) occurred as a result of subduction derived fluids in the case of Boyalı volcanics.

One of the lava samples show a trend somewhat distinct from the others in terms of shape and abundance of certain elements (K, Rb, Ba and P).

Negative Nb-Ta anomalies are diagnostic features of subduction-related arc volcanic rocks. (Pearce et al., 1984). Based on this assumption, Nb-Ta anomalies which are weakly developed might indicate transition from subduction related magmatism to within-plate magmatism; from previously erupted ones to younger ones. Among the samples the intensity of these negative anomalies differ. Especially one of the dyke samples display a Nb-Ta anomaly sharper than the others, straying from the general trend; whereas some samples display weaker anomalies. However, overall these are not notable enough to consider the above theory in Boyalı rocks.

High field strength elements (HFSE) are not compatible with the mantle phases;

therefore, are excluded from them and are left in residual melts. Consequently, accessory phases accommodate these elements. Given that apatite fractionation is observed, especially, depletion in P amounts is related to formation of this accessory phase in one of the lava samples.

Negative Ti anomaly is observed in variable amounts in the samples; whereas stronger negative Ti anomalies are evident in dyke samples. This is consistent with abundance of Fe-Ti oxides in which Ti is predominantly partitioned in, as indicated in the petrography section. This could have been reinforced by Ti substitution for Mg and Fe ions in silicate phases such as amphiboles and mica; in particular hornblende and biotite in the case of Boyalı dykes. Another reason for Ti anomalies could be crustal contamination as stated by Taylor and McLennan (1985).

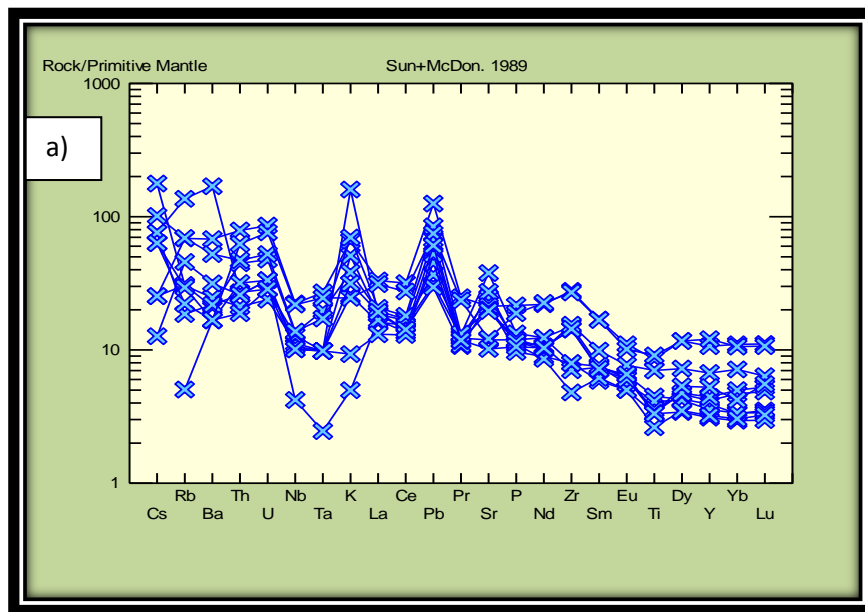


Figure 63. Primitive mantle-normalized trace element patterns of a) dyke samples b) lava samples (Normalized values are from Sun and McDonough, 1989).

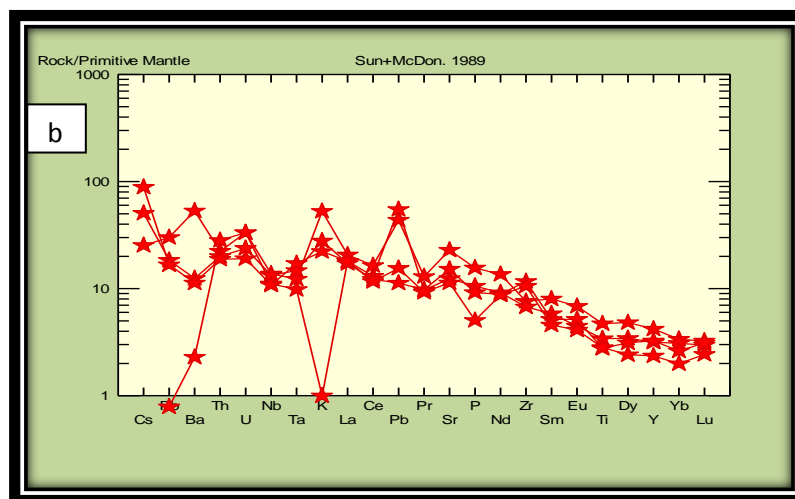


Figure 63. continued.

REE's are plotted on the diagram of Sun and McDonough (1989) to utilize them for petrogenetic interpretations (Figure 64). Chondrite normalization is applied to smoothen large differences in concentration between different REE's. A negative slope is observed for the plot of lava and dyke samples in heavy REE's; indicating garnet was present in the source magma as garnet tends to accommodate HREE's more compared to the LREE's.

Eu/Eu\* values vary between 0.07-0.09 in lava samples and 0.06-0.09 in dyke samples indicating small negative Eu anomaly. This is consistent with an Eu depleted magma for both lava and dyke samples; hence negative Eu anomalies as Eu incorporated into plagioclase.

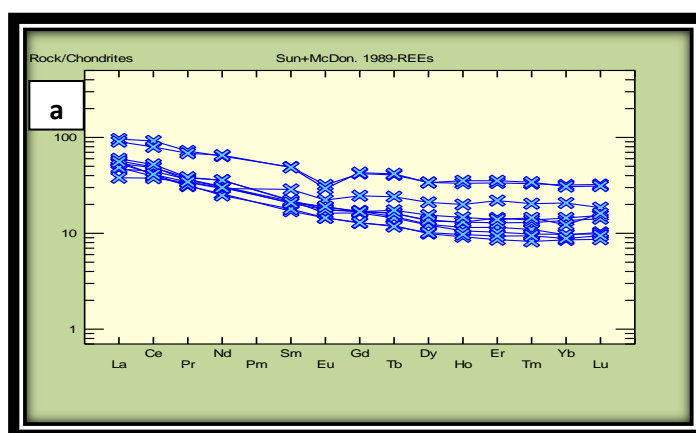


Figure 64. Chondrite normalized REE patterns a) for dyke samples b) for lava samples (Normalized values are from Sun and McDonough, 1989).

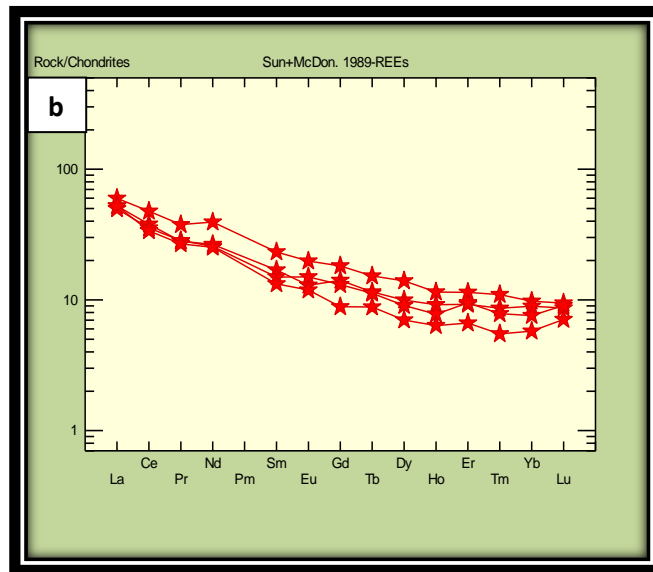


Figure 64. continued.

Typical subduction zone geochemical signatures and continental signatures are reflected in enrichments in LREE, K, Rb, Ba and Th and; depletions in Nb and HFSE. These changes are likely to have occurred mainly due to subduction fluids. A marked Eu anomaly is observed in dike samples, whereas this signature is almost absent in half of the lava samples (Figure 36). Eu anomalies lava and dyke samples indicate that plagioclase was a major fractionating phase.

Depleted HREE patterns are suggestive of garnet as a refractory phase in the source of these rocks; also indicative of depth of partial melting (>80 km; garnet lherzolite) as Wilson (1989) stated, residual garnet would cause HREE depletion due to their preferential retention.

For all examined samples, relative LREE enrichment is significant; indicated by approximately 40 to 100 times to chondrite; however it occurs on higher levels for two of the dyke samples; which is 90 and 100 times, that can be traced clearly from the pattern.

#### 4.6. Classification

Since the samples in this study are affected by alteration and having developed secondary alteration minerals in the vesicles and cracks, we utilized a diagram that makes use of abundances of immobile elements such as Zr, Ti, Nb and Y in the studied samples. A Zr/Ti vs Nb/Y diagram further developed by Pearce (1996) after Winchester and Floyd (1977) is chosen (Figure 65) and the samples are classified on the basis of these immobile elements. Samples mainly plot in the andesite and basalt+andesite, as well as basalt fields, half of the lavas plotting in the latter.

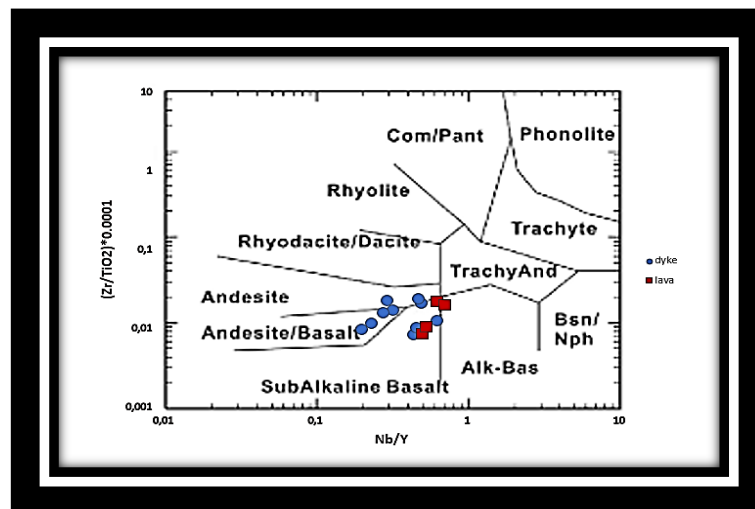


Figure 65. Chemical classification of the dykes and lavas of the Boyalı Volcanics on the basis of immobile elements (Winchester and Floyd, 1977).

#### 4.7. Tectonomagmatic Discrimination

In order to infer the tectonomagmatic affiliation of old rocks, geochemical data is plotted on tectonomagmatic discrimination diagrams to determine which boundary the investigated samples fall into and thus which tectonic setting they are generated in. As explained in Pandarinath and Verma (2013) these diagrams are based on the following assumptions:

1. Concentrations of the characteristic chemical elements being used in the discriminate diagrams differ widely in rocks, from one tectonic setting to the other.
2. These characteristic chemical elements of the rocks are relatively immobile from the period of rock formation to the present.

On the Ti vs Zr diagram (Pearce and Cann, 1973) most of the samples fall into the calc-alkali field with only two exceptions from dikes; one being left out of the determined borders and the other falling into the island arc tholeiite field (Figure 66).

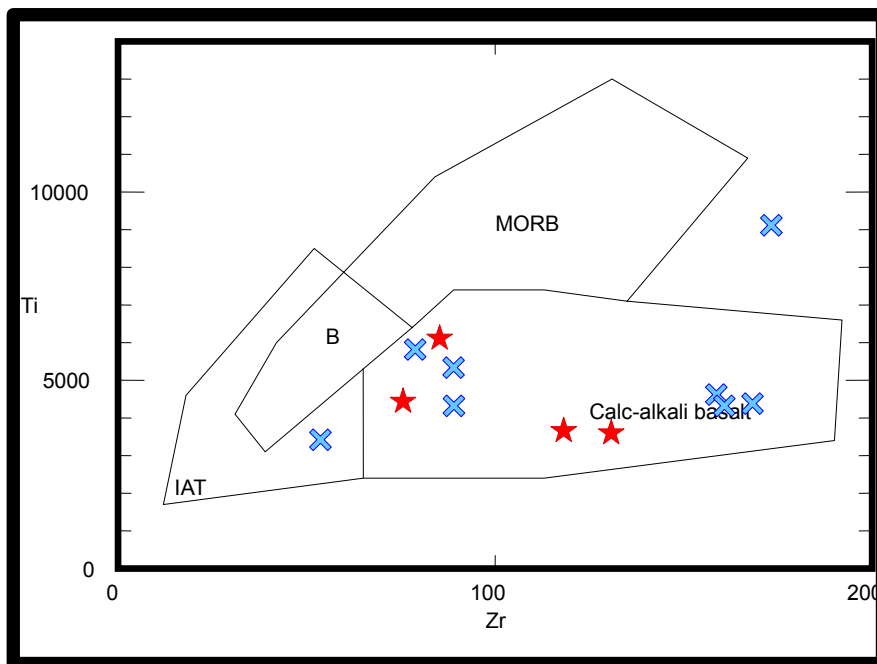


Figure 66. Zr vs Ti diagram of the Boyalı dykes (blue) and lavas (red) after Pearce (1982) .

Using the Zr-Ti/100-Y\*3 diagram (Pearce and Cann, 1973) important interpretations can be obtained (Figure 67).

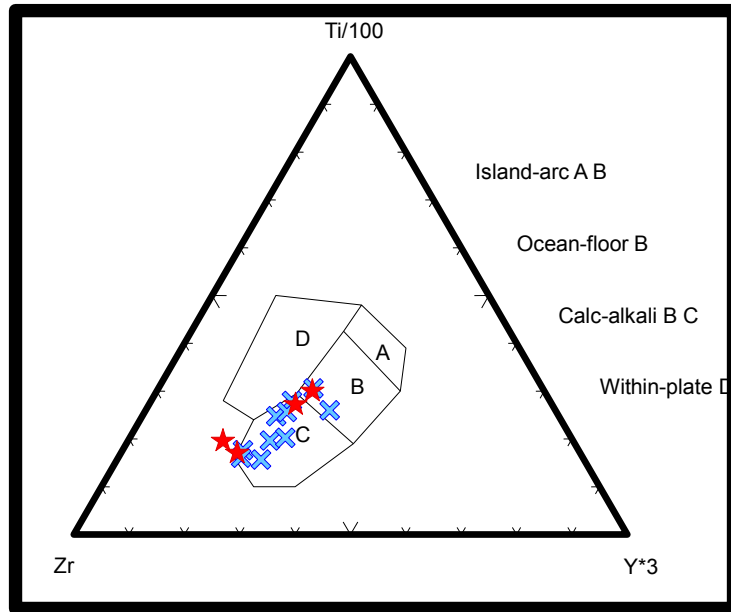


Figure 67. Zr-Ti/100-Y\*3 diagram (Pearce and Cann, 1973) of the Boyalı dykes (blue) and lavas (red).

Samples plotted on Zr/Y-Ti/Y diagram of Pearce and Gale (1977) (Figure 68) fall onto the plate margin basalts field, which is in correlation with previously plotted discriminations.

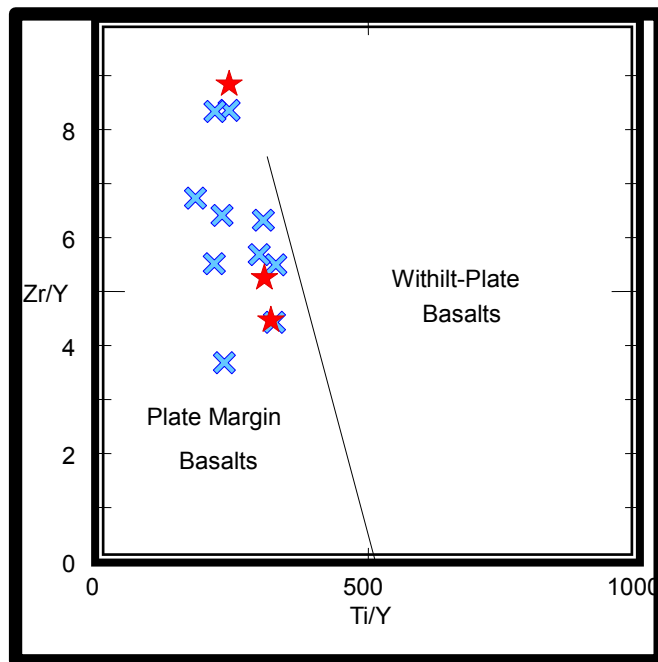


Figure 68. Zr/Y-Ti/Y diagram of the Boyalı dykes (blue) and lavas (red) after Pearce and Gale (1977)

The samples are distributed across a couple of fields using V and Ti elements (Figure 69) as designed by Shervais (1982).

On the other hand, as illustrated in Figure 70, with the help of the Zr-Ti/100-Y\*3 diagram of Pearce and Cann (1973), samples of the Boyalı lavas (red) and dykes (blue) plot into the calc-alkaline (fields B and C) and within-plate basalt fields (field D).

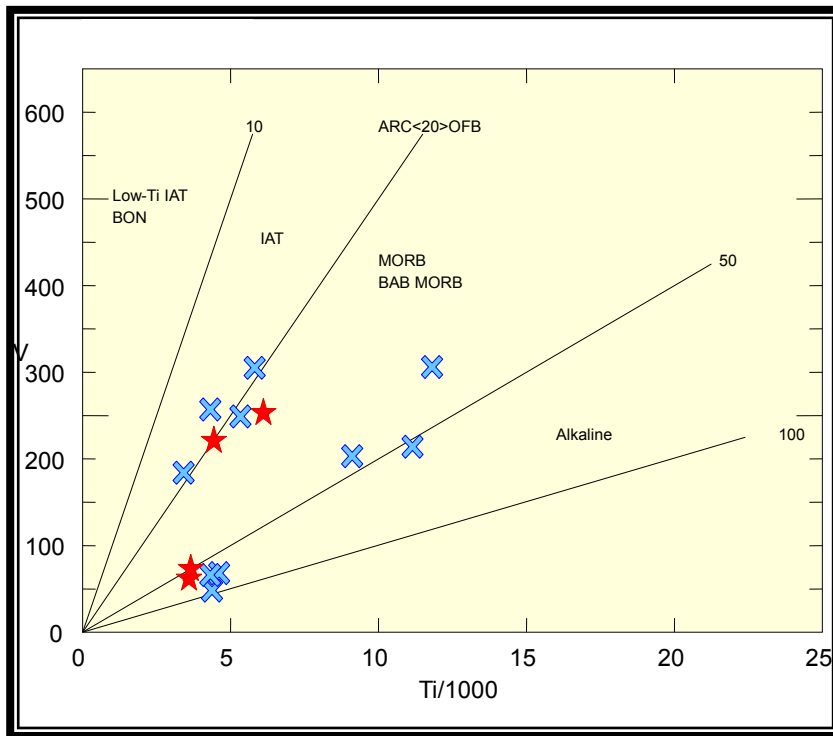


Figure 69. Ti/1000 vs V diagram of the Boyalı dykes (blue) and lavas (red) (Shervais, 1982).

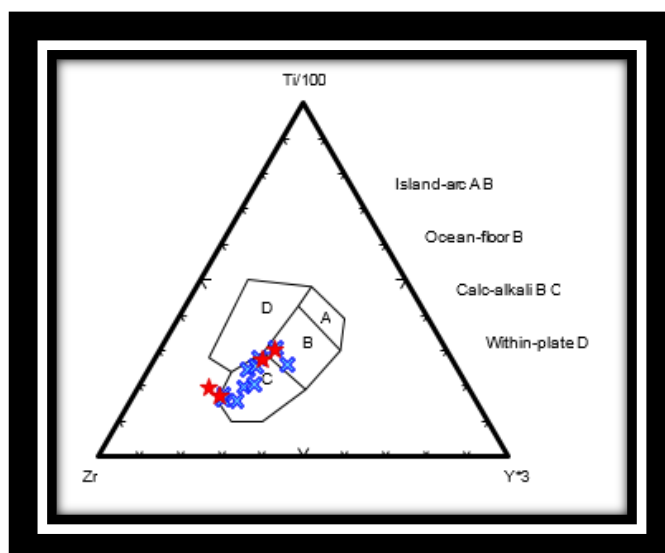


Figure 70. Zr-Ti/100-Y\*3 diagram of the Boyalı dykes (blue) and lavas (red) after Pearce and Cann (1973).

Th/Yb vs Ta/Yb diagram (Figure 71) appears to have an overall perpendicular trend observed on dyke samples. While, it is difficult to interpret the trend on lava samples due to scarcity of samples, the samples that have been obtained seem to show a partly similar trend to the dyke samples; with more inclination towards the crustal contamination vector. This could suggest that sources of the lavas that show a crustal contamination trend had different geochemistry.

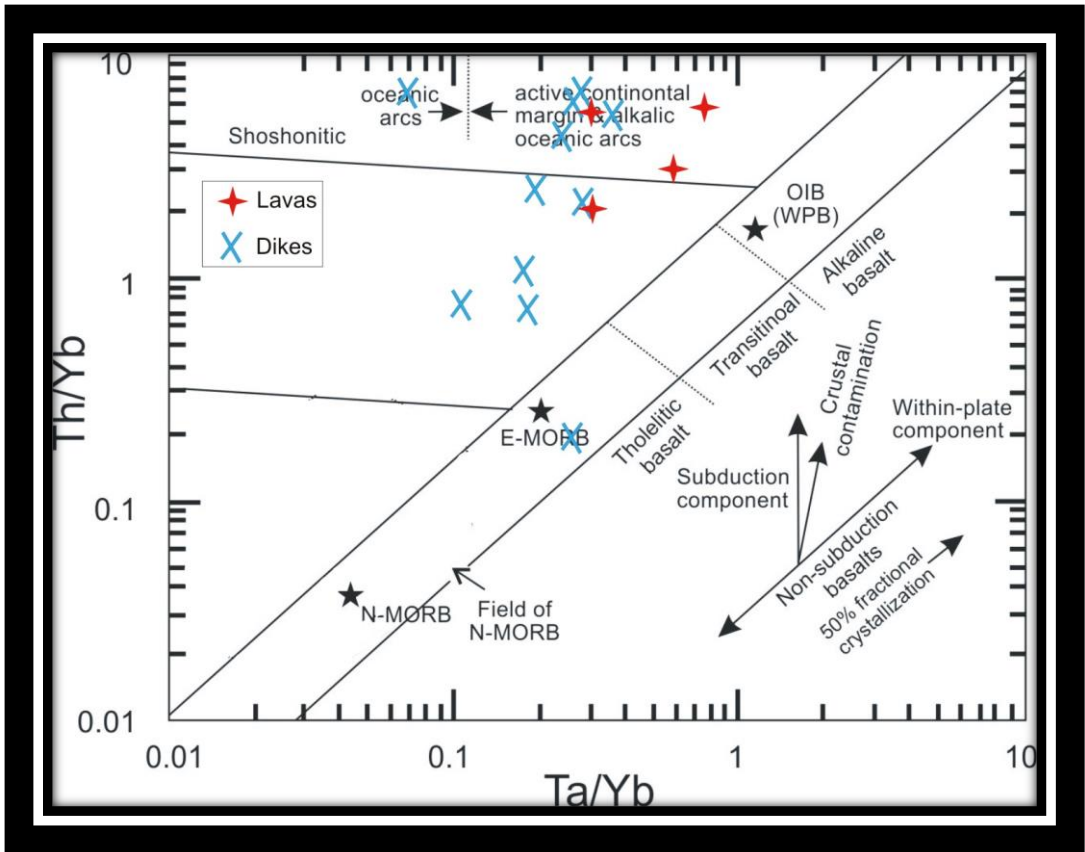


Figure 71. Evolution lines of the studied volcanic rocks in Th/Yb vs Ta/Yb diagram.

By this the geochemical data of the lavas as well as the dikes is in favour of a tectonic environment with combination of an arc with continental crust contamination. Such a tectonic environment is mainly interpreted as a continental back-arc (e.g. Stern, 1985)

#### 4.8. Source

To evaluate the source of the dikes and lavas of the studied volcanic rocks we considered the Th/Yb versus Ta/Yb diagram (Fig 69) and the REE pattern (Fig...) of the samples.

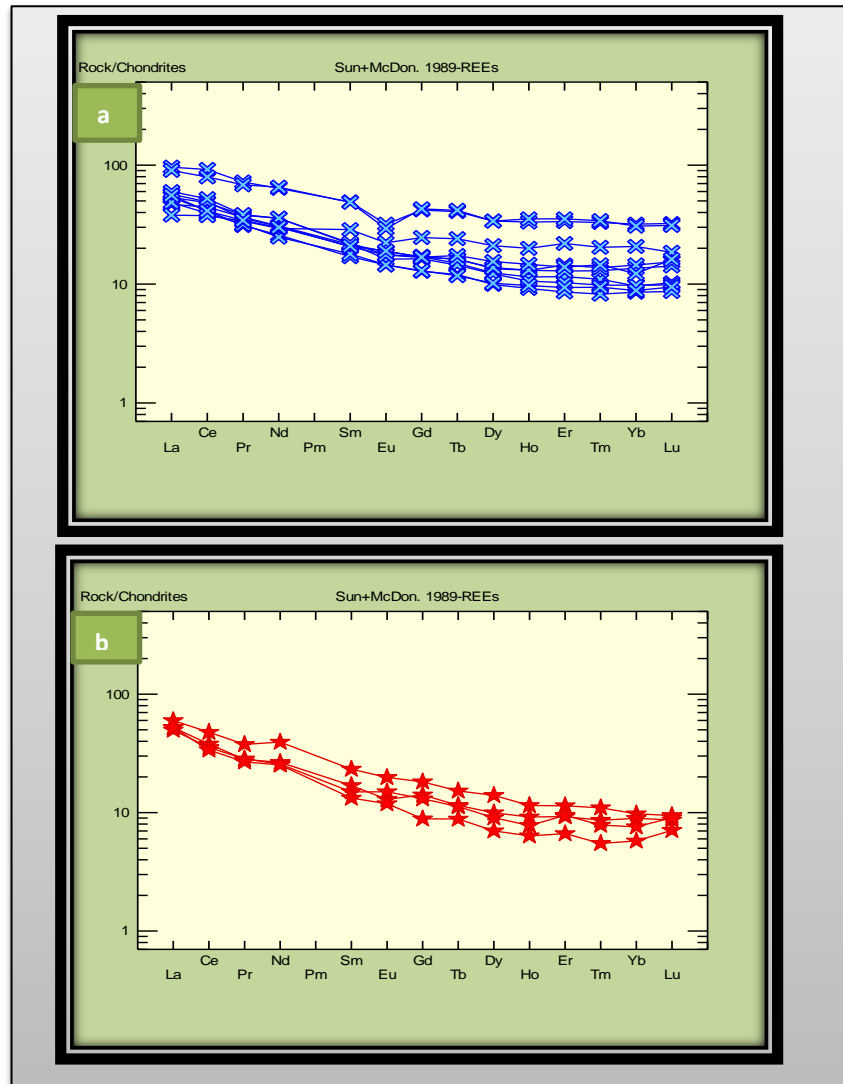


Figure 72. Chondrite normalized REE patterns a) for dyke samples b) for lava samples (Normalizing values are from Sun and McDonough, 1989).

“Genesis at Active Continental Margins” by Pearce et al.(1984) explained the generation of basalts in volcanic arc environments: usually enriched in LIL (Large Ion Lithophile elements) and in some cases in light rare-earth elements and P regardless of the nature of the mantle. Components of active continental margins are different than those of oceanic island arcs in terms of additional elements such as Nb, Ta, Zr and Hf which are not present in environments of subduction or crustal origin. Trace element enriched metasomatized subcontinental lithosphere. Geological patterns normalized to MORB values are used to demonstrate the relative contributions of the subduction and lithosphere components to the composition of active continental margin basalts. Rb, K, Ba, Th and Sr contents are mainly derived from the subduction

zone; Ce, Sm and P are provided by the lithosphere, in greater amounts compared to the contribution coming from the subduction zone. In addition all of Ta, Nb, Zr, Hf, Ti, Y and Yb are of lithospheric origin as well.

## CHAPTER 5

### DISCUSSION AND CONCLUSIONS

Volcanism in Boyalı has been investigated, first by field observations, then petrographic examinations and geochemical approaches. Volcanism has been revealed to be occurring in different forms: in addition to several dykes, pillow and massive lava flows are observed as syndimentary intercalations with the metaclastic and volcano-clastic successions and gravity-flow deposits. As a result of plotted rose diagrams and stereographic projections of the dikes, paleostress tensor is indicative of an extensional strike-slip tectonic regime for the formation of dykes, with horizontal maximum and minimum stress axes oriented NE-SW and NW-SE, respectively.

Petrographic investigations indicate that dyke and lava samples of porphyritic character are characterized by plagioclase, pyroxene and biotite as major phases. On plagioclases, sieve texture is commonly observed. Penetration of melt into the crystal structure resulted in this texture and possibly indicates placement into a magma which not in equilibrium by their composition,; therefore magma mixing. Petrographic evidences of magma mixing is further supported by partial resorption observed especially in the major minerals, Glassy inclusions are observed on some of the plagioclase phenocrysts. While these inclusions indicate rapid growth and related trapping of melt within the crystal; the fact that some minerals have experienced it;

and some have not is in favor of magma mixing.

Geochemically, the dike and lava samples are found to be mainly basalts, basaltic andesites and andesites, when plotted on the Zr/Ti vs Nb/Y diagram (Pearce 1996, after Winchester and Floyd, 1977)). Fractionation trends of Boyalı volcanics are monitored on Harker diagrams of elements plotted against SiO<sub>2</sub>, which indicate plagioclase, pyroxene and iron-titanium oxides. Lava and dyke samples are in correlation, which supports genetic relation of these volcanics. Correlations of Zr with other elements highlights the importance of fractional crystallization processes.

REE diagrams plotted are LREE enriched and have a negative slope for both of the lava and dyke samples. This indicates garnet was present in the source rock from which the magma formed. Eu anomalies observed on REE diagrams support petrographic observations that plagioclase is an important fractionation phase; however not in the same amount for all samples.

Samples plotted on the tectonomagmatic discriminations diagrams fall onto the calc alkali field and suggest generation in a destructive margin for Boyalı volcanics. Similarities in geochemical features, supported by petrographic examinations, on the other hand, suggest these dykes could be the feeders of lavas in the Boyalı region.

Regarding the source and tectono-magmatic setting of the dikes and lavas of the Boyalı Volcanics; the evaluation of trace element abundances, LILE and LREE enrichment is observed on both dyke and lava samples. It is likely that fluids expelled from the subducting slab that influx into the mantle wedge to initiate melting of the lithospheric mantle caused the generation of LILE enriched melts that formed Boyalı volcanics, which suggests arc affinity to them. Negative Nb-Ta anomalies further supports a subduction-related arc character of volcanic rocks examined. On the other hand the transitional character of the rocks to within-plate magmatics is of importance. Considering their geological setting as dikes cutting the Late Cretaceous foreland deposits and their Sakarya Composite Terrane-type basement (e.g. Catanzariti et al 2013) the Boyalı Volcanics are obviously formed in a within-plate setting. The orientation of the dikes further indicate that their formation is related to an extensional setting. The combination of these geochemical and geological data suggests that the geological setting of the studied volcanic rocks was a back-arc basin. On the basis of

regional geological constraints together with geochemical characteristics we suggest that the Boyalı Volcanic rocks were formed in relation to a back-arc basin within the Sakarya Composite Terrane above the N-ward subducting Izmir-Ankara oceanic lithosphere of Neotethys.

Similar volcanic rocks (Tafano Unit) were recently recognized in the SE part of the study area by Ellere et al (2016), just to south of Tosya in the Central Pontides. In this area basalts, basaltic andesites and their pyroclastic are found within the Late Cretaceous (late Santonian-middle Campanian age marly-calcareous turbidite formation. The geochemistry of the volcanic rocks reveals an active continental margin setting as evidenced by the enrichment in Th and LREE over HFSE, and the Nb-enriched nature of these lavas relative to N-MORB. In their tectonic evaluation, Ellere et al (2016) discuss alternative geodynamic reconstructions previously proposed and conclude that this tectonic unit could represent a slice derived from the northern continental margin of the Intra-Pontide or Izmir-Ankara-Erzincan oceanic basins.

In the Boyalı area, the structural position of the Taraklı Flysch is well-established by the previous study of Catanzariti et al (2013). Here, the basement of the flysch basin is the Mesozoic cover of the Sakarya Composite Terrane. Hence, the extension-related basin formation and the Boyalı volcanism were developed on its continental crust. By this, we favour a model suggesting that the studied area was on the northern continental margin of the Izmir-Ankara-Erzincan oceanic basin, behind the continental arc formed during the northward subduction of its lithosphere beneath the Sakarya microcontinent.

Following conclusions can be obtained from our study:

- The Boyalı volcanic rocks occur as dikes and lava flows within the Late Cretaceous turbidites known as the Taraklı Flysch. They are mainly basalts, andesites and basaltic andesites. Their petrographic and geochemical characteristics suggest that they are co-genetic.
- The dikes were emplaced as more or less parallel sheets and extend in NE-SW direction indicating a NW-SE extension within the flysch basin during their formation.
- Geochemically the dykes and lavas range from sub alkaline to alkaline basalts in composition. Majority of lava and dyke samples are of calc alkaline

character. Based on immobile REE and trace element diagrams the source of the magmatism is interpreted as a subduction-modified mantle with crustal contamination. Tectono-magmatic evaluation combined with regional geological constraints suggests a continental back-arc extension for the formation of Boyalı volcanics.

- Considering the regional geological setting, it is put forward that the Boyalı volcanic rocks were formed within the Sakarya continental crust in relation to an extensional back-arc basin above the N-ward subducting Neotethyan Izmir-Ankara oceanic lithosphere.

## REFERENCES

- Anderson, C.A., and Blacet, P.M., 1972. Precambrian geology of the northern Bradshaw Mountains, Yavapai Country, Arizona, Bulletin 13-36.
- Akartuna, M., 1968. Geology of the Armutlu Peninsula. Istanbul Üniversitesi Fen Fakültesi Monografileri, 20), 105p.
- Altner, D., Koçyiğit, A., Farrinacci, A., Nicosia, U., Conti, M. A. 1991. Jurassic-Lower Cretaceous Stratigraph and Paleogeographic Evolution of the Southern Part of North-Western Anatolia (Turkey): Geology and Paleontology of Western Pontides, Turkey. (Ed.). A.Farrinacci, D. V. Ager, U. Nicosia), *Geologica Romana*, v. XXVII, Roma.
- Altunkaynak, Ş. and Dilek, Y., 2013 Eocene mafic volcanism in northern Anatolia: its causes and mantle sources in the absence of active subduction. *International Geology Review*, vol. 55(13), 1641-1659.
- Bektaş, O., 1987. Volcanic belts as markers of the Mesozoic-Cenozoic active margin of Eurasia—discussion. *Tectonophysics*, 141(4), 345-347.
- Bozkurt, E., 2001. Neotectonics of Turkey—a synthesis. *Geodinamica Acta*, 14(1-3), 3-30.
- Bozkurt, E., Piper, J.D. and Winchester, J.A. eds., 2000. Tectonics and magmatism in Turkey and the surrounding area. Geological Society of London.
- Catanzariti, R., Ellero, A., Göncöoğlu, M.C., Marroni, M., Ottria, G., Pandolfi, L., 2013. The Taraklı Flysch in the Boyalı area (Sakarya Terrane, Northern Turkey): Implications for the Tectonic History of the IntraPontide Suture Zone. *Compte Rendu Geosciences* 345, 454–461.

Chen, J.F., Yan, J., Xie, Z., Xu, X., Xing, F., 2001. Nd and Sr isotopic compositions of igneous rocks from the Lower Yangtze region in eastern China: constraints on sources. *Physics and Chemistry of the Earth, Part A*, 26, 719–731.

Delaloye, M., and Bingol, E., 2000. Granitoids from western and northwestern Anatolia: Geochemistry and modeling of geodynamic evolution. *International Geology Review*, 42, 241-268.

Dercourt, J., Zonenshain, L.P., Ricou, L.E., Le Pichon, X., Knipper, A.L., Grandjaquet, C., Sbertshikov, I.M., Geussant, J., Lepvrier, C., Pechersku, D.H., Boulin, J., Bazhenov, M.L., Lauer, J.P., Biju-Duval, B., 1986. Geological evolution of the Tethys belt from the Atlantic to the Pamirs since the Lias. *Tectonophysics* 123, 241 – 315.

Elmas A. and Yigitbas E., 2001. Ophiolite emplacement by strike–slip tectonics between the Pontide Zone and the Sakarya Zone in northwestern Anatolia, Turkey. *Int. J. Earth Sci. (Geol.Rundsch.)*, 90, 257-269.

Floyd, P. A., Yaliniz, M. K., and Göncüoğlu, M. C., 1998. Geochemistry and petrogenesis of intrusive and extrusive ophiolitic plagiogranites, Central Anatolian Crystalline Complex, Turkey. *Lithos*, 42(3), 225-241.

Göncüoğlu, M.C., Erendil, M., Tekeli, O., Aksay, A., Kuşu, Ü., 1987. Geology of the Armutlu Peninsula. IGCP Project 5, Guide Book. Field Excursion along W-Anatolia, 12–18.

Göncüoğlu, M. C., and Erendil, M., 1990. Pre-Late Cretaceous tectonic units of the Armutlu Peninsula. In *Proceedings, 8th Petroleum Congress of Turkey*, 161-168.

Göncüoğlu, M.C., Erler, A., Toprak V., Yaliniz, M.K., Olgun, E., Rojay, B., 1992. Orta Anadolu masifinin bati bölümünün jeolojisi Bolum 2: Orta kesim. TPAO Report No. 3155. 76 pp.

Göncüoğlu, M. C., and Türeli, K., 1993. Petrology and geodynamic interpretation of plagiogranites from Central Anatolian Ophiolites (Aksaray-Turkey). *Turkish Journal of Earth Sciences*, 2, 195-203.

Göncüoğlu, M.C., Dirik, K., and Kozlu, H., 1997. Pre-Alpine and Alpine Terranes in

Turkey: explanatory notes to the terrane map of Turkey. *Annales Geologique de Pays Hellenique*, 37, 515-536.

Göncüoğlu, M.C., and Kozur, H.W., 1998. Facial development and thermal alteration of Silurian rocks in Turkey. In: J.C. Guitierrez-Marco, and I. Rabano, (eds.), *Proceedings of 1998 Field-Meeting, IUGS Subcomission on Silurian Stratigraphy, Temas Geologico-Mineros*, 23, 87-90.

Göncüoğlu M.C., 2001, Turhan, N., Şentürk, K., Özcan, A. and Uysal, Ş. 2000. A geotraverse across NW Turkey: tectonic units of the central Sakarya region and their tectonic evolution. In: Bozkurt, E., Winchester, J. and Piper, J.A. (eds), *Tectonics and Magmatism in Turkey and the Surrounding Area. Geological Society, London, Special Publications 173*, 139–161.

Görür, N., Şengör, A.M.C., Akkök, R. and Yılmaz, Y., 1983. Pontidlerde Neotetisin kuzey kolunun açılmasına ilişkin sedimentolojik veriler. *Bulletin of the Geological Society of Turkey*, 26, 11-20.

Harris, N.B.W., Kelley, S.P. and Okay, A.I., 1994. Postcollision magmatism and tectonics in northwest Turkey: *Contrib. Mineral. Petrol.*, 117, 241-252.

Kadıoğlu Y. K., Dilek Y., 2010. Structure and geochemistry of the adakitic Horoz granitoid, Bolkar Mountains, southcentral Turkey, and its tectonomagmatic evolution, *International Geology Review*, 52 (4–6), 505–535.

Kaya O. and Kozur H., 1987. A new and different Jurassic to Early Cretaceous Sedimentary assemblage in northwestern Turkey (Gemlik, Bursa): Implications for the pre-Jurassic to Early Cretaceous tectonic evolution. *Yerbilimleri* 14, 253-268.

Ketin, I., 1951. Bayburt bölgesinin jeolojisi hakkında. *Ist-Üni. Fen Fak. Mecm.*, 21, 113-127.

Nzegge, O.M., Satir, M., Siebel, W. and Taubald, H., 2007. Geochemical and isotopic constraints on the genesis of the Palaeozoic Deliktas and Sivrikaya granites from the Kastamonu granitoid belt (Central Pontides, Turkey). *Neues Jahrbuch für Mineralogie*, 183(3), 27.

Saner, S. 1977. Geyve–Osmaneli–Gölpazarı–Taraklı Alanının Jeolojisi; Eski Çökeltme Ortamları ve Çökeltmenin Evrimi, Yüksek lisans Tezi, İstanbul Üniversitesi.

Saner, S., 1980. Mudurnu - Göynük havzasının Jura ve sonrası çökeltim nitelikleriyle paleocoğrafya yorumlaması. Türkiye Jeol. Kur. Bült., 23, 39 - 52.

Okay, A.I. 1989. Tectonic units and sutures in the Pontides, northern Turkey. In: ŞENGÖR, A.M.C. (ed), Tectonic Evolution of the Tethyan Region. Kluwer Academic Publications, Dordrecht, 109–115.

Okay, A. I., Şengör, A. C., and Görür, N., 1994. Kinematic history of the opening of the Black Sea and its effect on the surrounding regions. *Geology*, 22(3), 267-270.

Okay, A. I., and Monié, P., 1997. Early Mesozoic subduction in the Eastern Mediterranean: Evidence from Triassic eclogite in northwest Turkey. *Geology*, 25(7), 595-598.

Okay, A.I., and Tüysüz, O., 1999. Tethyan sutures of northern Turkey, in Durand, B., Jolivet, L., Horváth, F., and Séranne, M., The Mediterranean basins: Tertiary extension within the Alpine orogen: Geological Society [London] Special Publication 156, 475–515.

Okay, A.I., Monod, O. and Monié, P., 2002. Triassic blueschists and eclogites from northwest Turkey: vestiges of the Paleo-Tethyan subduction. *Lithos*, 64, 155–178.

Okay, A.I., Satır, M. and Siebel, W., 2006. Pre-Alpide Palaeozoic and Mesozoic orogenic events in the Eastern Mediterranean region. Geological Society, London, *Memoirs*, 32(1), 389-405.

Okay, A.I., Bozkurt, E., Satır, M., Yiğitbaş, E., Crowley, Q.G. and Shang, C.K., 2008. Defining the southern margin of Avalonia in the Pontides: geochronological data from the Late Proterozoic and Ordovician granitoids from NW Turkey. *Tectonophysics*, 461(1), 252-264.

Nakamura, K. 1977. Volcanoes as possible indicators of tectonic stress orientation – principle and proposal. *Journal of Volcanology and Geothermal Research*. 2 (1), 1-16.

- Pandarínath, K., Verma, S. K., 2013. Application of four sets of tectonomagmatic discriminant function based diagrams to basic rocks from northwest Mexico. *Journal of Iberian Geology*, 126, 322-352.
- Pandit, M. K., Sial, A. N., Jamrani, S. S. and Ferreira, V. P., 2001. Carbon isotopic profile across the Bilara Group rocks of trans-Aravalli Marwar Supergroup in Western India: Implications for Neoproterozoic–Cambrian transition; *Gondwana Res.* 4, 387–394.
- Pearce, J.A., Cann, J.R., 1973. Tectonic setting of basic volcanic rocks determined using trace element analysis, *Earth and Planetary Science Letters*, 19, 290-300.
- Pearce, J. A. and Gale, G. H. 1977: Identification of ore deposition environments from trace element geochemistry of associated igneous host rocks. In (Anonymous), *Volcanic processes in ore genesis* and. Inst. Mining Metallurg. , London, 14-24.
- Pearce, J.A., Harris, B.W., Tindle, A.G., 1984. Trace element discrimination diagrams for the tectonic interpretation of granitic rocks. *J. Petrol.*, 25, 956-983.
- Pearce, J. A., 1996. A user's guide to basalt discrimination diagrams. In: Wyman, D. A. (ed.) *Trace Element Geochemistry of Volcanic Rocks: Applications for Massive Sulphide Exploration*. Geological Association of Canada, Short Course Notes 12, 79–113.
- Peccerillo A. and Taylor S.R., 1976. Geochemistry of Eocene calc-alkaline volcanic rocks of the Kastamonu area, northern Turkey. *Contrib Mineral Petrol*, 58, 63- 81.
- Robertson, A.H.F., and Dixon, J.E., 1984. Introduction. In Dixon, J.E., and Robertson, A.H.F. (Eds.), *The Geological Evolution of the Eastern Mediterranean*. Geol. Soc. Spec. Publ. London, 17,1-74.
- Robertson A.H.F. and Ustaömer T., 2004. Tectonic evolution of the Intra-Pontide suture zone in the Armutlu Peninsula, NW Turkey. *Tectonophysics*, 381, 175-209.
- Robertson, A. H., Ustaömer, T., Pickett, E. A., Collins, A. S., Andrew, T., and Dixon, J. E. 2004. Testing models of Late Palaeozoic–Early Mesozoic orogeny in Western Turkey: support for an evolving open-Tethys model. *Journal of the Geological Society*, 161(3), 501-511.

Sayit, K., Tekin, U.K. and Göncüoğlu, M.C., 2011. Early-middle Carnian radiolarian cherts within the Eymir Unit, Central Turkey: Constraints for the age of the Palaeotethyan Karakaya Complex. *Journal of Asian Earth Sciences*, 42(3), 398-407.

Sevin, M. and Aksay, A., 2002. 1/100.000 Ölçekli Türkiye Jeoloji Haritaları Bolu-G28 Paftası (1/100.000 scaled geological map of Turkey-Bolu G28 section). Geological Research Department, MTA (General Directorate of Mineral Research and Exploration), 35p.

Shervais, J.W., 1982. Ti–V plots and the petrogenesis of modern ophiolitic lavas. *Earth Planet. Sci. Lett.*, 59, 101–118.

Stampfli, G.M. 2000. Tethyan oceans. In: E. Bozkurt, J.A. Winchester and J.D.A. Piper (Eds.), *Tectonics and magmatism in Turkey and surrounding area*. Geological Society of London, Special Publication, 173, 163-185.

Stern, T. A., 1985. A back-arc basin formed within continental lithosphere: The Central Volcanic region of New Zealand. *Tectonophysics*, 122, 385-409.

Sun, S.S. and McDonough, W.F., 1989. Chemical and isotopic systematics of oceanic basalts; implications for mantle composition and processes. In: *Magmatism in the ocean basins*. Saunders, A.D. and Norry, M.J. (Editors), Geological Society of London, London. 42, 313-345.

Şengör, A.M.C. ve Yılmaz, Y., 1981, Tethyan evolution of Turkey : A plate tectonic approach: *Tectonophysics*, 75,181 - 241.

Şengör, A. M. C., Yılmaz Y., and Ketin I. 1981. "Remnants of a pre-Late Jurassic ocean in northern Turkey: fragments of a Permian-Triassic Paleotethys: *Geological Society of American Bulletin*, 91 , 599-609.

Şengör, A.M.C., Yılmaz, Y and Sungurlu, O., 1984. Tectonics of the Mediterranean Cimmerides: natures and evolution of the western termination of Palaeo-Tethys. *Geological Society, London, Special Publications*, 17, 77-112.

Taylor, S.R. and McLennan, S.M., 1985. The continental crust: its composition and

evolution Blackwell Scientif. Publ., Oxford, 312 pp.

Temizel, İ., Arslan, M. and Ruffet, G. 2007. Petrochemical and  $^{40}\text{Ar}/^{39}\text{Ar}$  geochronological evidence of postcollisional Tertiary calc-alkaline volcanism in the Ulubey (Ordu), eastern Pontide, NE Turkey. Special Supplement, 17th Annual V.M. Goldschmidt Conference, Geochronology of Tectonic Processes, *Geochimica et Cosmochimica Acta* 71, A1013.

Topuz, G., Altherr, R., Kalt, A., Satır, M., Werner, O. and Schwarz, W.H., 2004. Aluminous granulites from the Pular complex, NE Turkey: a case of partial melting, efficient melt extraction and crystallisation. *Lithos*, 72(3), 183-207.

Ustaömer T, Robertson AHF., 1993. A late Palaeozoic-Early Mesozoic marginal basin along the active southern continental margin of Eurasia: evidence from the Central Pontides (Turkey) and adjacent regions. *Geol J*, 28, 219-238.

Ustaömer, T. and Robertson, A.H., 1999. Geochemical evidence used to test alternative plate tectonic models for pre-Upper Jurassic (Palaeotethyan) units in the Central Pontides, N Turkey. *Geological Journal*, 34(1-2), 25-53.

Ustaömer, T. and Robertson, A., 1997. AAPG Memoir 68: Regional and Petroleum Geology of the Black Sea and Surrounding Region. Chapter 14: Tectonic-Sedimentary Evolution of the North Tethyan Margin in the Central Pontides of Northern Turkey.

Wilson, M., 1989. Review of Igneous Petrogenesis: A global Tectonic Approach. *Terra Nova*, 1(2), 218-222.

Winchester J. A., Floyd P. A., 1976. Geochemical magma type discrimination: Application to altered and metamorphosed igneous rocks. *Earth and Planetary Science Letters*, 28, 459-69.

Winchester, J.A., Floyd, P.A., 1977. Geochemical discrimination of different magma series and their differentiation products using immobile elements. *Chem. Geol.* 20, 325-343.

Yalınz, M.K., Floyd, P.A. and Göncüoğlu, M.C., 1996. Supra-subduction zone ophiolites of Central Anatolia: geochemical evidence from the Sarikaraman ophiolite, Aksaray, Turkey. *Mineralogical Magazine*, 60(5), 697-710.

Yanev, S., Göncüoğlu, M.C., Gedik, I., Lakova, I., Boncheva, I., Sachanski, V., Okuyucu, C., Özgül, N., Timur, E., Maliakov, Y., Saydam, G., 2006. Stratigraphy, correlations and palaeogeography of Palaeozoic terranes of Bulgaria and NW Turkey: a review of recent data. In: Robertson, A.H.F., Mountrakis, D. (Eds.), *Tectonic Development of the Eastern Mediterranean Region*. Geological Society, London, Special Publications, 260, 51–67.

Yılmaz, O. and Boztuğ, D., 1986. Kastamonu granitoid belt of northern Turkey: First arc plutonism product related to the subduction of the Paleo-Tethys. *Geology*, 14, 179-183.

Yılmaz, Y., 1981. Sakarya kıtası güney kenarının tektonik evrimi. *İst. Üniv. Yerbilimleri Dergisi*, 1(1-2), 33-52 (in Turkish).

Yılmaz, Y., Genç, Ş. C., Yiğitbaş, E., Bozcu, M., and Yılmaz, K., 1995. Geological evolution of the late Mesozoic continental margin of Northwestern Anatolia. *Tectonophysics*, 243(1), 155-171.

Yılmaz, Y., Tüysüz, O., Yiğitbaş., Genç, Şengör, A.M.C. 1997. Geology and tectonic evolution of the Pontides. In: ROBINSON, A.G. (ed), *Regional and Petroleum Geology of the Black Sea and Surrounding Regions*. American Association of Petroleum Geologists Memoir 68, 183–226.

Yiğitbaş, E. ve Elmas, A. 1997. Bolu – Eskipazar – Devrek – Çaycuma dolayının jeolojisi. TPAO Raporu, 112p.

Yiğitbaş, E., Elmas, A., and Yılmaz, Y., 1999. Pre-Cenozoic tectono-stratigraphic components of the Western Pontides and their geological evolution. *Geological Journal*, 34(1-2), 55-74.